Warm DM vs. Cold DM Scenario for the formation of Cosmic Structures

N. Menci
Osservatorio Astronomico di Roma - INAF

Outline

Critical Issues Concerning CDM on Small Scales (Dwarf Galaxies)

Solutions based on Astrophysical Processes

vs

Solutions based on Warm Dark Matter (candidates with mass m_X~keV)

Some properties of WDM galaxy formation

Constraining the Warm Dark Matter particle mass: getting rid of uncertainties due to modelling of astrophysical processes

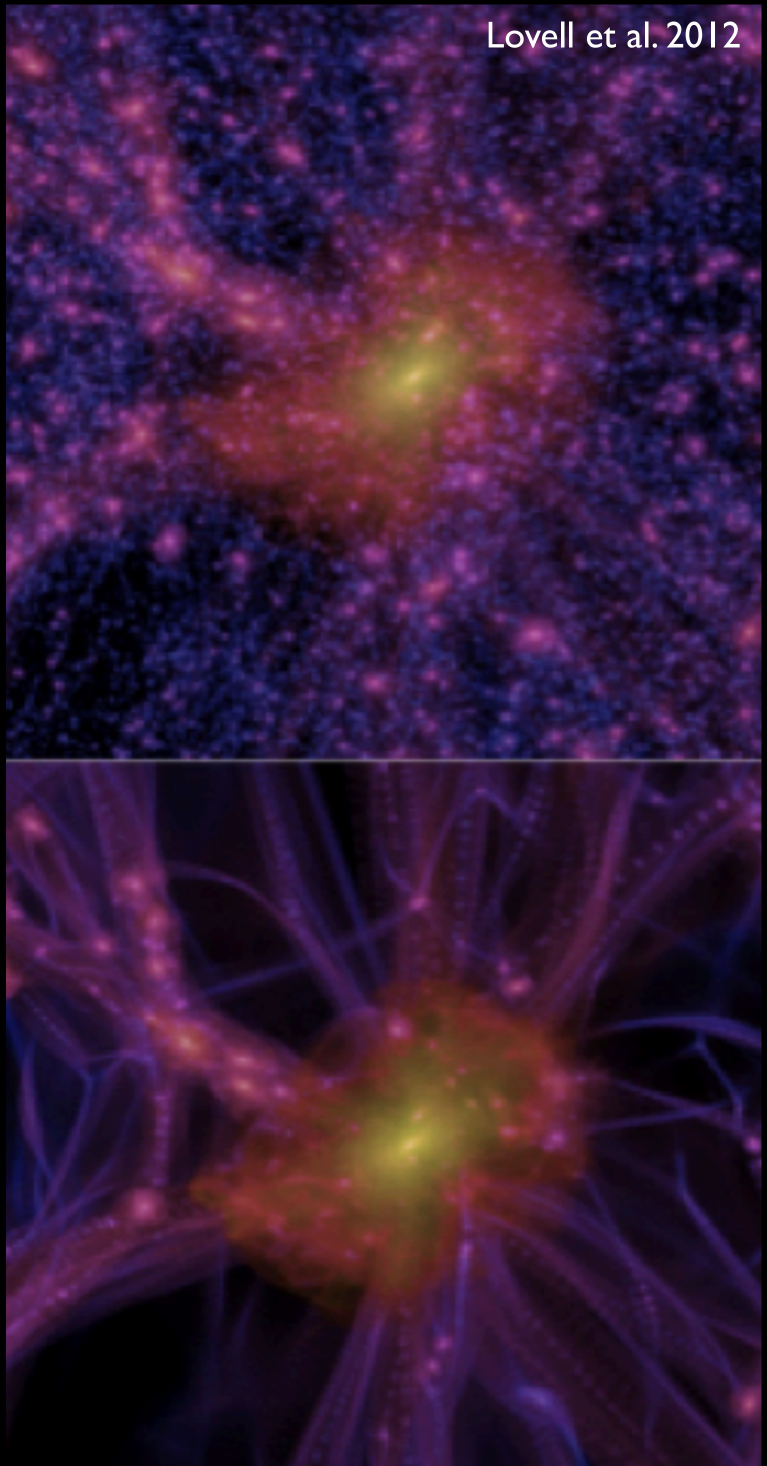

DARK MATTER
and
STRUCTURE FORMATION

Cosmic Structures form from the collapse of overdense regions in the DM primordial density field, and grow by gravitational instability

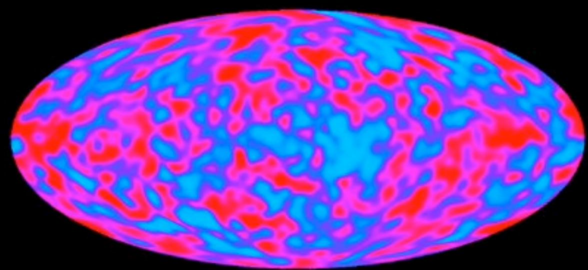

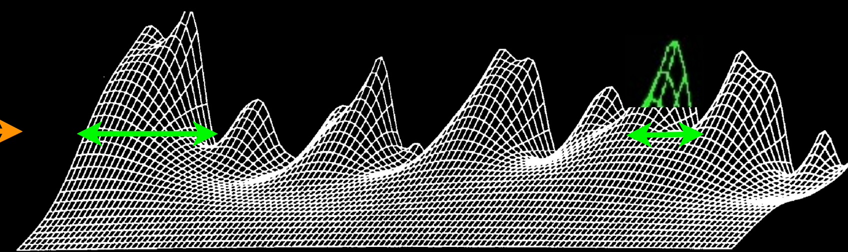

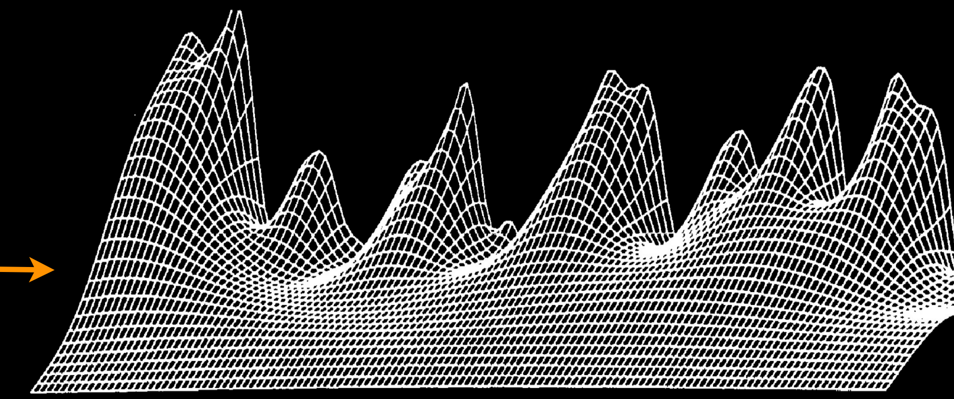

R=2π/k

$$M = \frac{4\,\pi}{3}\,\rho\,R^3$$

$$\langle \delta_M^2 \rangle = \sigma^2(M)\,g(t)$$

Gaussian Random field

$$\delta = \frac{\delta\rho}{\rho}$$

$$p(\delta_k) = \frac{1}{\sqrt{2\pi}\,\sigma_k}\,e^{-\frac{\delta_k^2}{2\,\sigma_k^2}}$$

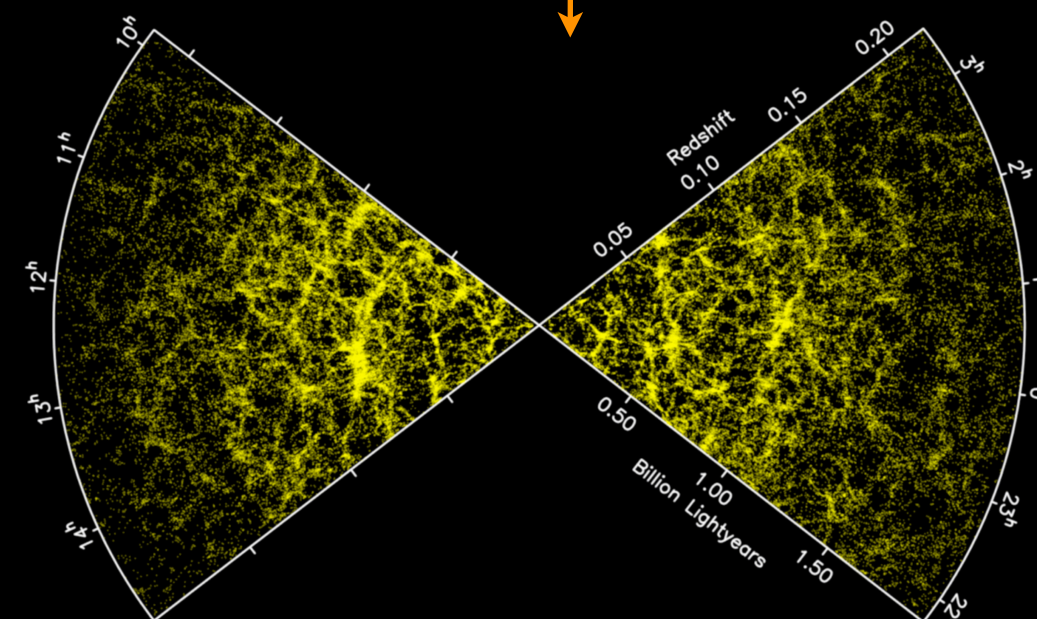

Mean (square) value of perturbations of size R(~1/k) enclosing a mass M

$$P(k) = \frac{1}{V}\,\langle |\delta_k|^2 \rangle$$

$$\sigma_M^2 = \frac{1}{(2\pi)^3\,V}\int^{M\leftrightarrow k} dk\,k^2\,P(k)$$

$$\sigma_M^2 \leftrightarrow P(k)$$

Variance σ(M) quantifies the typical amplitude of density perturbations on a given mass scale

The Variance of the perturbation field

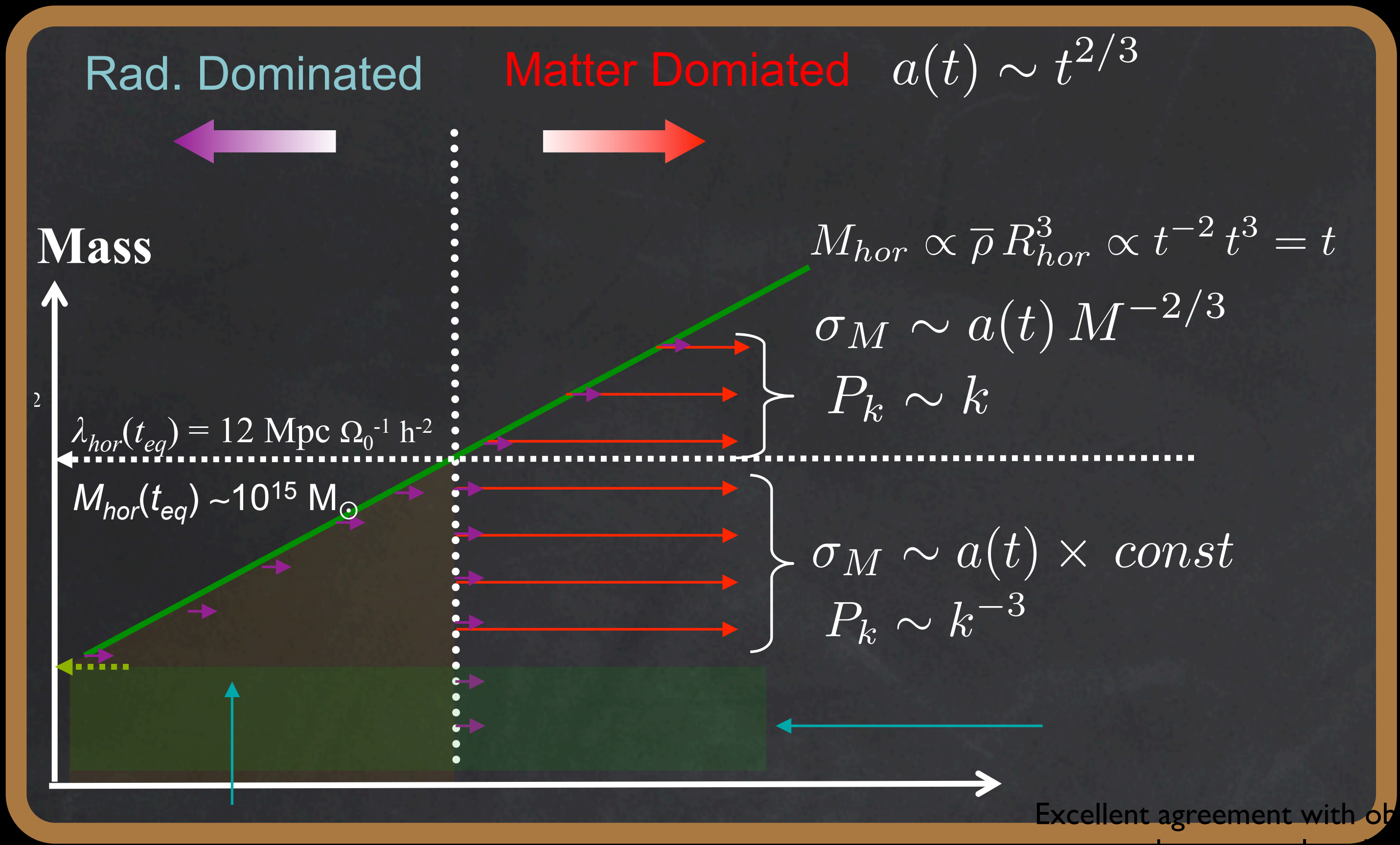

Cold Dark Matter

non relativistic at decoupling

no dissipation down to small scales < 10^6 $M_\odot$

Variance is an ever-increasing inverse function of the mass scale.

Huge number of small-scale structures

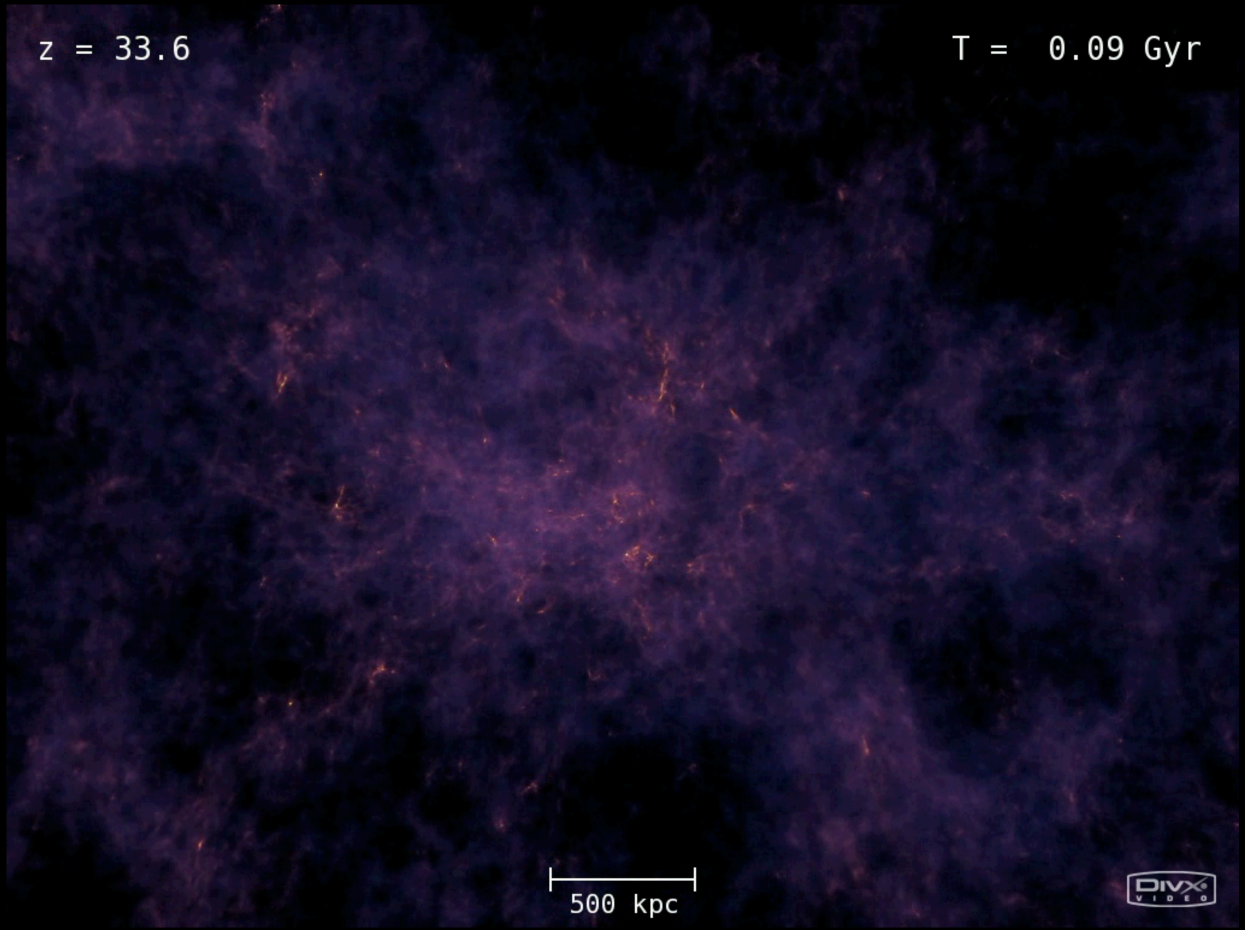

Springel et al. 2009

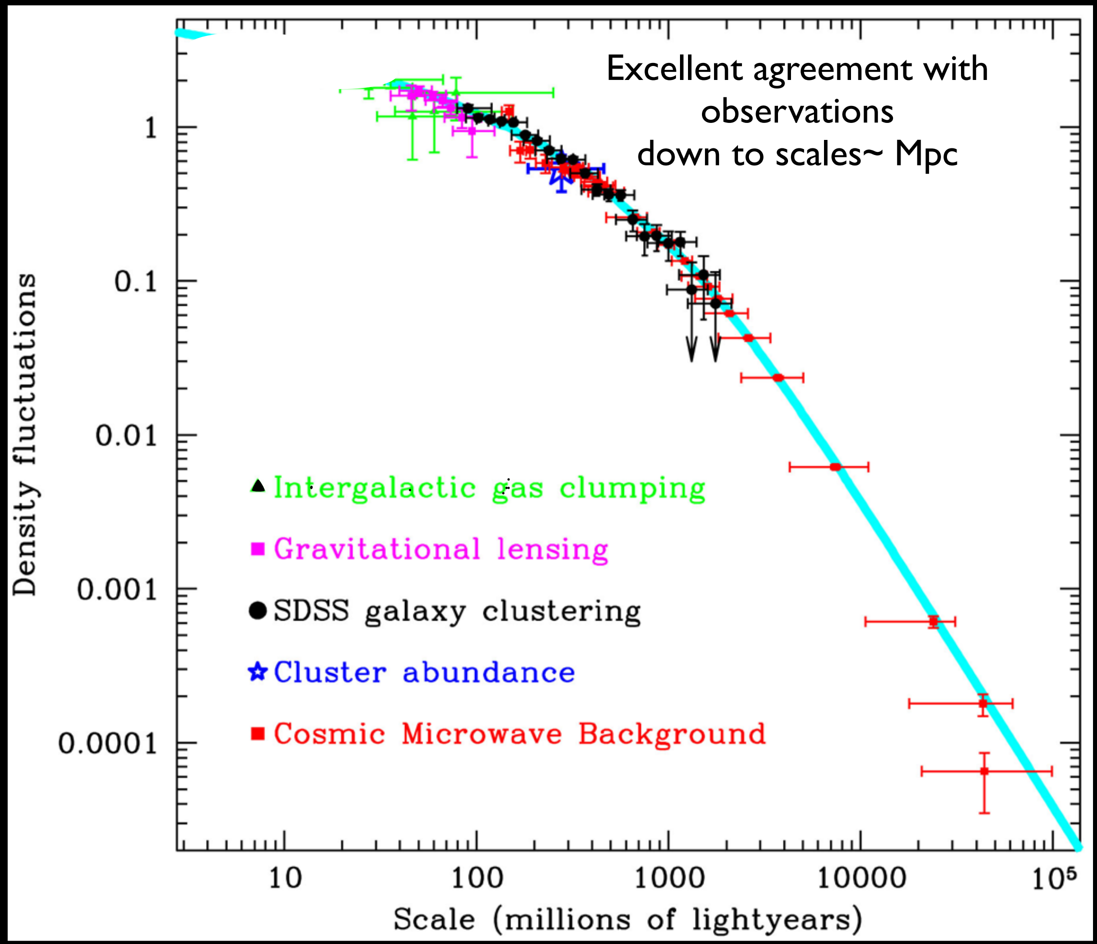

Dissipation, free-streaming scale

$$r_{fs} = \int_0^t \frac{v(t)}{R(t)}$$

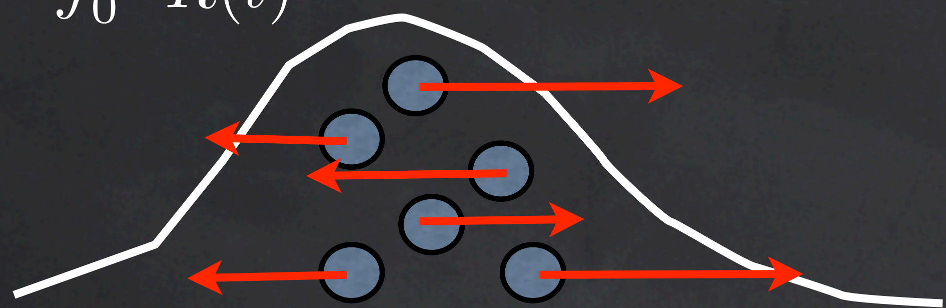

$$\sigma_\chi \propto a^{-1}\, m_\chi^{-1/2}$$

$$M_{fs} = 4 \times 10^{15} \left(\frac{m_\nu}{30\ \text{eV}} \right)^{-2} M_\odot$$

Lighter and faster Dark Matter particles stream out of density perturbations

CDM: the free streaming length is much smaller than any scale involved in galaxy formation (≪Mpc)

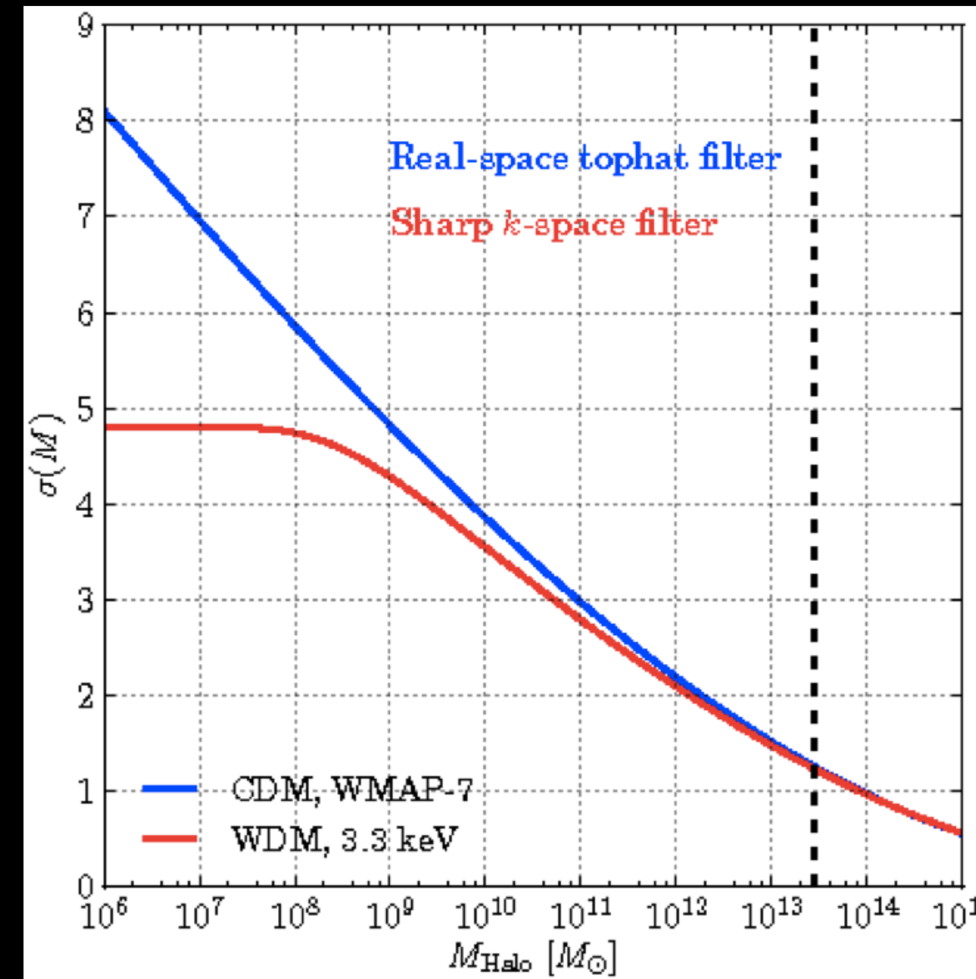

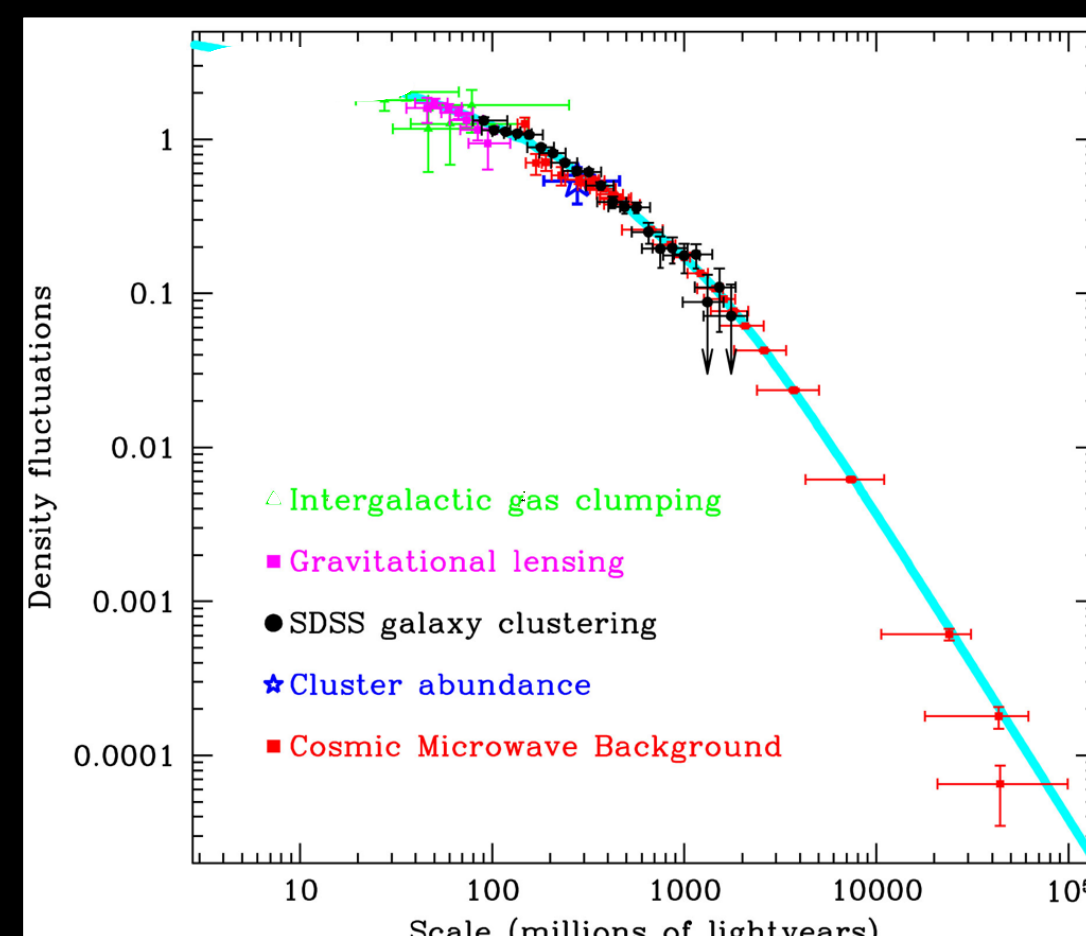

Dissipation, free-streaming scale

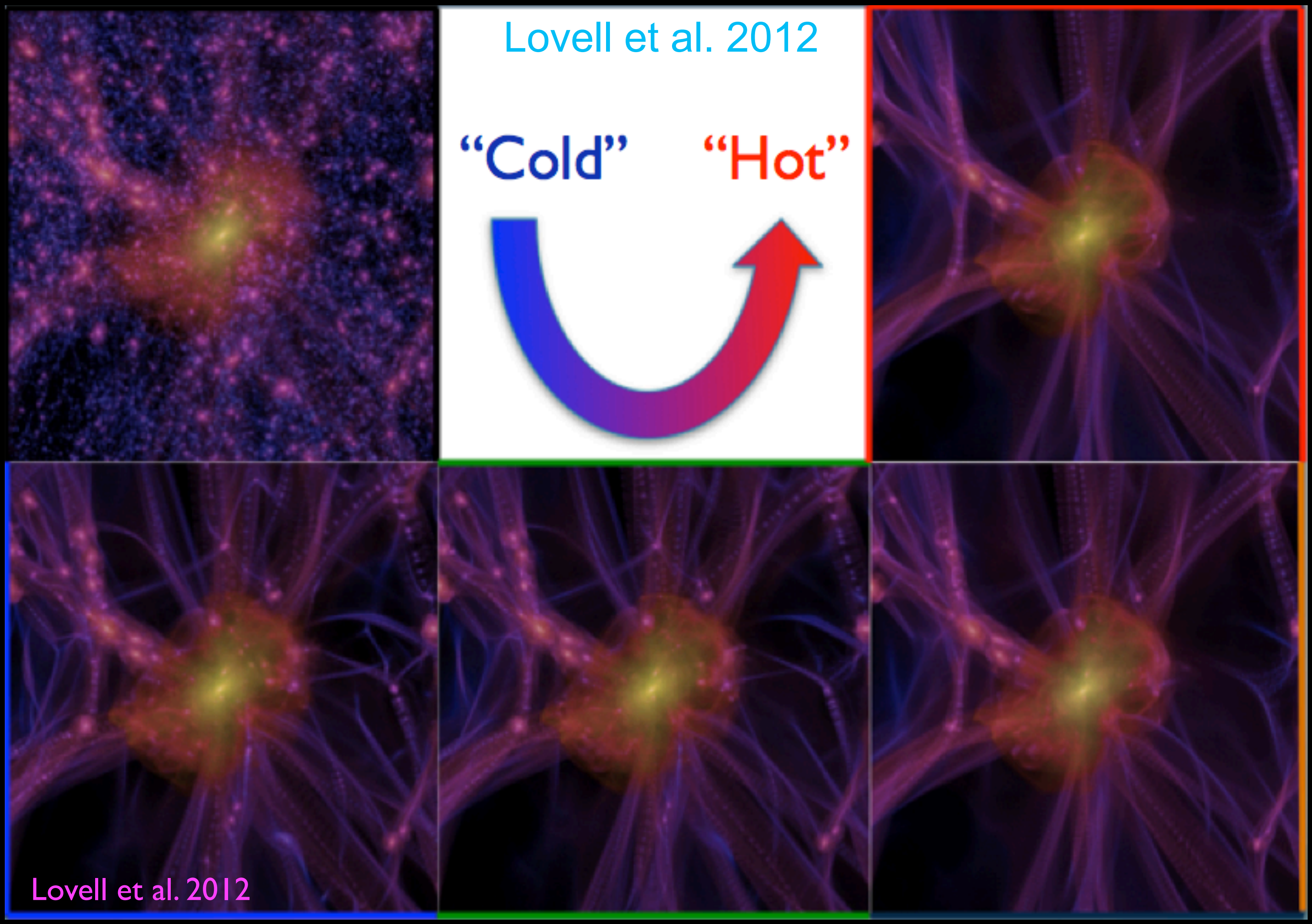

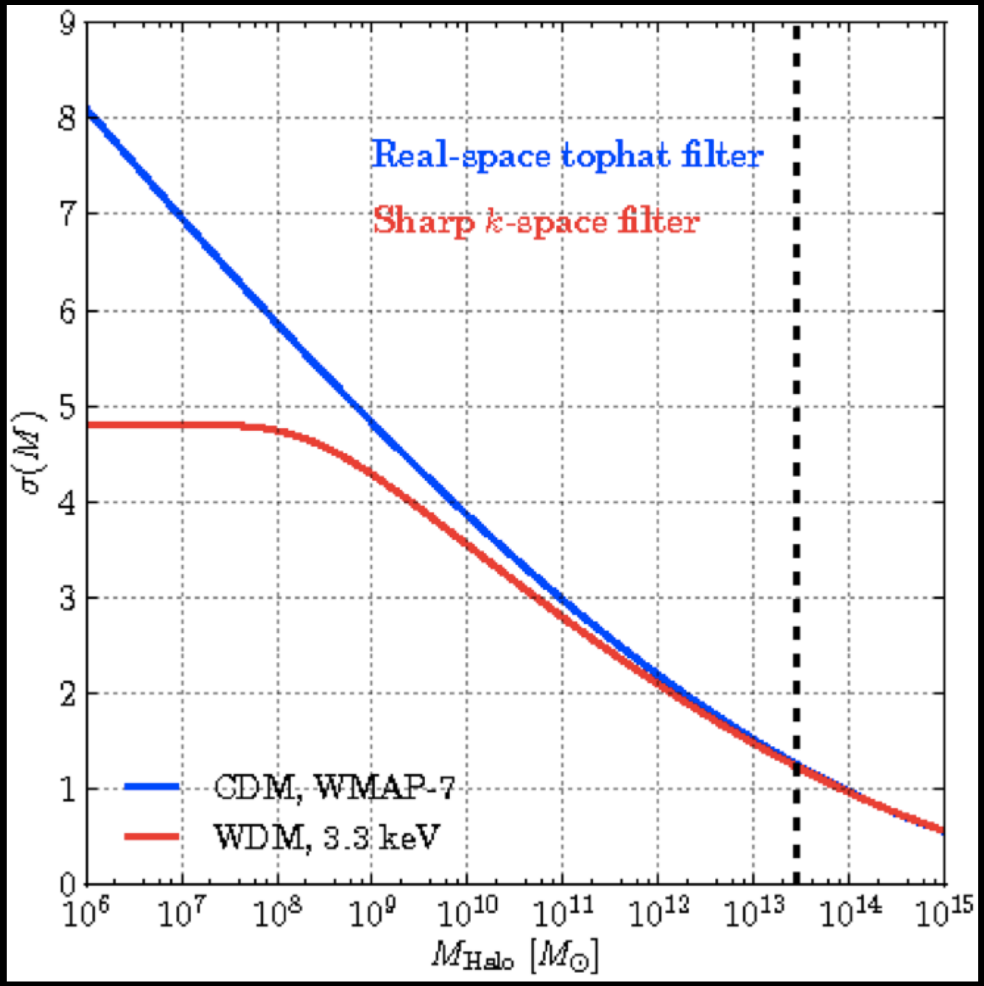

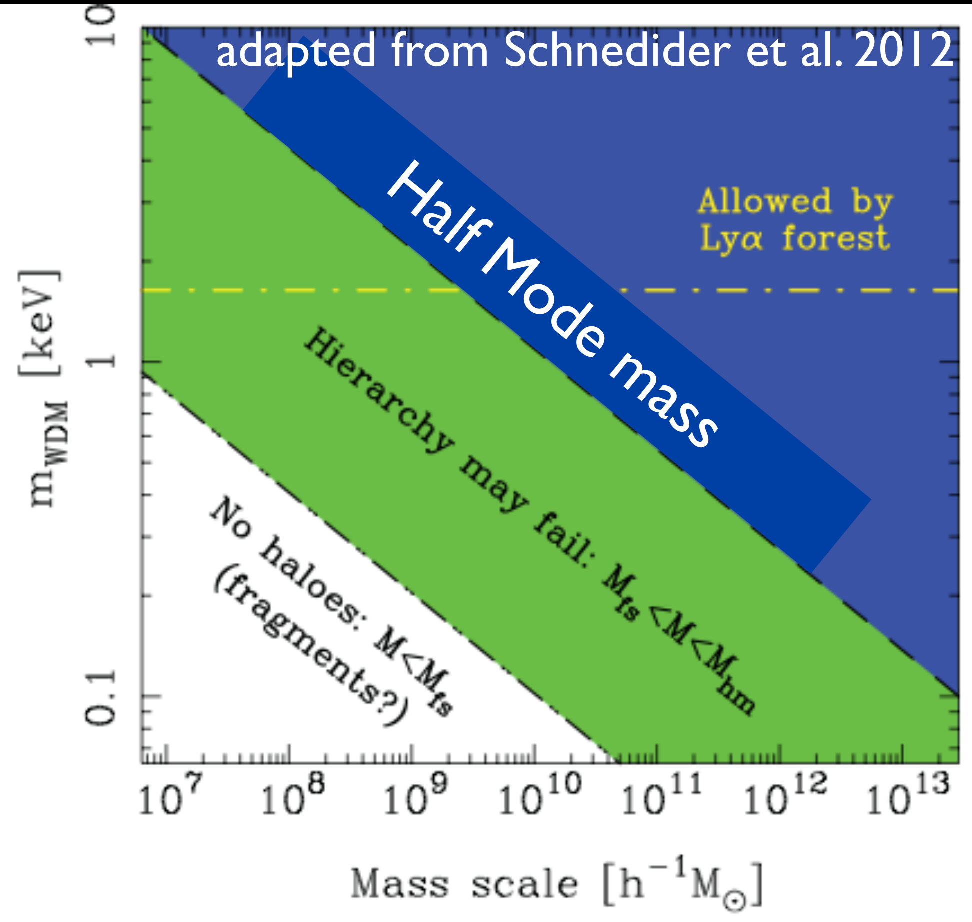

Dissipation, free-streaming scale

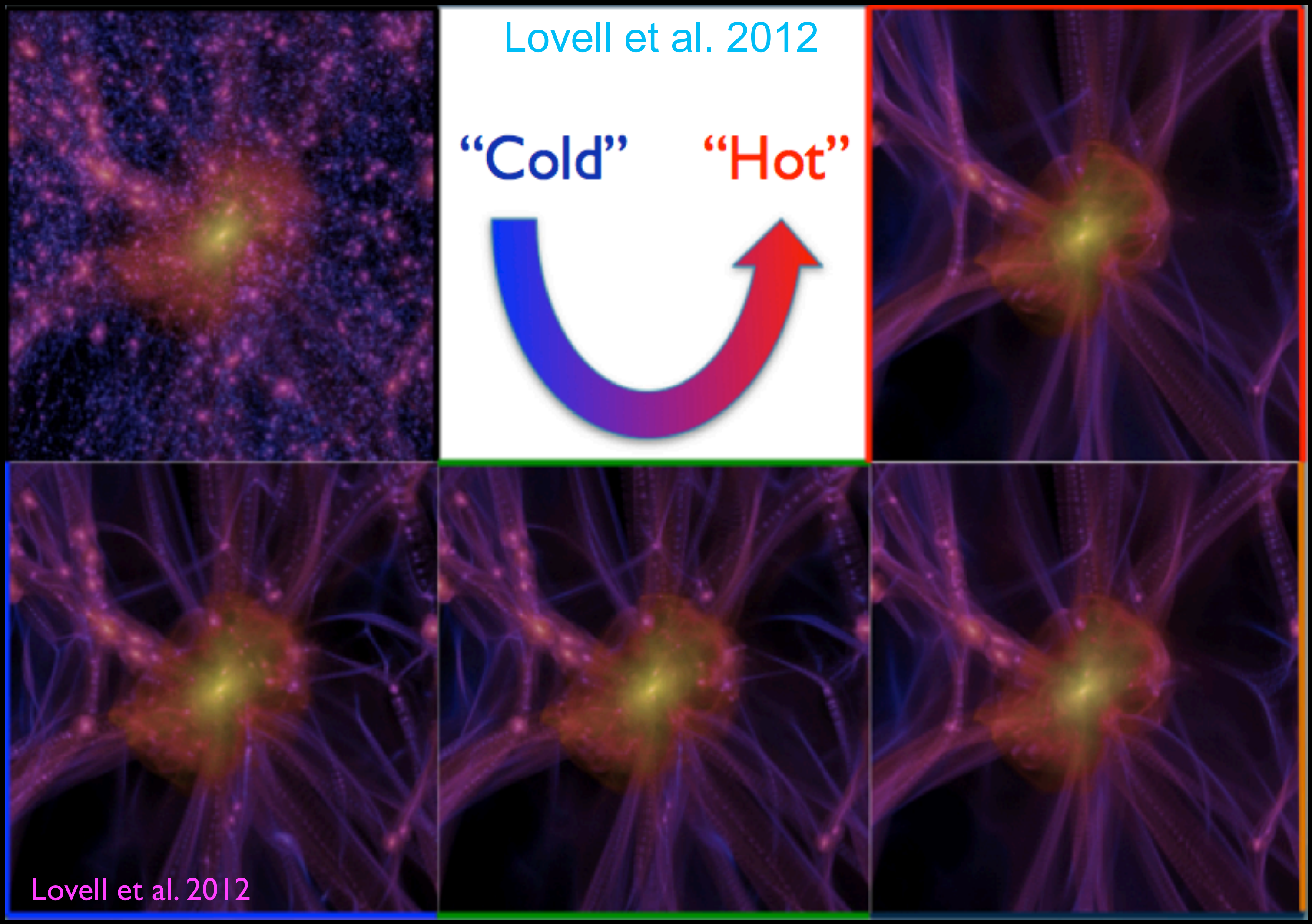

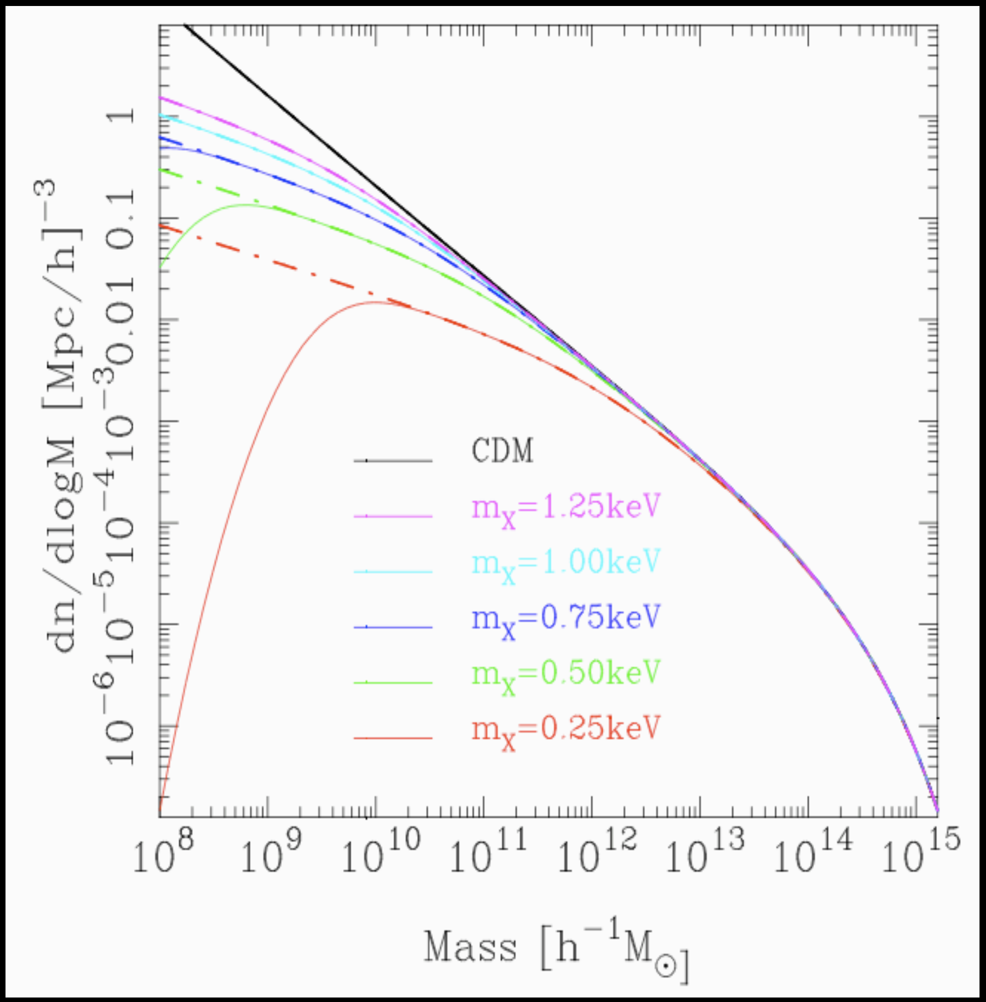

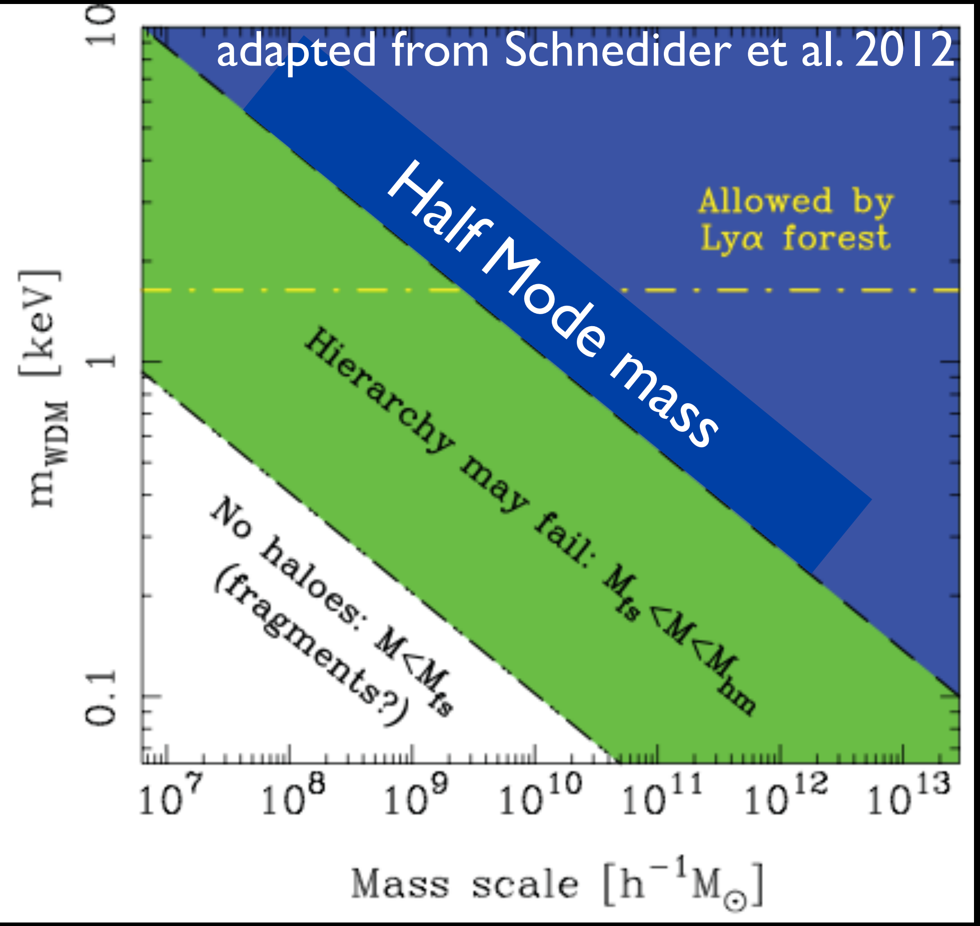

Compared to CDM, in WDM models the abundance of low-mass structures is suppressed below the half mode mass

CRITICAL ISSUES CONCERNING
COLD DARK MATTER
AT SMALL GALACTIC SCALES

Critical Issues (concerning structure formation)

Overabundance of low-mass objects

i) abundance of satellite DM haloes
ii) density profiles
iii) abundance of faint galaxies
iv) the M_*-M_{halo} relation
v) star formation histories of satellites

1) Dependence on specific theoretical model
2) Dependence on star formation and feedback effects
3) Solutions in WDM scenario

Critical Issues

Overabundance of low-mass objects

i) abundance of satellite DM haloes
ii) density profiles
iii) abundance of faint galaxies
iv) the M_*-M_{halo} relation
v) star formation histories of satellites

CDM Substructure in simulated cluster and galaxy haloes look similar.

Expected number of satellites in Milky Way- like galaxies in CDM largely exceeds the observed abundance.

Kravtsov, Klypin, Gnedin 2004

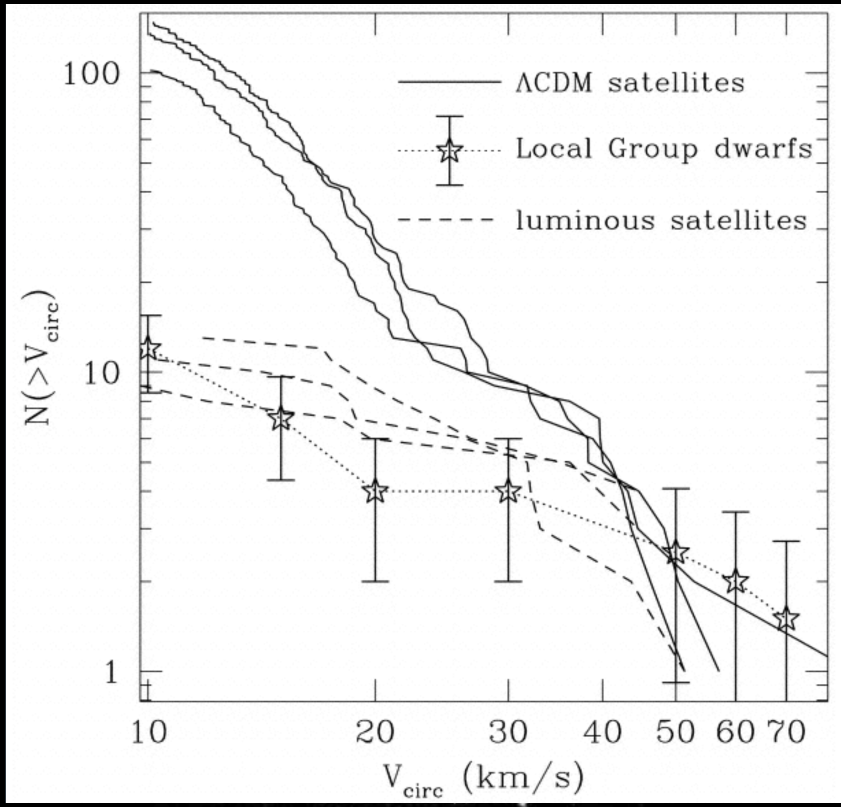

Via Lactea simulation of a Milky Way - like galaxy
Diemand et al. 2008

Critical Issues

Overabundance of low-mass objects

i) abundance of satellite DM haloes
ii) density profiles
iii) abundance of faint galaxies
iv) the M_{*}-M_{halo} relation
v) star formation histories of satellites

Moore et al. 2002

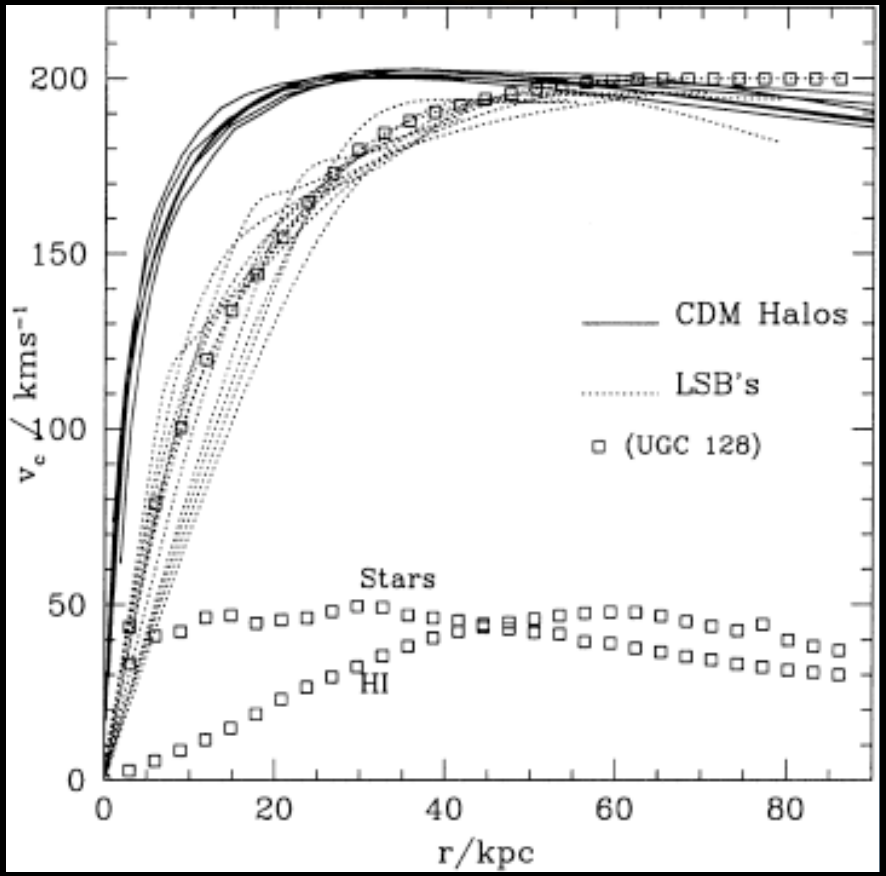

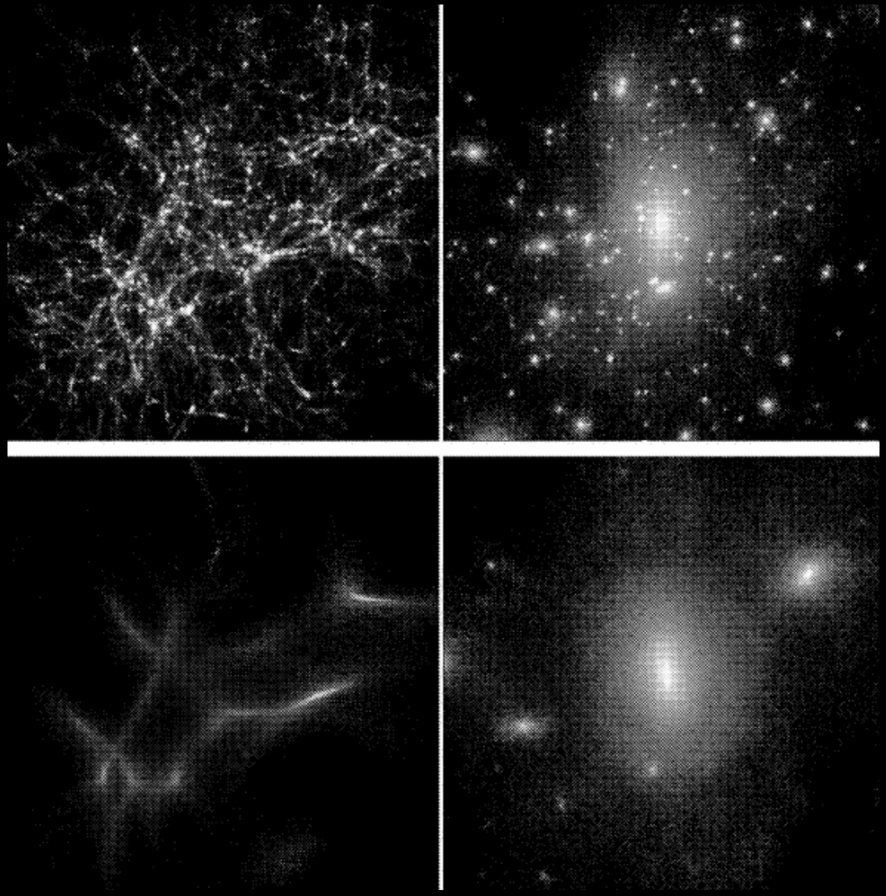

Most observed dwarf galaxies consist of a rotating stellar disk embedded in a massive dark-matter halo with a near-constant-density core. Models based on the dominance of CDM, however, invariably form galaxies with dense spheroidal stellar bulges and steep central dark-matter profiles, because low-angular- momentum baryons and dark matter sink to the centres of galaxies through accretion and repeated mergers.

SOLUTIONS BASED ON REFINED MODELING OF ASTROPHYSICAL PROCESSES

The DM-Feedback Degeneracy

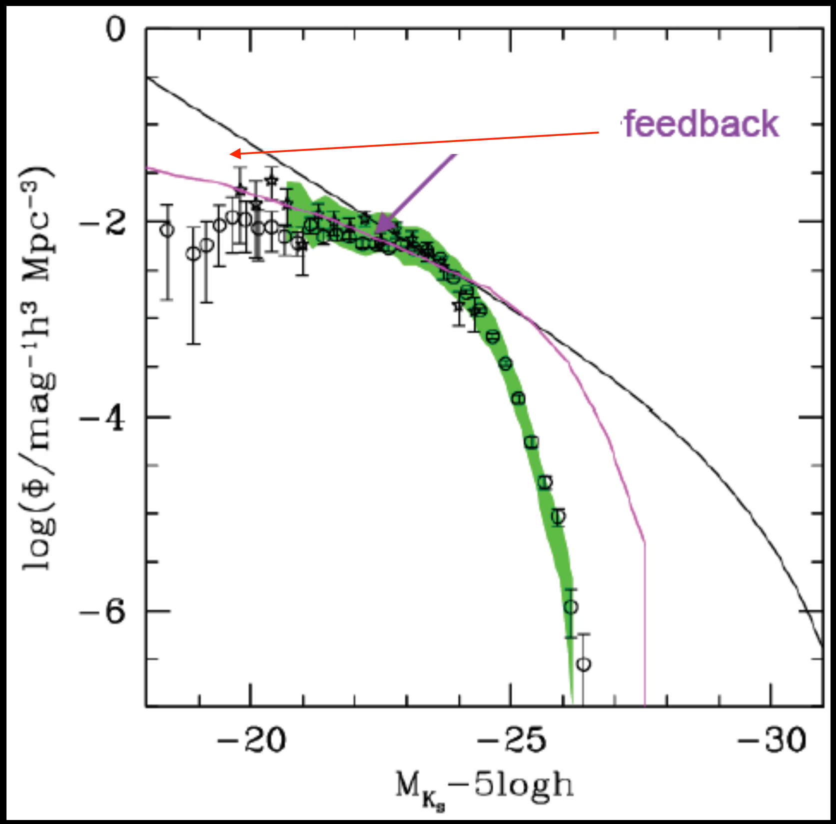

The origin of the problem:
The CDM halo Mass function has a steep log slope $N \sim M^{-1.8}$
While the Observed Galaxy Luminosity Function
has a much flattter slope $N \sim L^{-1.2}$

A Possible Solution:
Suppress luminosity (star formation) in low-mass haloes $L/M \sim M^{\beta}$ $\beta=1\text{-}3$
Heat - Expell Gas from shallow potential wells
- Enhanced SN feedback
- UV background

$$E_{SN} \approx 10^{51}\,\eta_0\eta_{IMF}\,\Delta M_* erg/s$$

$$v_{SN} = \sqrt{E_{SN}/M_{gas}} \approx 100 \;\; km/s$$

At Z=0 the mass scale at which SN can effectively espell gas from DM potential wells

$$M_{SN} \sim 10^{10}\, M_\odot$$

Vogelsberger et al. 2014

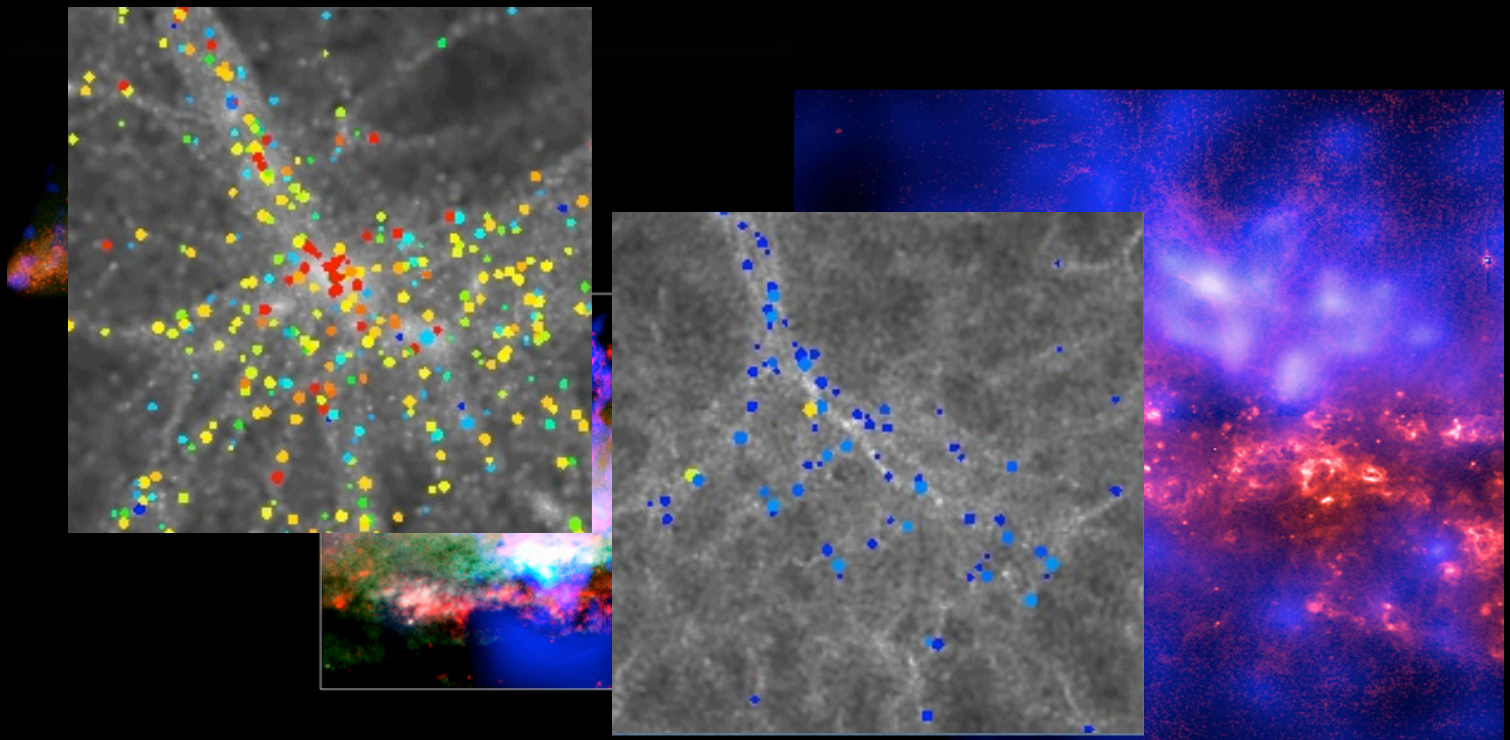

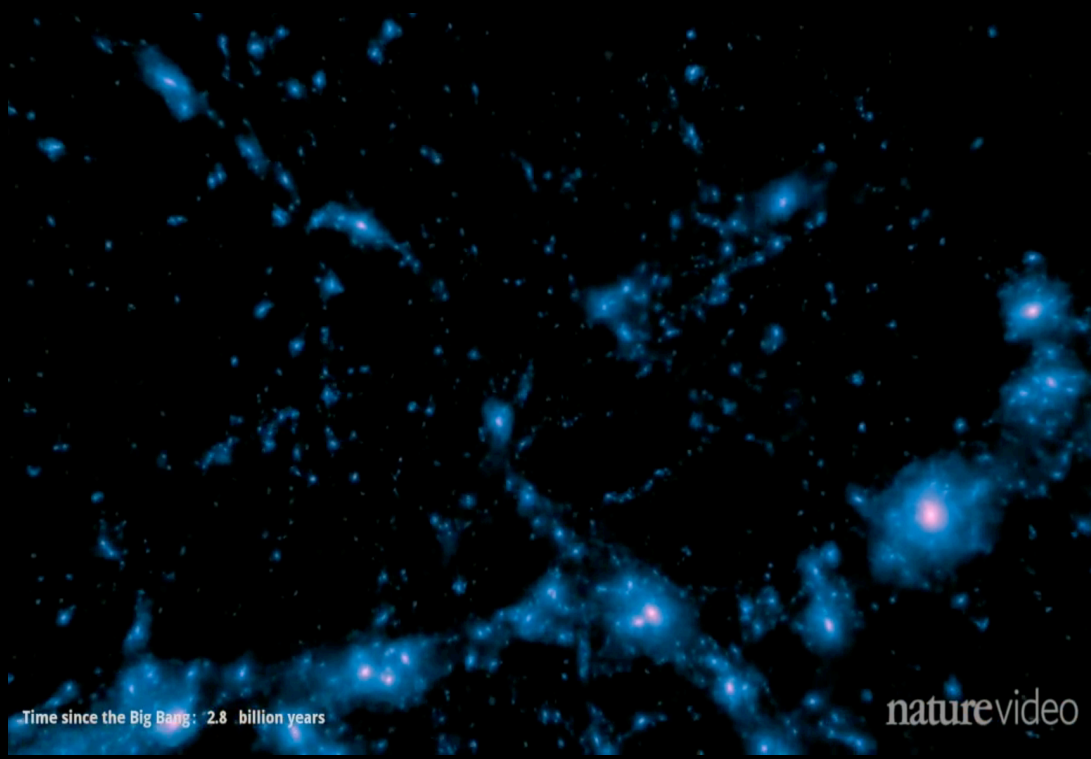

Galaxy Formation in a Cosmological Context

relating gas and star formation to the evolution of DM halos

Hydrodynamcal N-body simulations

Pros

include hydrodynamics of gas
contain spatial information

Cons

numerically expensive
(limited exploration of parameter space)
requires sub-grid physics

Semi-Analytic Models Monte-Carlo realization of collapse and merging histories

Pros

Physics of baryons linked to DM halos through scaling laws, allows a fast spanning of parameter space

Cons

Simplified description of gas physics
Do not contain spatial informations

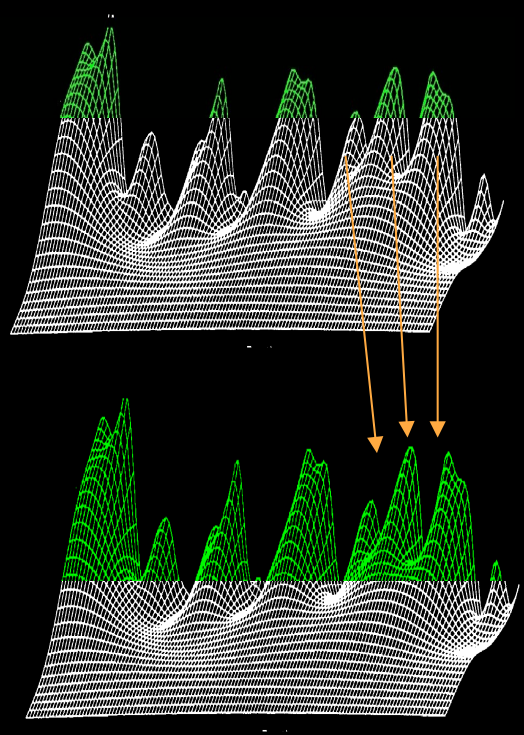

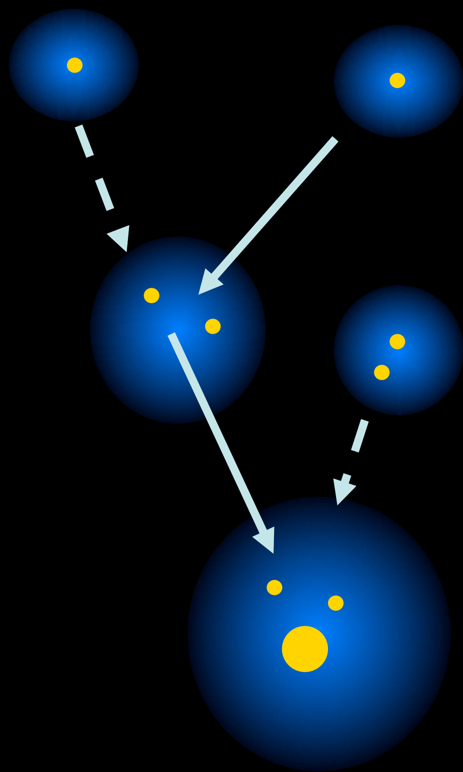

Sub-Halo dymanics:
dynamical friction, binary aggregation

Halo Properties
Density Profiles
Virial Temperature

Gas Properties
Profiles
Cooling - Heating Processes
Collapse, disk formation

Star Formation Rate

Gas Heating (feedback)
SNae
UV background

Evolution of stellar populations

Growth of Supermassive BHs
Evolution of AGNs

The DM-Feedback Degeneracy

Solutions from Feedback Processes

i) the abundance of satellite galaxies

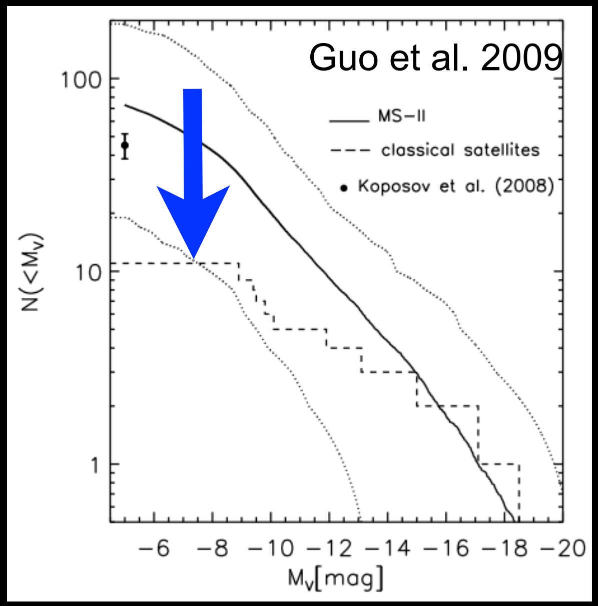

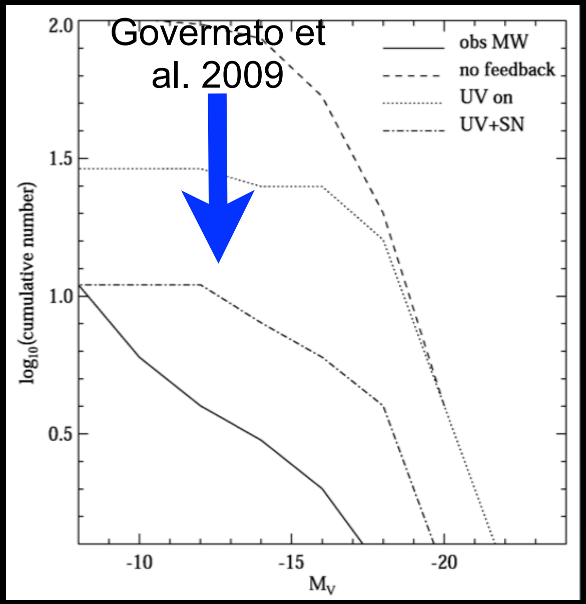

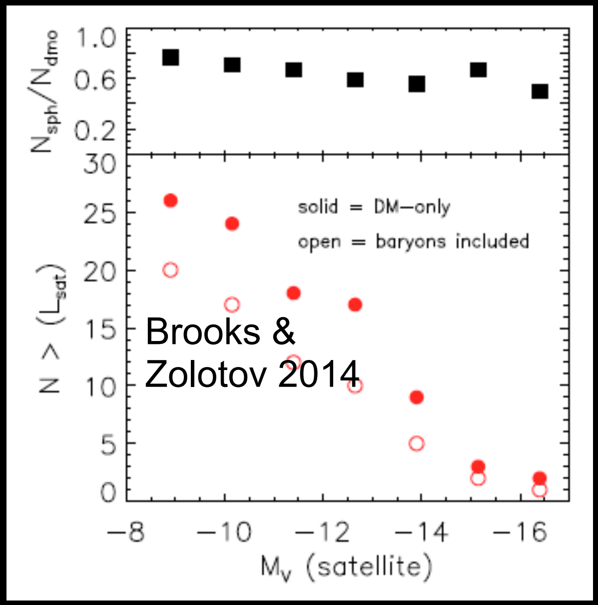

ii) the density profiles

A proposed solution at low redshift

"... The rapid fluctuations caused by episodic feedback progressively pump energy into the DM particle orbits, so that they no longer penetrate to the centre of the halo" (Weinberg et al. 2013, Governato et al. 2012)

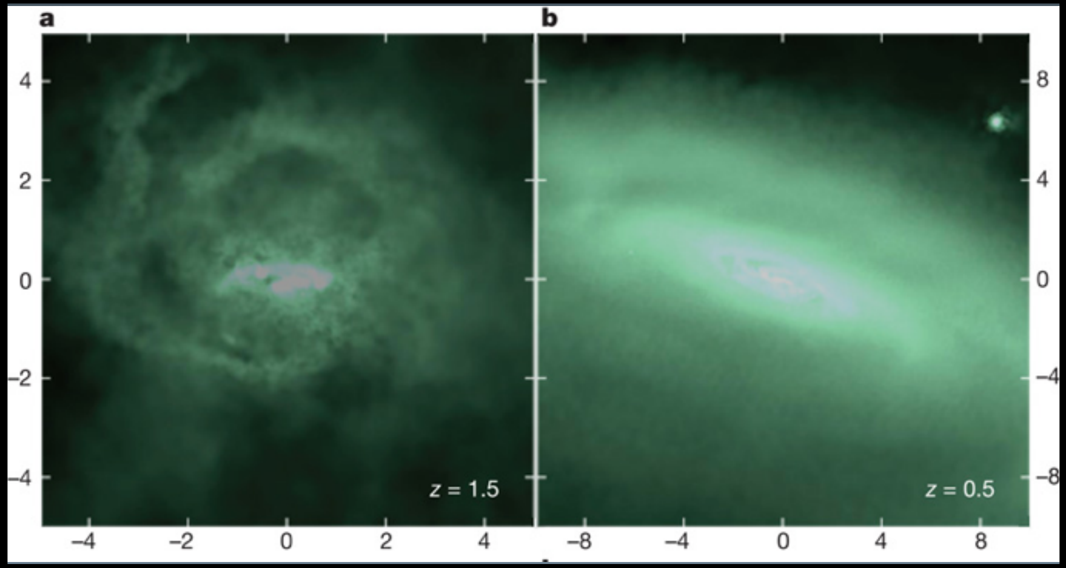

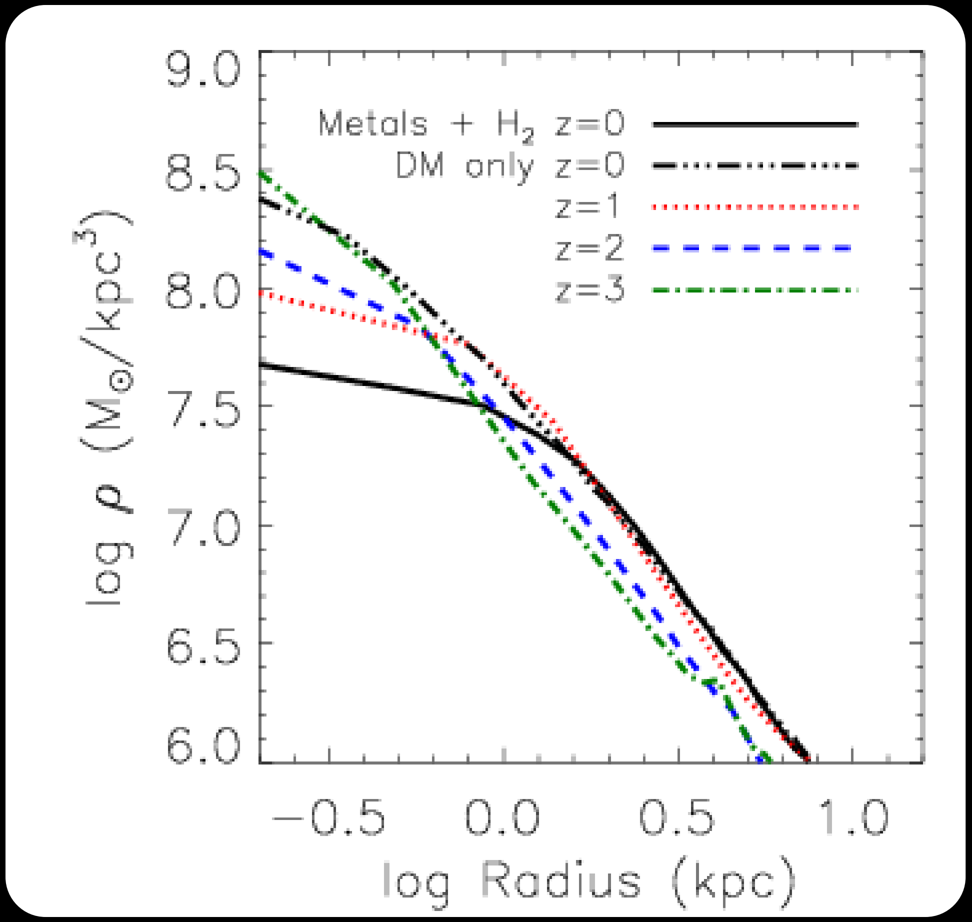

Problems with Solutions based on Feedback

1: Profiles and Abundances of low-mass galaxies at high redshifts

- Steeper central profiles are expected at z>1

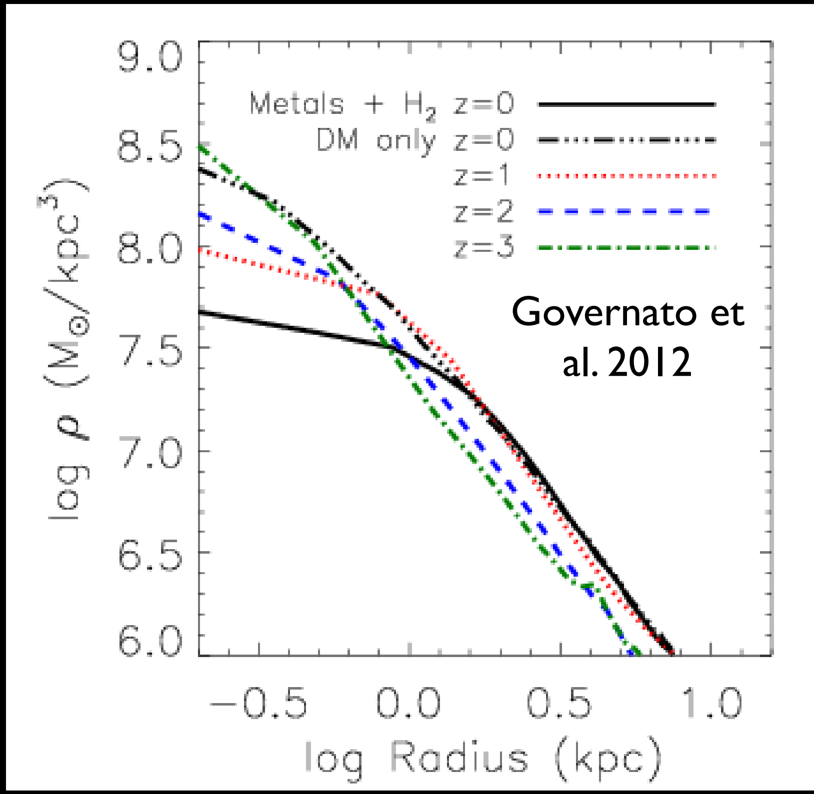

- Steeper luminosity functions are expected at z>1

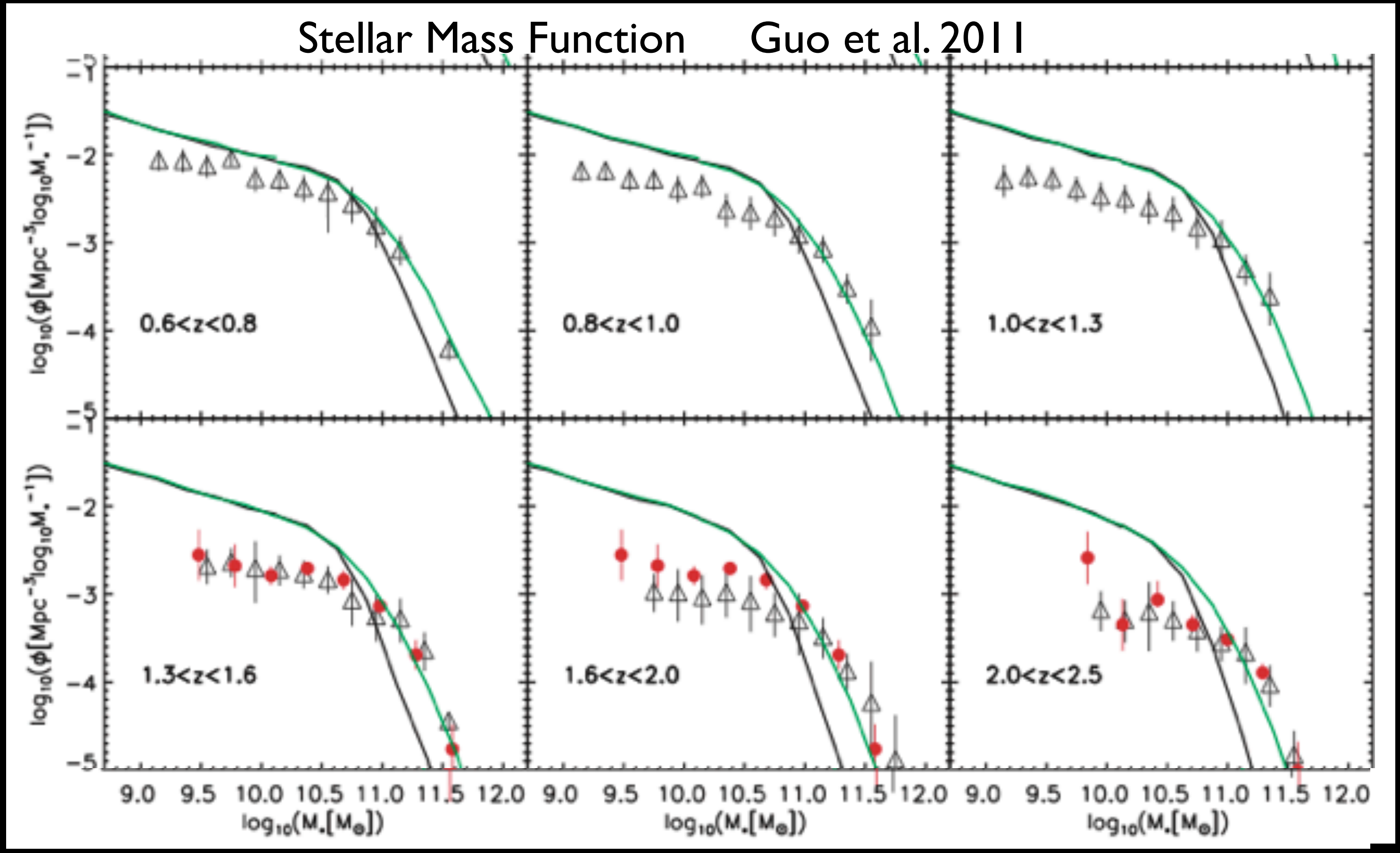

Problems with Solutions based on Feedback

I: Profiles and Abundances of low-mass galaxies at high redshifts

Velocities corresponding to Supernovae Feedback

$$v_{SN} = \sqrt{E_{SN}/M_{gas}} \approx 100 \quad km/s$$

$$M \approx (v_{esc}^2/G)\, r$$

$$r \propto (M/\rho)^{1/3}$$
$$\rho = 180\,\rho_u = 180\,\rho_u\,(1+z)^3$$
$$A \equiv \sqrt{3/G^3\,4\pi\,\rho_u}$$

$$M \approx A\,v_{esc}^3\,(1+z)^{-3/2}$$

$$v_{esc} = v_{SN}$$

Mass scale at which SN can effectively expel gas from DM halodecreases with redshift

$$M_{SN} \approx 10^{10}\,M_\odot\,(1+z)^{-3/2}$$

At high-z
larger densities imply
larger escape velocity
even for low-mass
galaxies:
feedback increasingly
ineffective

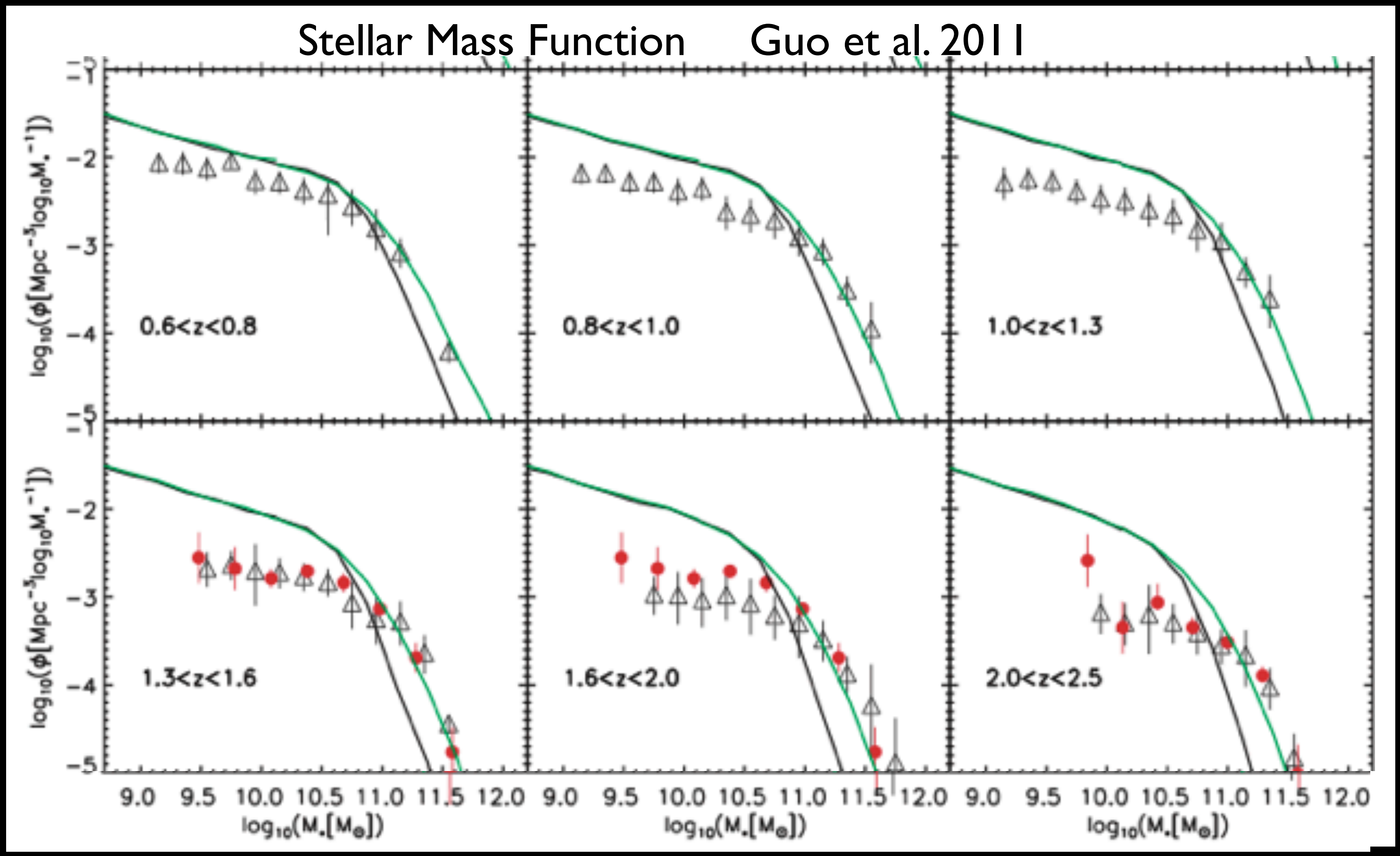

Problems with Solutions based on Feedback

II: The L/M ratio of low-mass galaxies

Enhancing the feedback results into inefficient star formation for given DM halo (suppress L/M).

This seems at variance with observed M_{star}-M relation

3926 *C. B. Brook and A. Di Cintio*

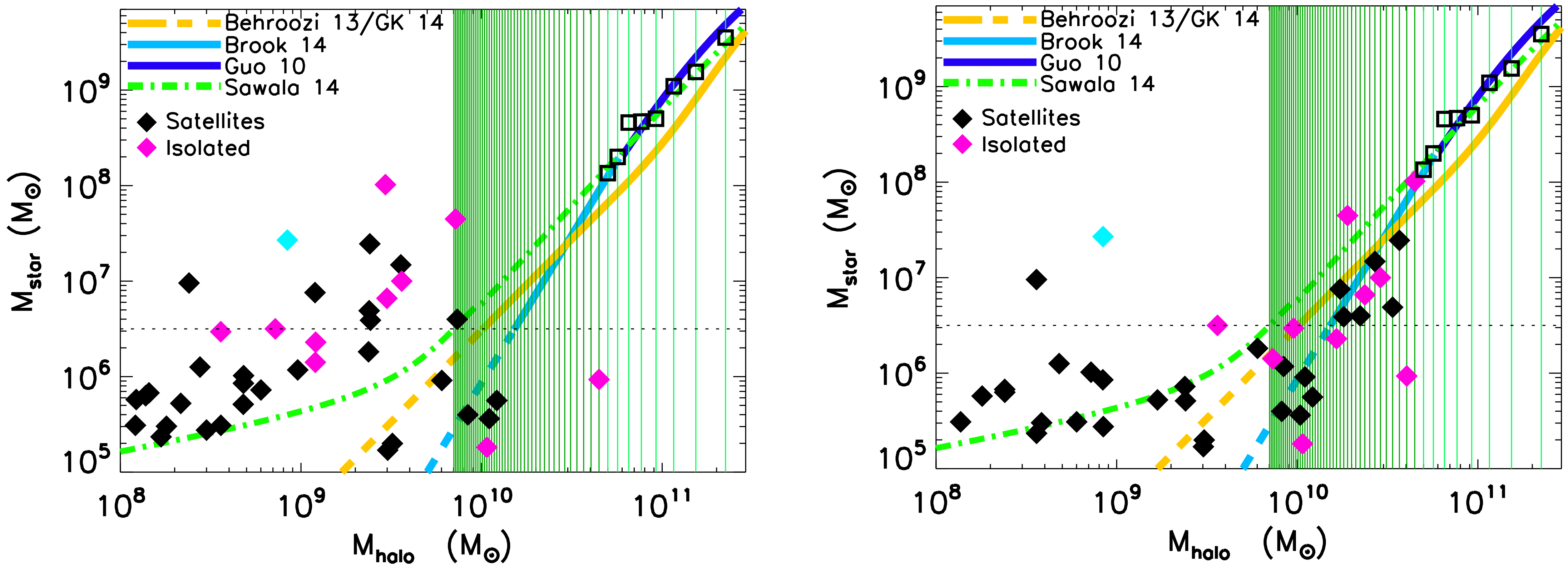

Figure 2. The relation between observed stellar mass and derived halo mass for LG galaxies. The halo mass has been found by fitting kinematical data and assuming two different halo profiles. The results for an NFW profile are shown in the left-hand panel, while the mass-dependent DC14 halo profile has been used in the right-hand panel. Satellites and isolated galaxies are shown in different colours, with Sagittarius dwarf irregular, highly affected by tides, shown in cyan. Several abundance matching predictions are indicated, in particular the Brook et al. (2014) one has been constrained using the LG mass function, and it is shown as dashed line below the observational completeness limit of the LG.

Problems with Solutions based on Feedback

III: The Distribution of Gas Rotation Velocities

21-cm survey done with Arecibo Telescope: 3000 deg^2; 11000 detections

measures: redshift, velocity width, integrated flux

No spatial resolution (size, inclination, shape)

Directly measures
the depth of the potential well:
less prone to physics of gas (feedback)

To match the observatons, observed rotation velocities should correspond to huge host DM halos with large V_{halo} so as to suppress the V_{rot}/V_{halo} ratio at low V_{rot}

$$\frac{dN}{dV_{rot}} = \frac{dN}{dV_{Halo}} \frac{dV_{Halo}}{dV_{rot}}$$

Abundance of galaxies as a function of their velocity width (gas rotation velocity)

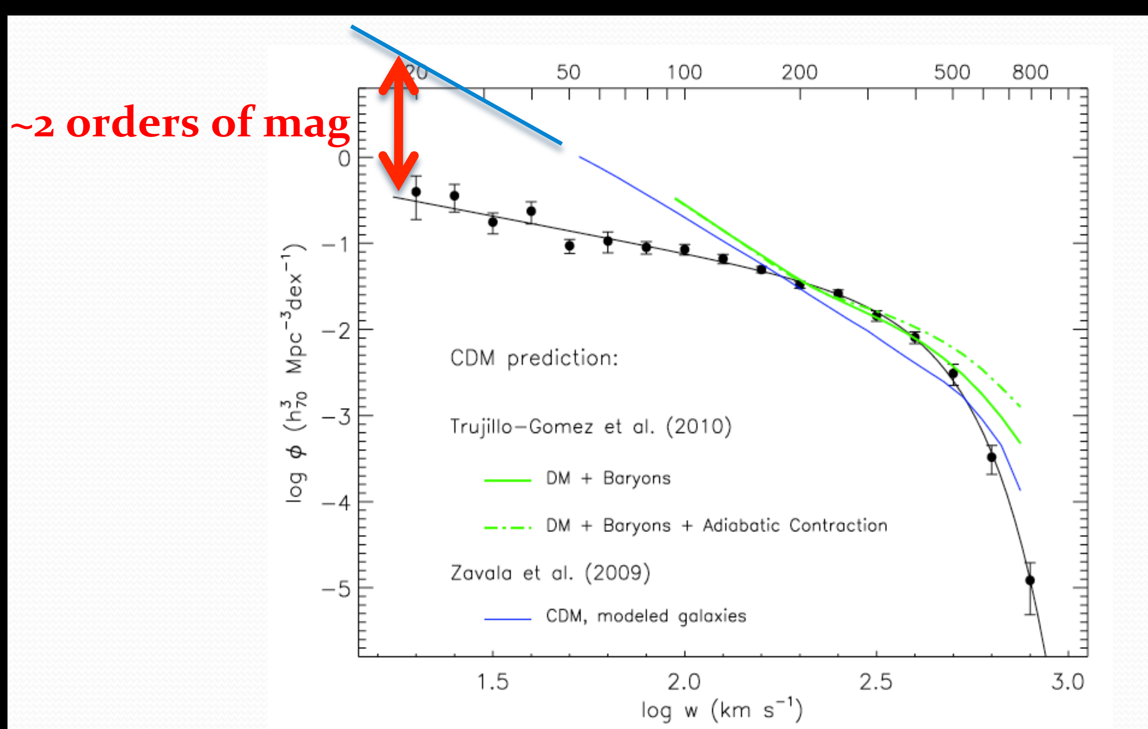

Papastergis+ (2011)

Papastergis et al. 2015

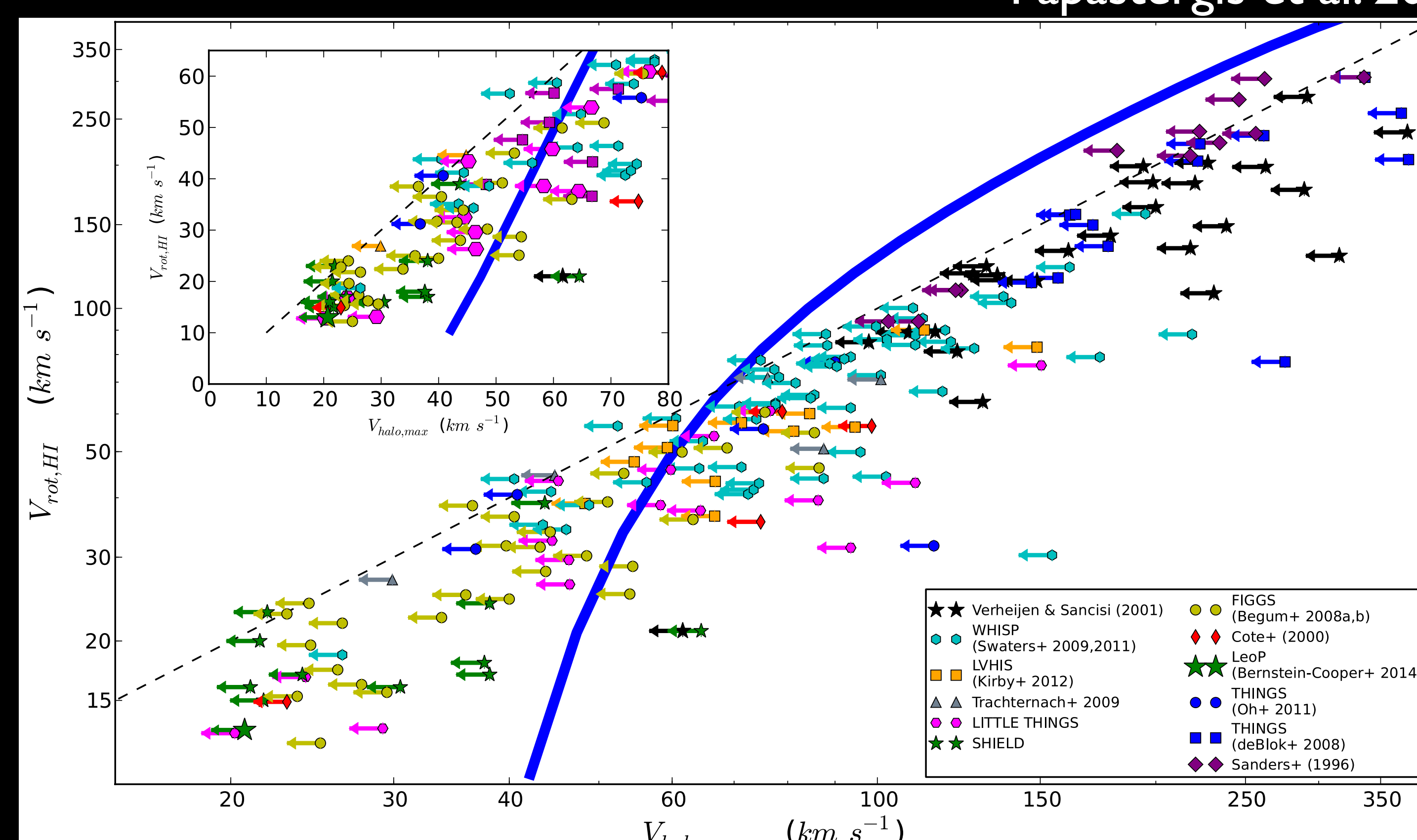

SOLUTIONS BASED ON ASSUMED DARK MATTER MODEL

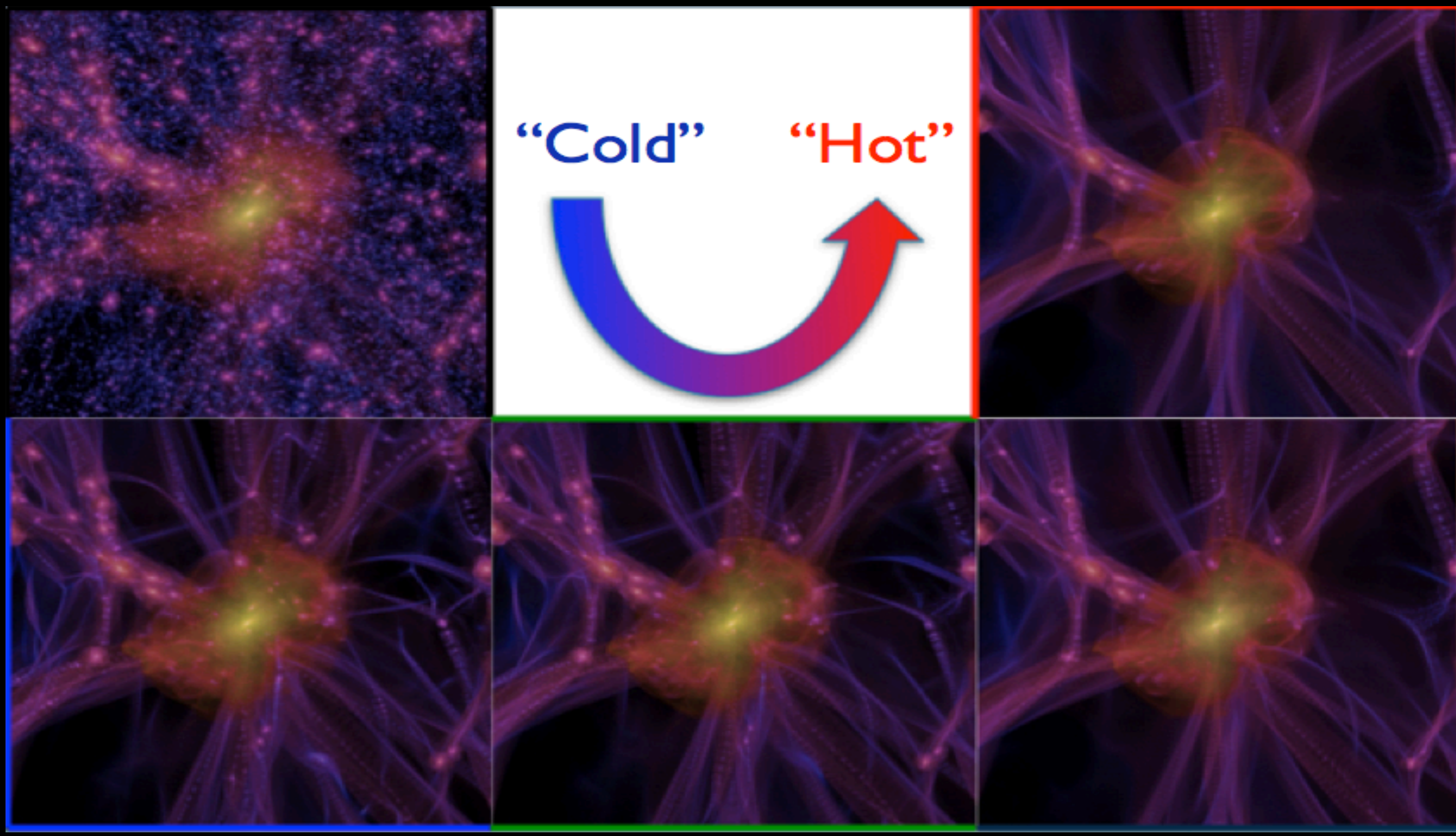

Implementing WDM power spectrum in the galaxy formation model

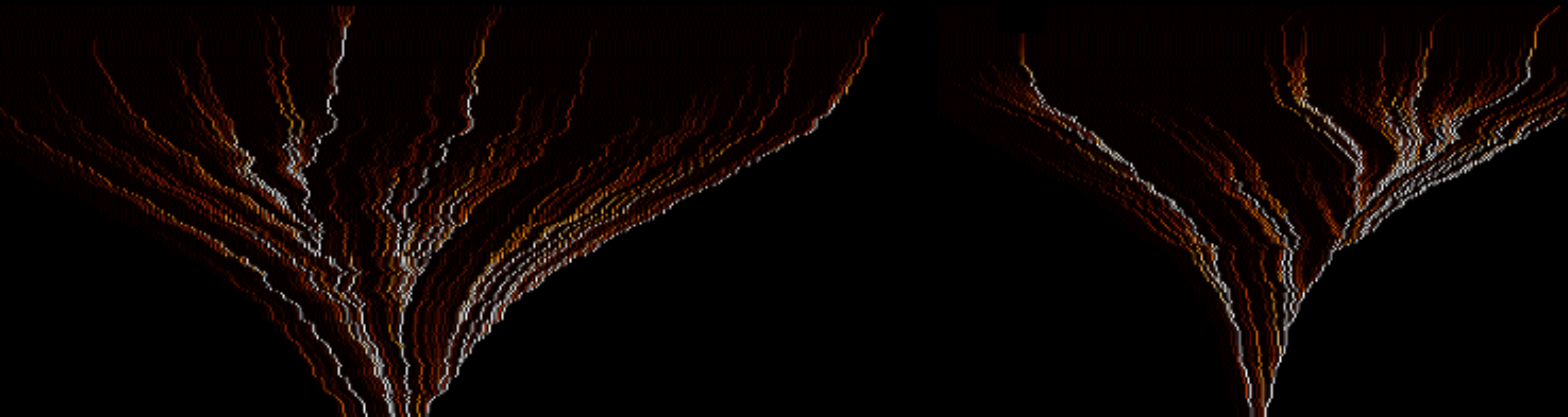

Halo Properties	Gas Properties	Star Formation	Gas Heating (feedback)	Evolution of stellar populations
Density Profiles Virial Temperature	Profiles Cooling - Heating Collapse Disk formation		SNae UV background	

WDM

Galaxy formation in WDM implies computing how modifications of the power spectrum propagate to the above processes

$$r_{fs} \approx 0.2 \left[\frac{\Omega_X\, h^2}{0.15}\right]^{1/3} \left[\frac{m_X}{rmkeV}\right]^{-4/3} \mathrm{Mpc} \qquad \frac{P_{WDM}(k)}{P_{CDM}(k)} = \left[1 + (\alpha\, k)^{2\,\mu}\right]^{-5\,\mu}$$

$$\alpha = 0.049 \left[\frac{\Omega_X}{0.25}\right]^{0.11} \left[\frac{m_X}{\mathrm{keV}}\right]^{-1.11} \left[\frac{h}{0.7}\right]^{1.22} h^{-1}\ \mathrm{Mpc}$$

From Thermal Relics to Sterile Neutrinos

The cutoff in the power spectrum is conventionally "labelled" according to the mass of "thermal relic" WDM particles

The same cutoff can be achieved through WDM sterile neutrinos assuming different production mechanisms

correspondence between thermal relic mass m_X and sterile neutrino mass m_ν (yielding the same power spectrum) depends on the assumed production mechanism
E.g. for the Shi-Fuller mechanism $m_\nu \approx 2.5\, m_X$

In the following we shall show the results in terms of the equivalent thermal relic mass

Suppression with respect to CDM

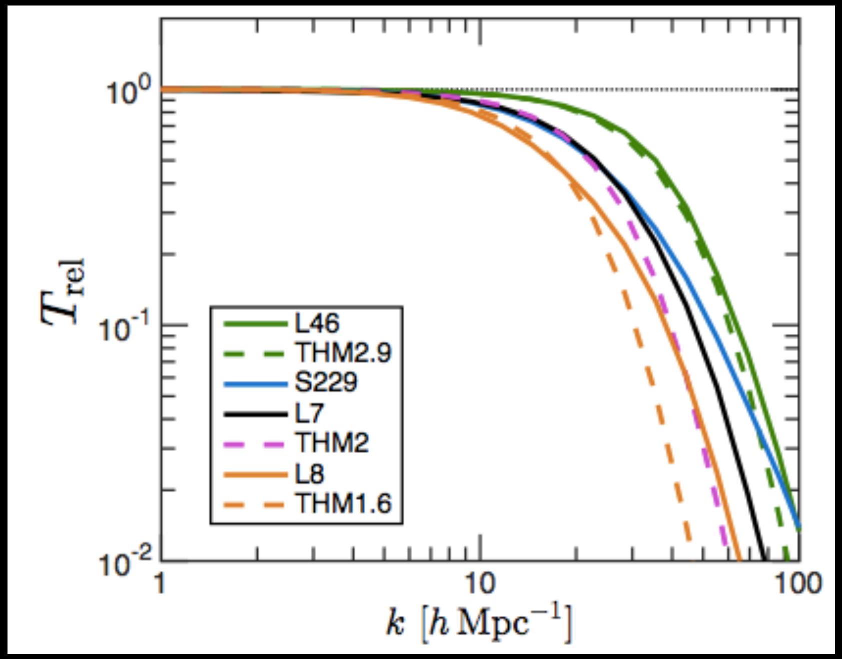

Bozek et al. 2015

Sterile Neutrinos

are produced in primordial plasma through

- off-resonance oscillations. Dodelson, Widrow; Abazajian, Fuller; Dolgov, Hansen;Asaka, Laine, Shaposhnikov et al.
- oscillations on resonance in presence of lepton asymmetry. Shi Fuller

- production mechanisms which do not involve oscillations
  - inflaton decays directly into sterile neutrinos Shaposhnikov, Tkachev
  - Higgs physics: both mass and production Petraki
  - decays of scalars in the early Universe Merle & Totzauer

From Thermal Relics to Sterile Neutrinos

Suppression with respect to CDM

The cutoff in the power spectrum is conventionally “labelled” according to the mass of “thermal relic” WDM particles

The same cutoff can be achieved through WDM sterile neutrinos assuming different production mechanisms

correspondence between thermal relic mass m_X and sterile neutrino mass m_ν (yielding the same power spectrum) depends on the assumed production mechanism
E.g. for the Shi-Fuller mechanism $m_\nu \approx 2.5\, m_X$

In the following we shall show the results in terms of the equivalent thermal relic mass

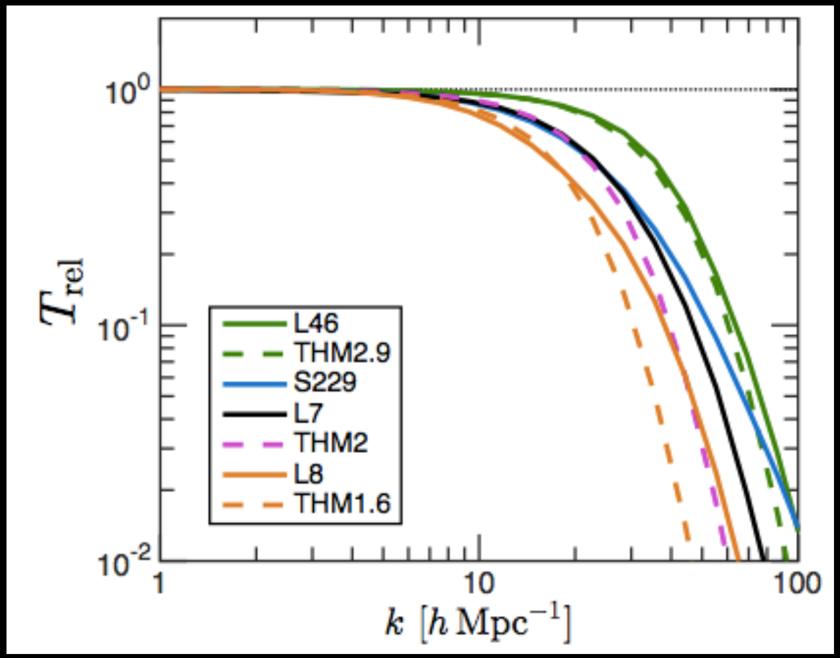

Bozek et al. 2015

Stacked XMM spectra (MOS and PN) of 73 bright galaxy clusters, blue-shifted to the same cluster rest frame

Searched for any unidentified emission lines in 2–10 keV band

Detected a very weak line at E = 3.55–3.57 keV rest-frame energy: IF due to WDM corresponds to the decay of

$m_\nu \approx 7$ keV $\rightarrow m_X \approx 2.5$ keV

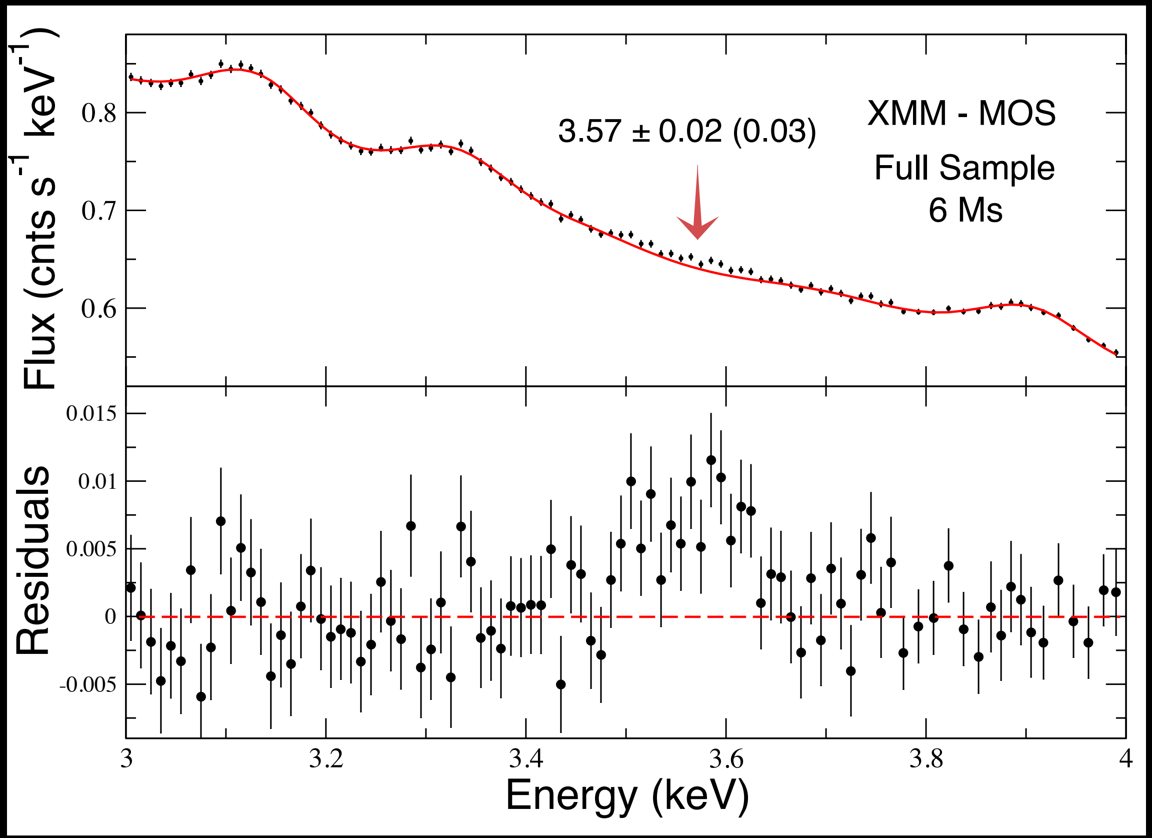

X-ray line reported in stacked observations of X-ray clusters with the XMM-Newton X-ray Space telescope with both CCD instruments aboard the telescope, and the Perseus cluster with the Chandra X-ray Space Telescope (Bulbul et al. 2014; independent indications of a consistent line in XMM-Newton observations of M31 and the Perseus Cluster is reported in Boyarsky et al. 2014)

WDM models with m_X=1-4 can provide a solution to

Density profiles & Rotation curves in WDM

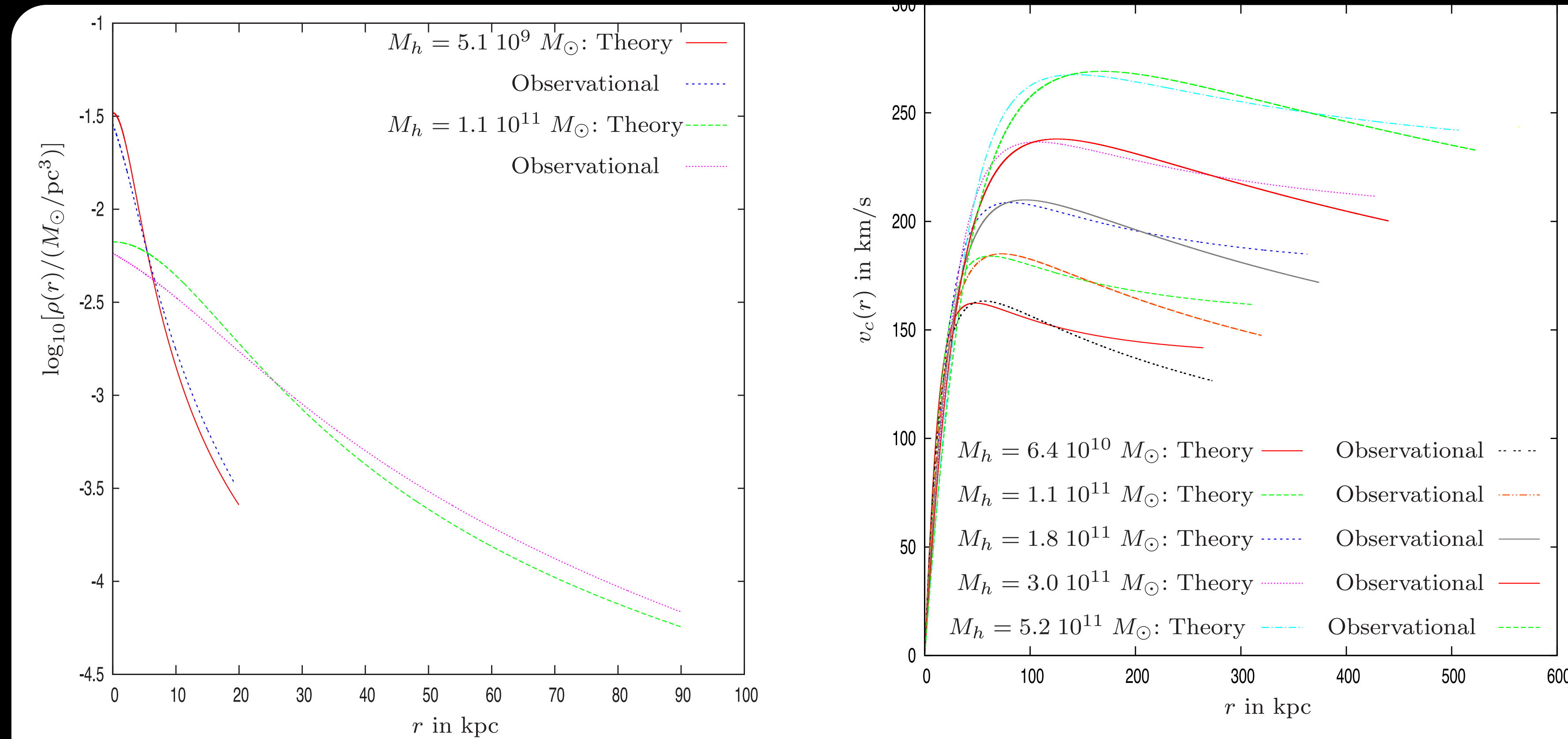

De Vega, Salucci, Sanchez 2014

Abundance of low-mass satellites

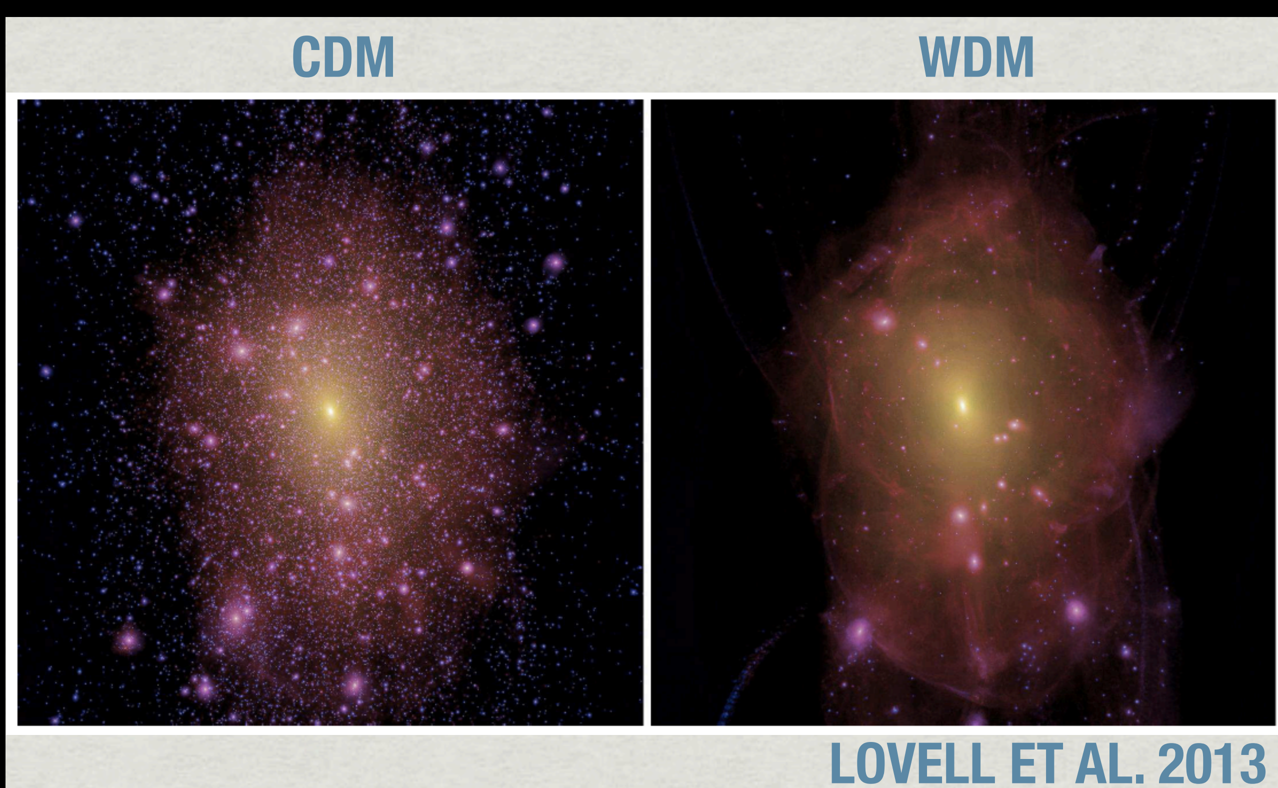

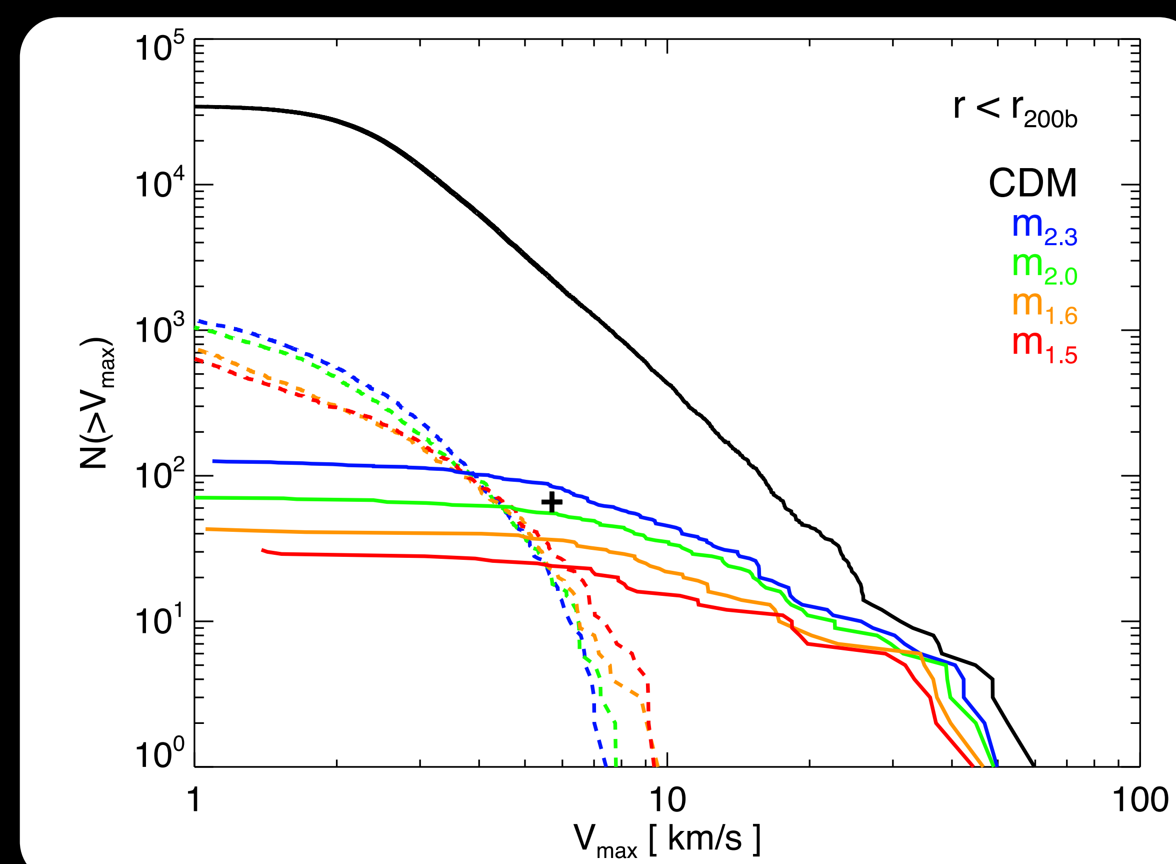

WDM models with m_X=1-4 constitutes a viable framework for galaxy formation

NM+2012

Are being investigated by several groups

Maccio et al. 2012, Benson et al. 2013,
Dayal, Mesinger, Pacucci 2014, Herpich et al.2014,
Governato et al. 2014, Kennedy et al. 2015
Bose et al. 2016, Chau, Mayer, Governato 2016

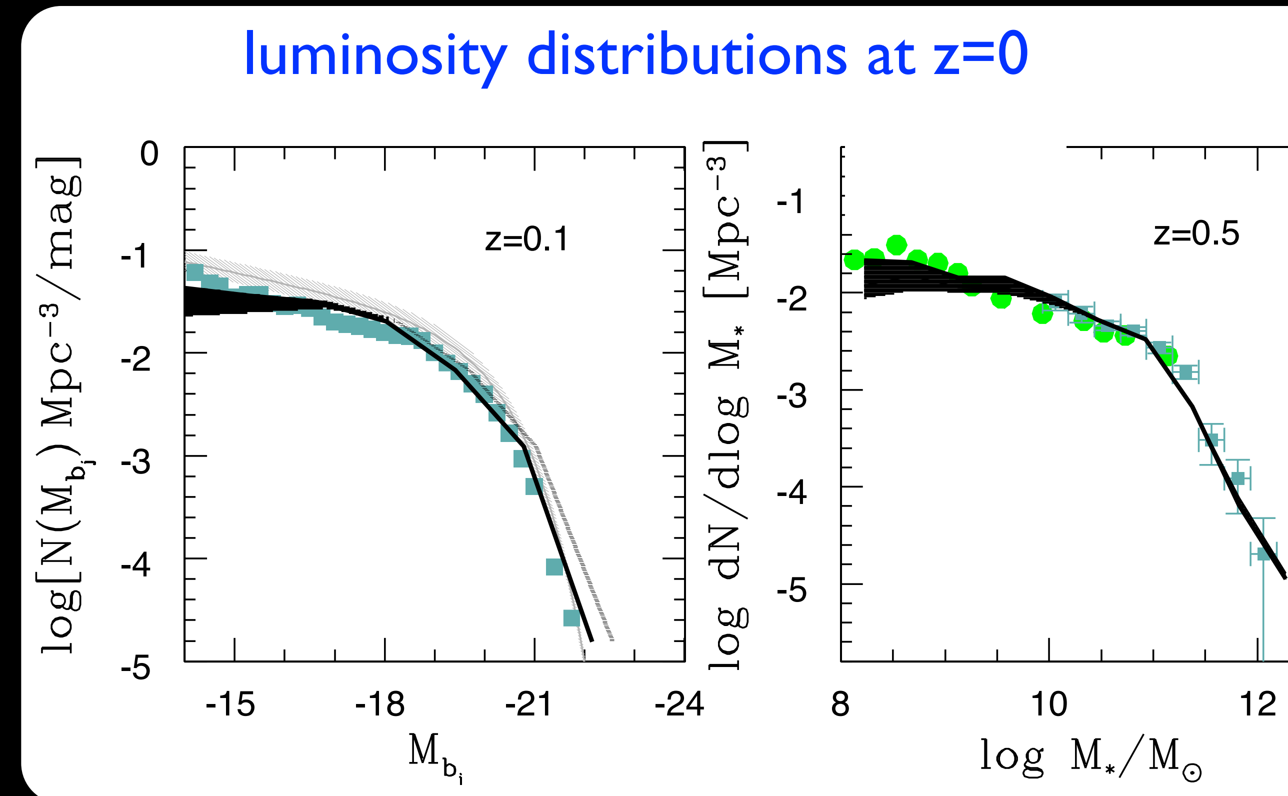

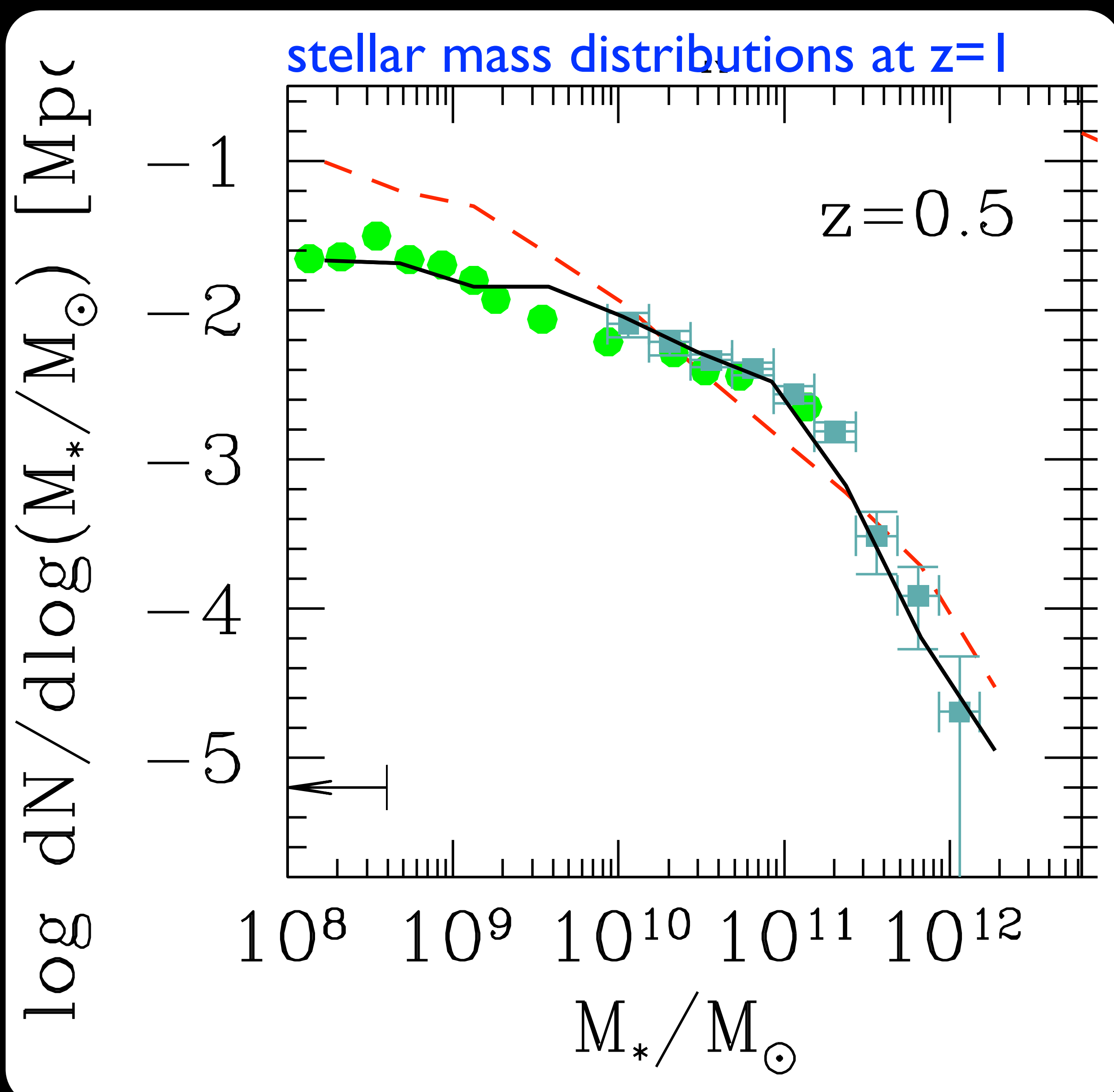

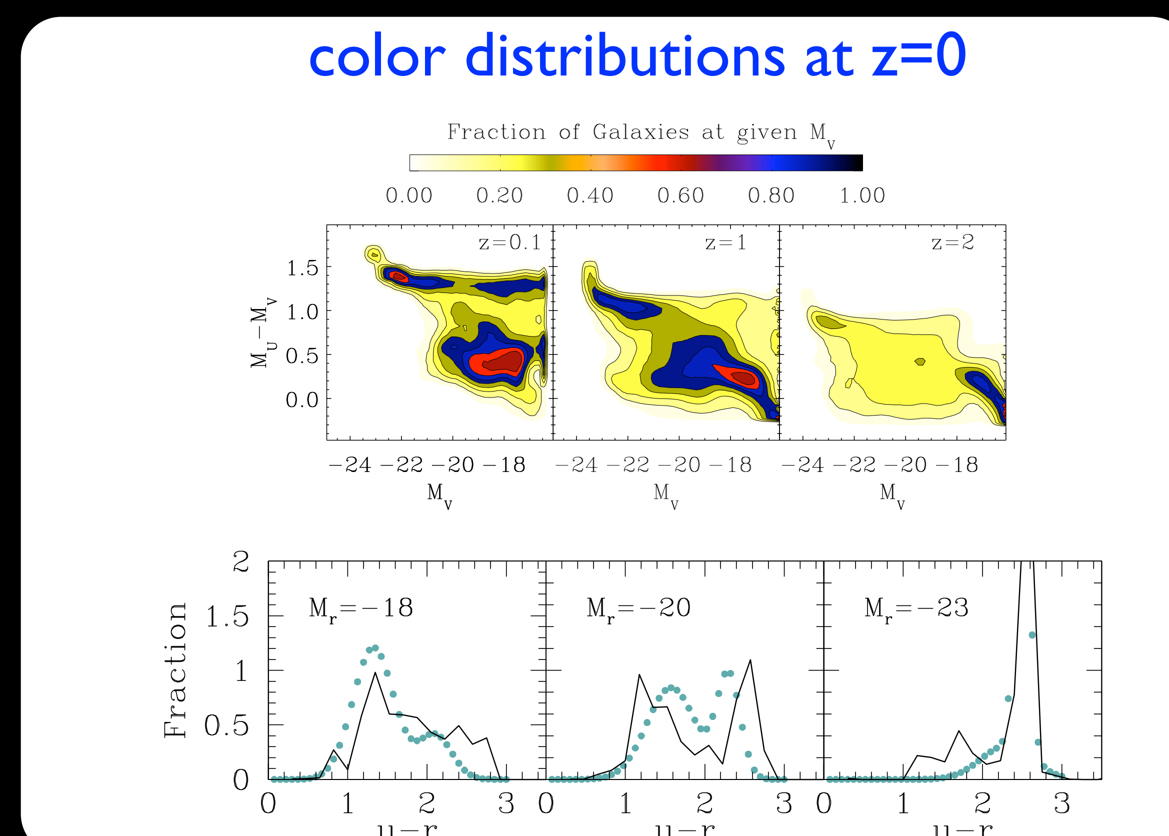

SOME PROPERTIES OF WDM GALAXY FORMATION

A Delayed Growth of Stellar Mass in WDM galaxy formation

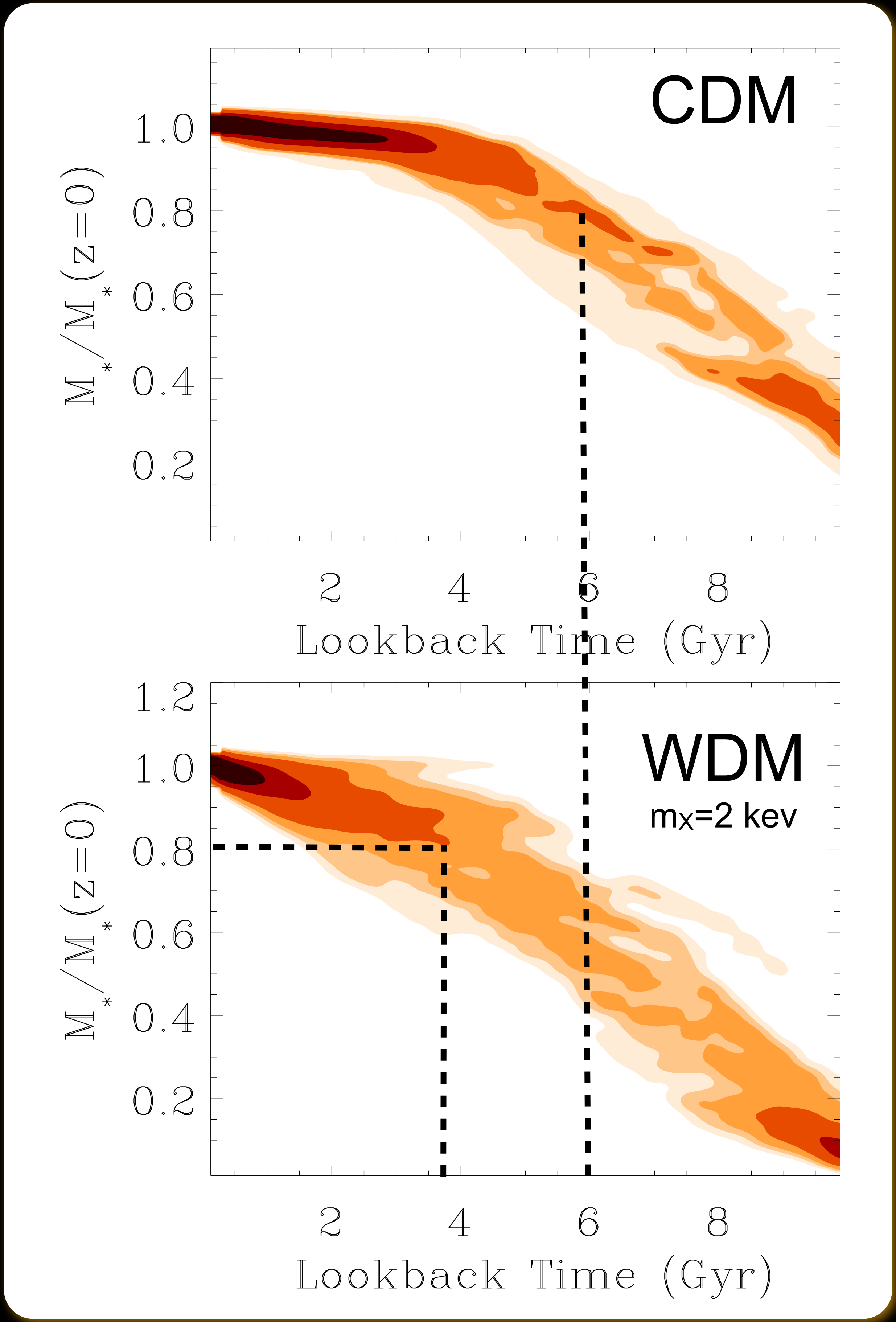

The suppression of progenitors
of satellite galaxies with high SFR yields
Slower growth of stellar mass in WDM

CDM: 80 % of mass formed 6 Gyr ago
WDM: 80 % of mass formed 4 Gyr ago

Approx. delay ~ 2 Gyr

Independent works based on hydro-Nbody
simulations confirm such a result
(Governato et al. 2014)

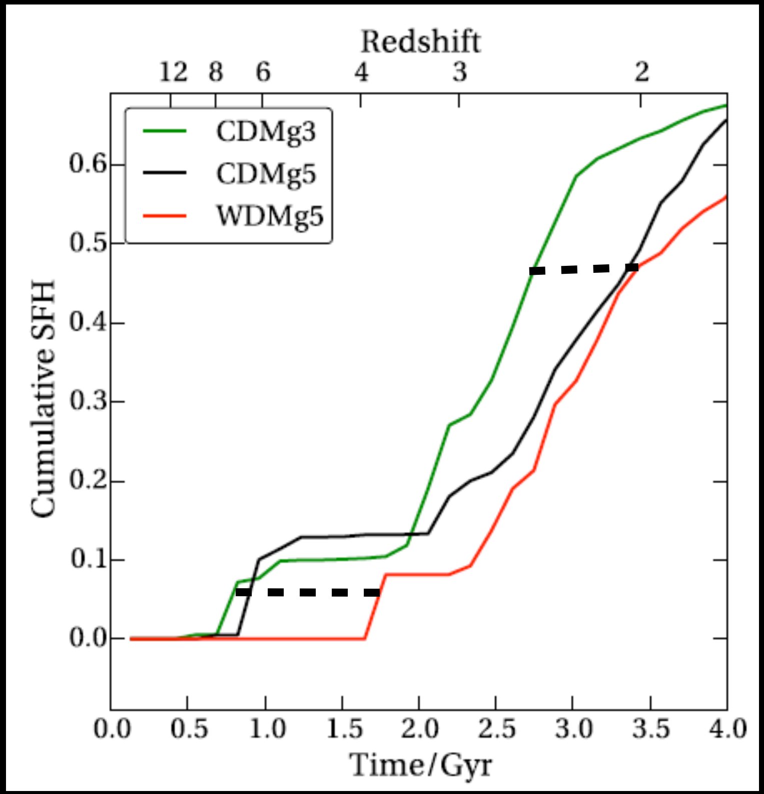

N-body simulations

Star formation from cooled gas in simulations if

- it is bound, and has a central gravitational potential minimum
- is Jeans unstable
- is converging

Semi-analytic Models

Star formation from cooled gas

$$m_* = \frac{m_{gas}}{\tau_*} \qquad \tau_* \propto \tau_{dyn}$$

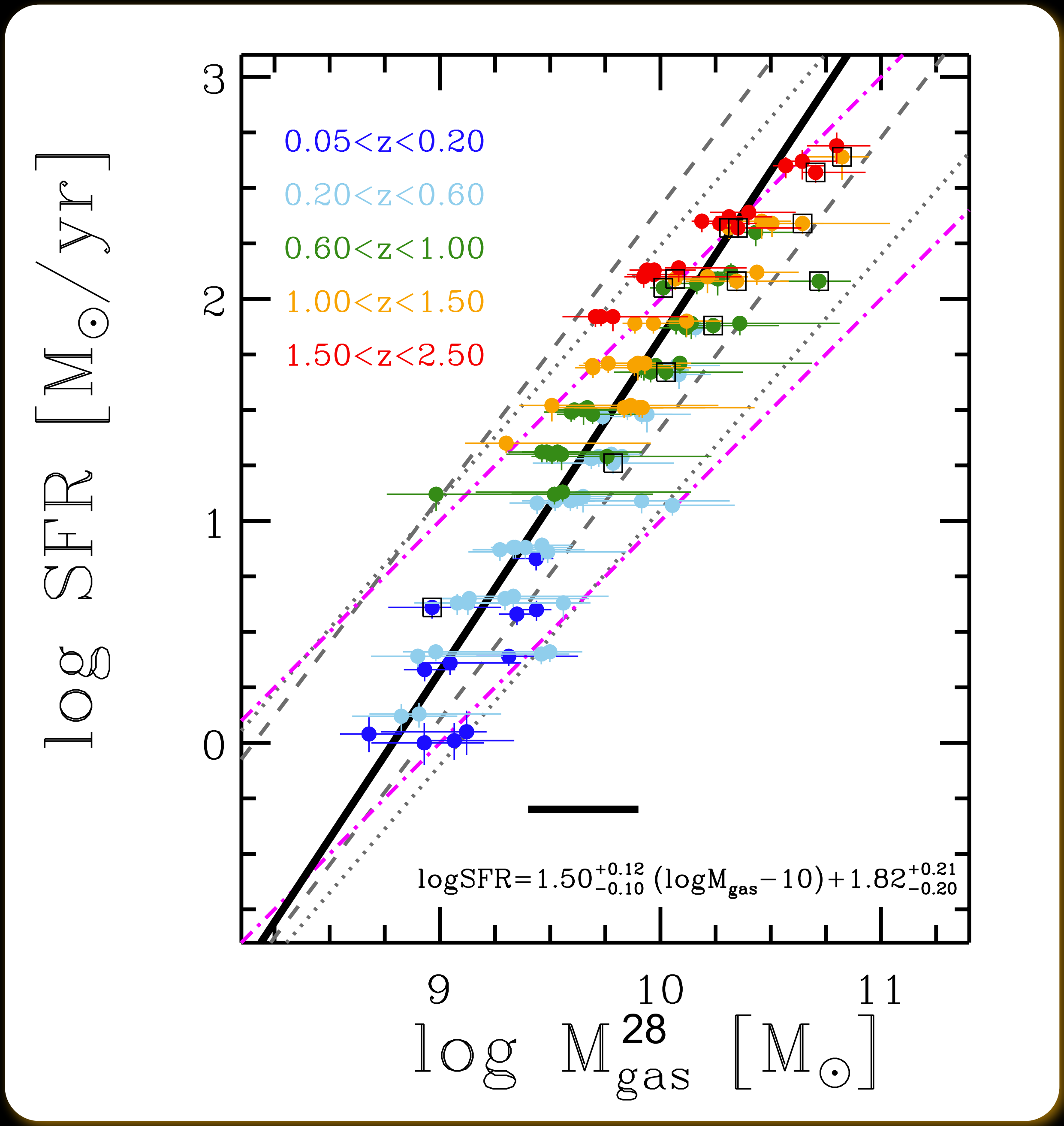

THE FRACTION OF QUIESCENT SATELLITE GALAXIES

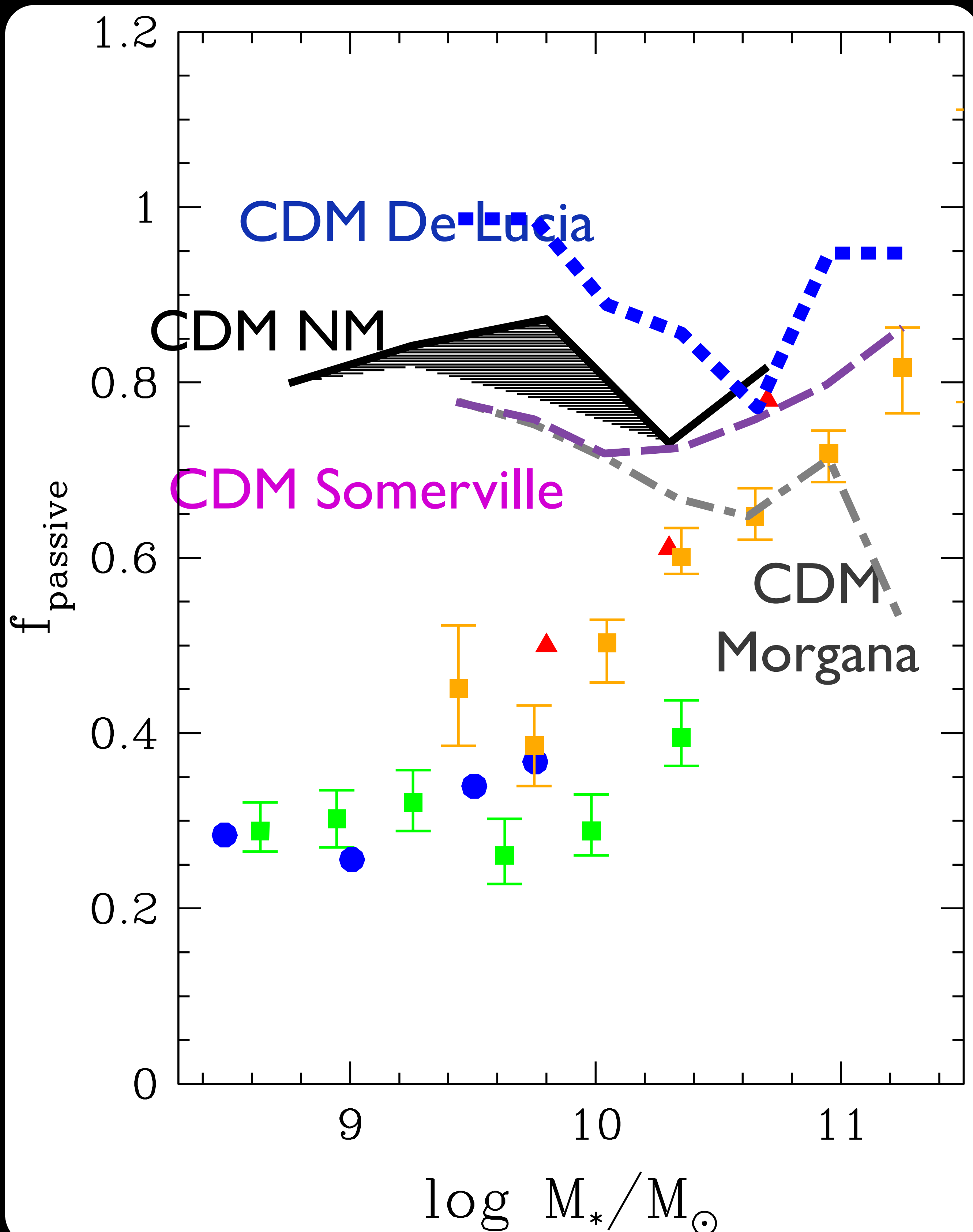

Specific Star Formation Rate SSFR measures the current star formation activity with respect to the past

$$SSFR = \dot{M}_*/M*$$

Quiescent Fraction SSFR<10^{-11} yrs
corresponds to minimum in the SSFR distribution (to form M_* it would need $3t_H$ at current SF rate)

Result robust with respect to different CDM models with different feedback modelling

Due to the large number of dense DM clumps collapsed at high redshifts gas rapidly converted into stars at high-redshifts

- Cold gas converted into stars at high z
- Hot gas stripped when they were incorporated into larger DM haloes

No further star formation at low redhsift

NM 2014;
Data from Wetzel et al. 2013, Kimm et al. 2014, Phillips 2014, Geha 2012

THE FRACTION OF QUIESCENT SATELLITE GALAXIES

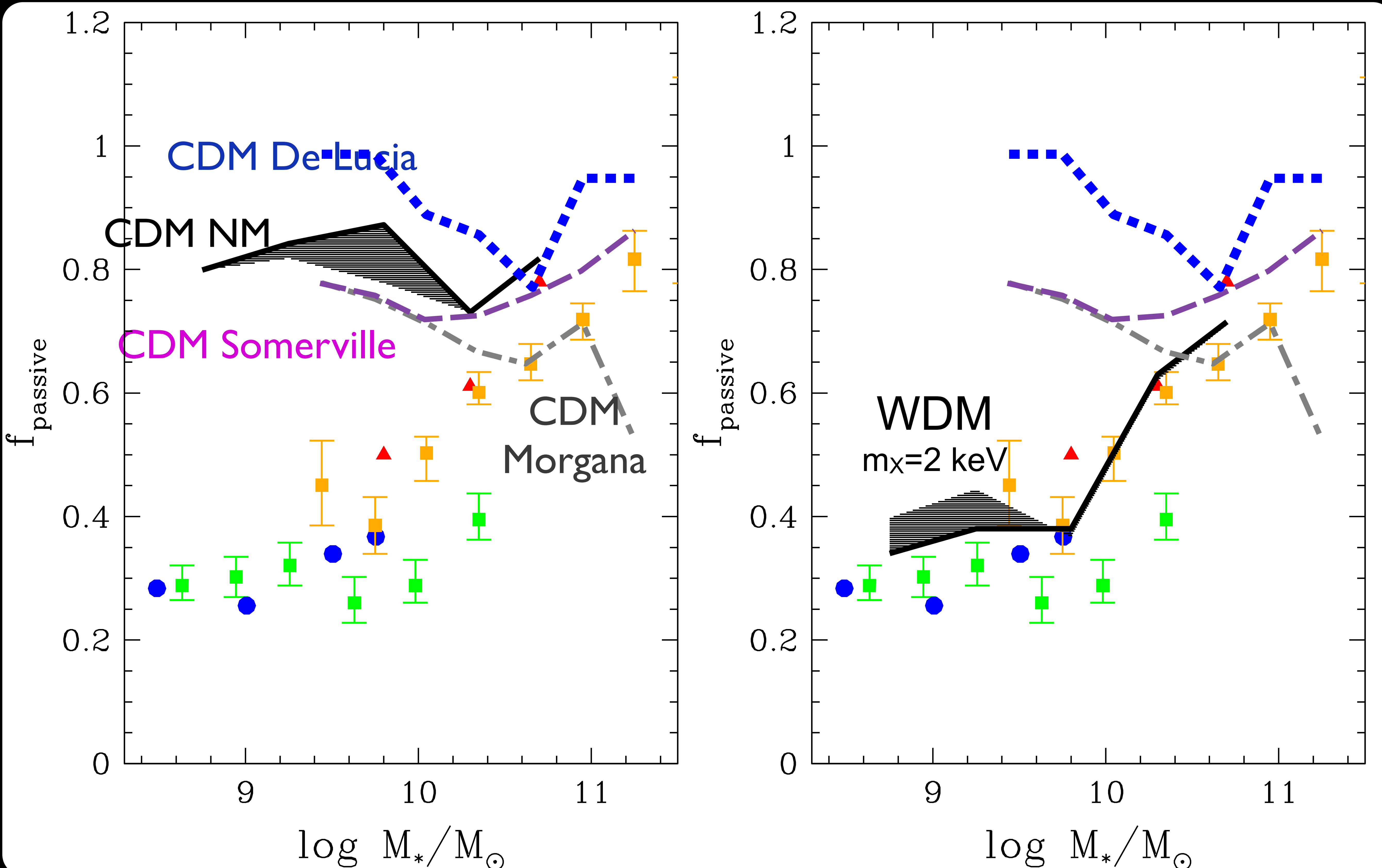

Problems with Solutions based on Feedback

II: The L/M ratio of low-mass galaxies

Enhancing the feedback results into inefficient star formation for given DM halo (suppress L/M).

This seems at variance with observed M_{star}-M relation

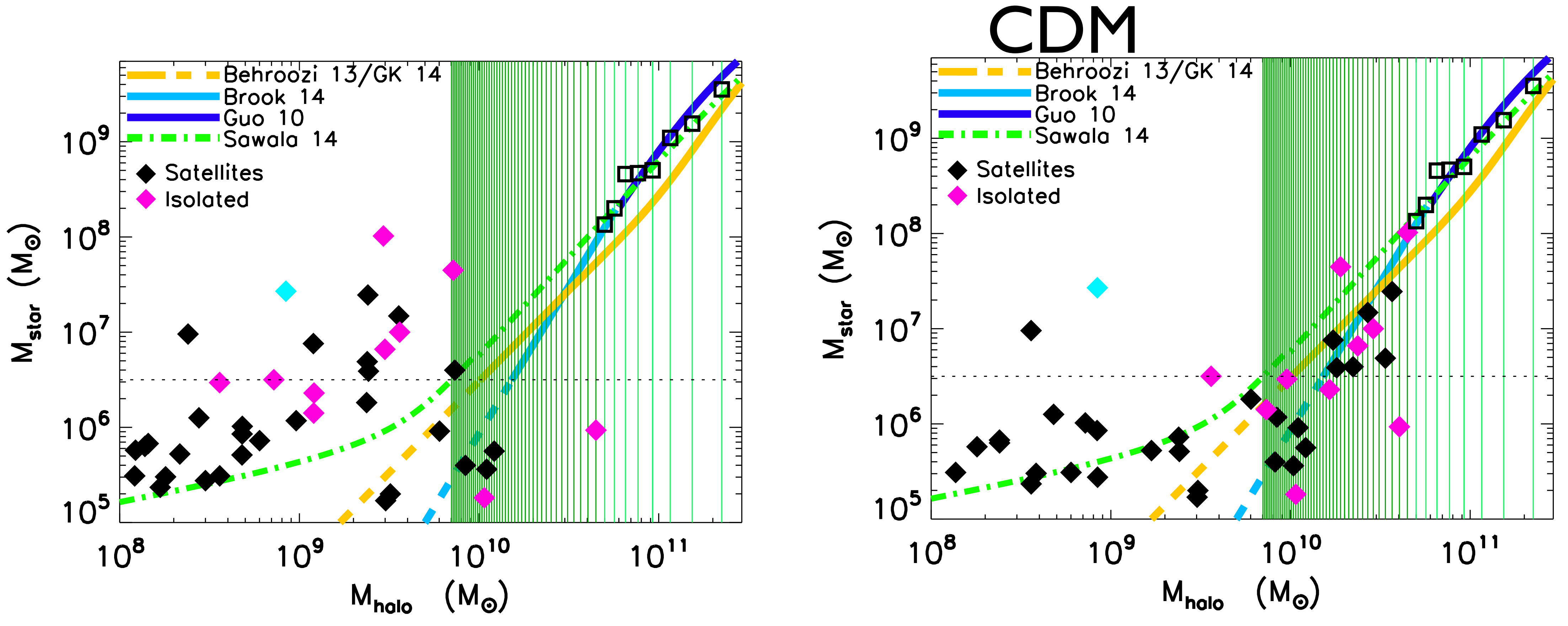

Figure 2. The relation between observed stellar mass and derived halo mass for LG galaxies. The halo mass has been found by fitting kinematical data and assuming two different halo profiles. The results for an NFW profile are shown in the left-hand panel, while the mass-dependent DC14 halo profile has been used in the right-hand panel. Satellites and isolated galaxies are shown in different colours, with Sagittarius dwarf irregular, highly affected by tides, shown in cyan. Several abundance matching predictions are indicated, in particular the Brook et al. (2014) one has been constrained using the LG mass function, and it is shown as dashed line below the observational completeness limit of the LG.

Problems with Solutions based on Feedback

II: The L/M ratio of low-mass galaxies

Enhancing the feedback results into inefficient star formation for given DM halo (suppress L/M).

In WDM the flatter shape of the LF allows for larger L/M ratios

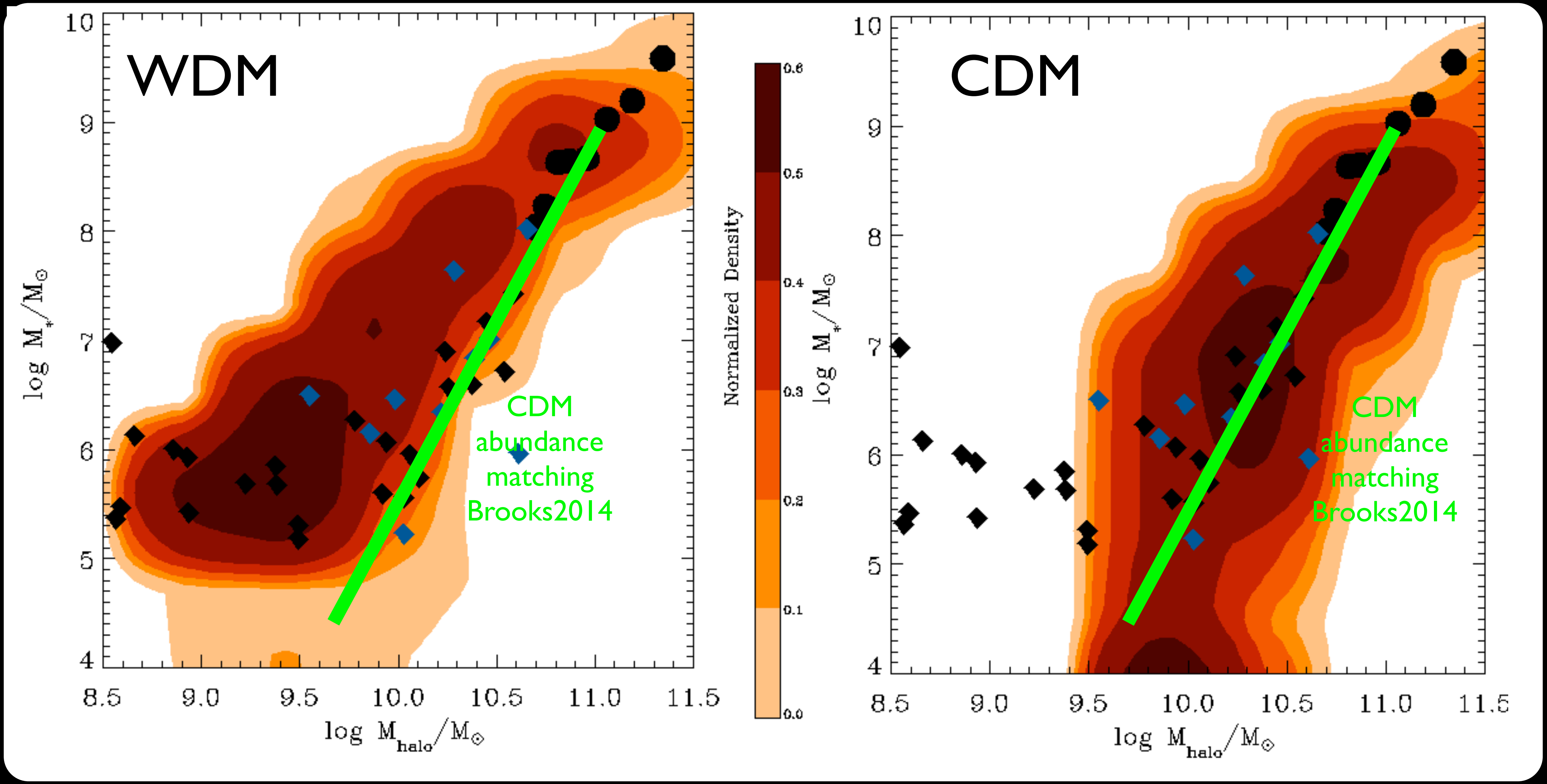

The Age of stellar populations in low-mass galaxies

CDM predicts early collapse of a huge number of low-mass halos, which remain isolated at later times retaining the early-formed stellar populations; as a result, CDM-based SAMs generally provide flat age-mass relations (Fontanot et al. 2009; Pasquali et al. 2010; De Lucia & Borgani 2012).

Increasing the stellar feedback worsen the problem

Early SF: WDM induces delay in star formation, affects small-mass objects(see, e.g., Angulo et al. 2013)

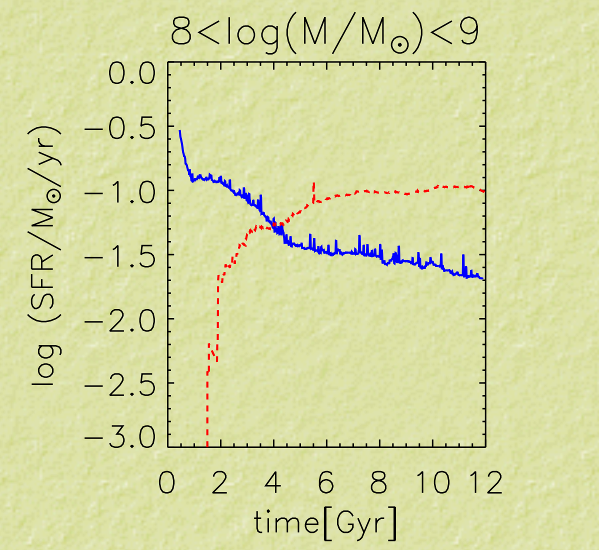

$$Age(t_0) = \frac{\int_0^{t_0} (t_0 - t)\, \psi(t)\, dt}{\int_0^{t_0} \psi(t)\, dt}$$

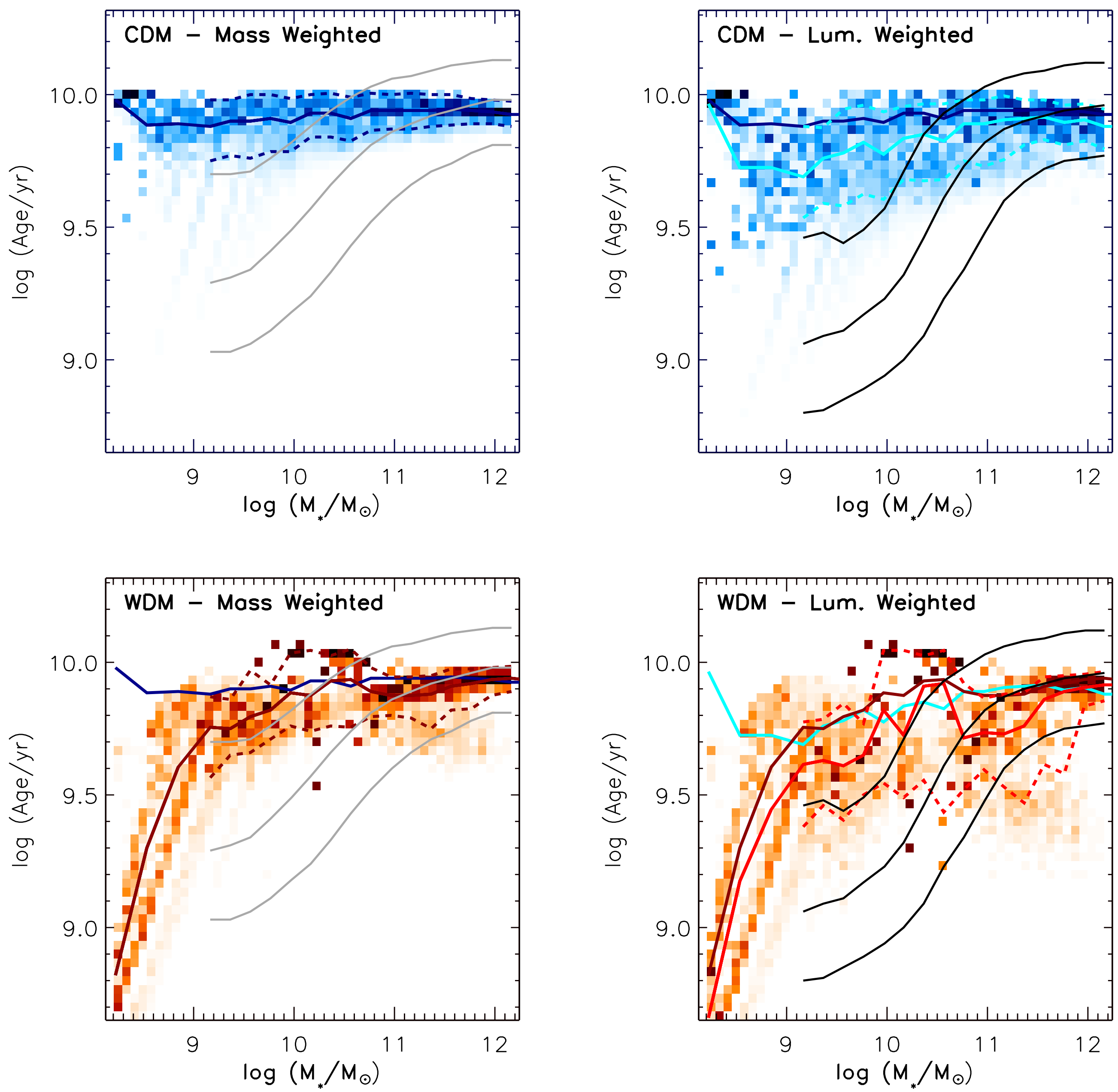

Calura, NM, Gallazzi 2014

The upper, the middle and the lower grey (black) curves represent the 16th, the 50th (median) and the 84th percentiles of the observed distribution in mass-(light-)weighted stellar age (Gallazzi et al. 2008)

CONSTRAINING THE WDM PARTICLE MASS

In terms of thermal relic mass m_X
(conversion to sterile neutrino masses depends on production mechanism)

E.g.
Dodelson-Widrow mechanism $m_\nu \approx 2.9\ m_X$
Shi-Fuller mechanism $m_\nu \approx 2.5\ m_X$

$m_X > 4$ keV is indistinguishable from CDM from the point of view of galaxy formation

WDM particle mass: limits from the Ly-α forest vs. Hydro-Simulations

Viel et al. 2005-2013

m_{WDM}>3.3 keV	Thermal relics WDM
m_{ν}>12 keV	Sterile ν WDM (DW) **Dodelson-Widrow**

Results subject to further investigations

Still affected by the difficult-to-characterize physics of intergalactic gas. Degeneracy between WDM effects and Jeans and Doppler broadening of the absorption lines. These are affected by the IGM temperature

WDM particles are 10^{68} times heavier (10^5 $M_\odot$) than the real WDM particles. This makes difficult to infer the initial velocity distribution of the effective particles from the known initial velocity distribution of the real WDM particles (Lovell et al. 2012, 2014; Maccio` et al. 2012; Viel et al. 2013).

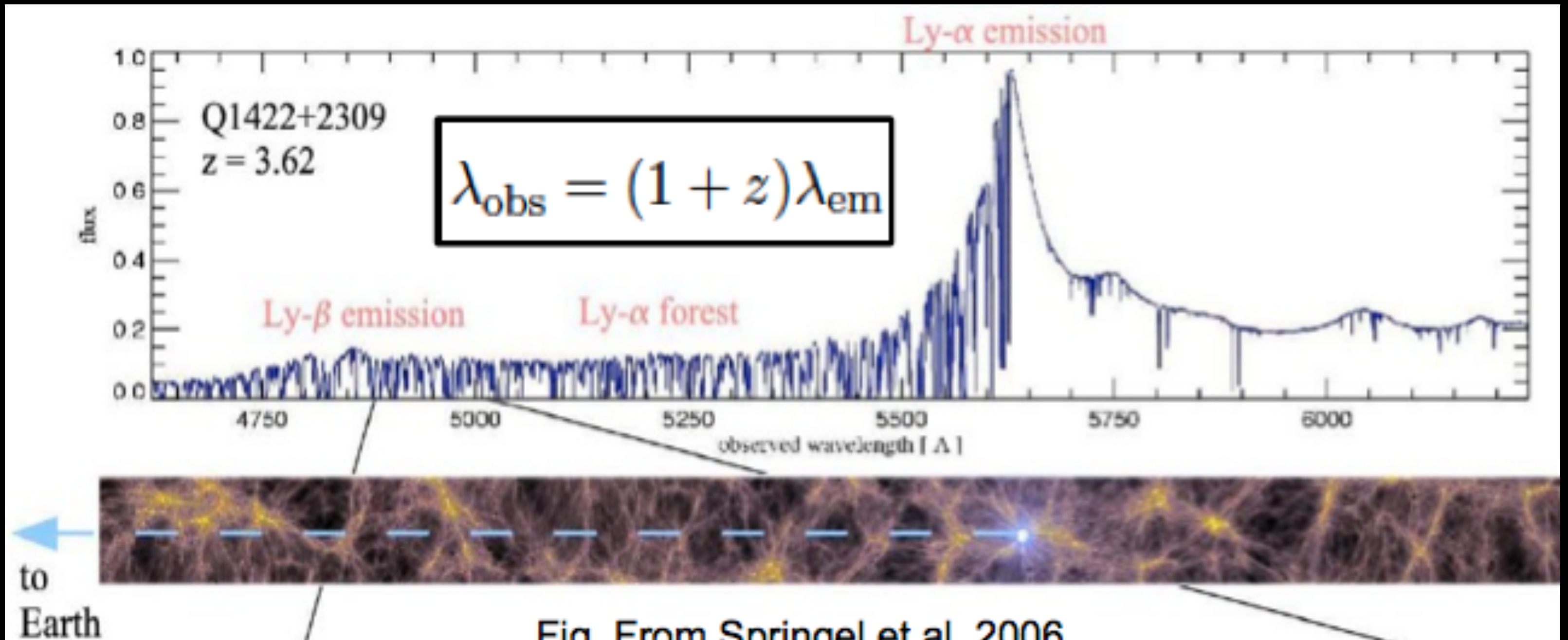

Fig. From Springel et al. 2006

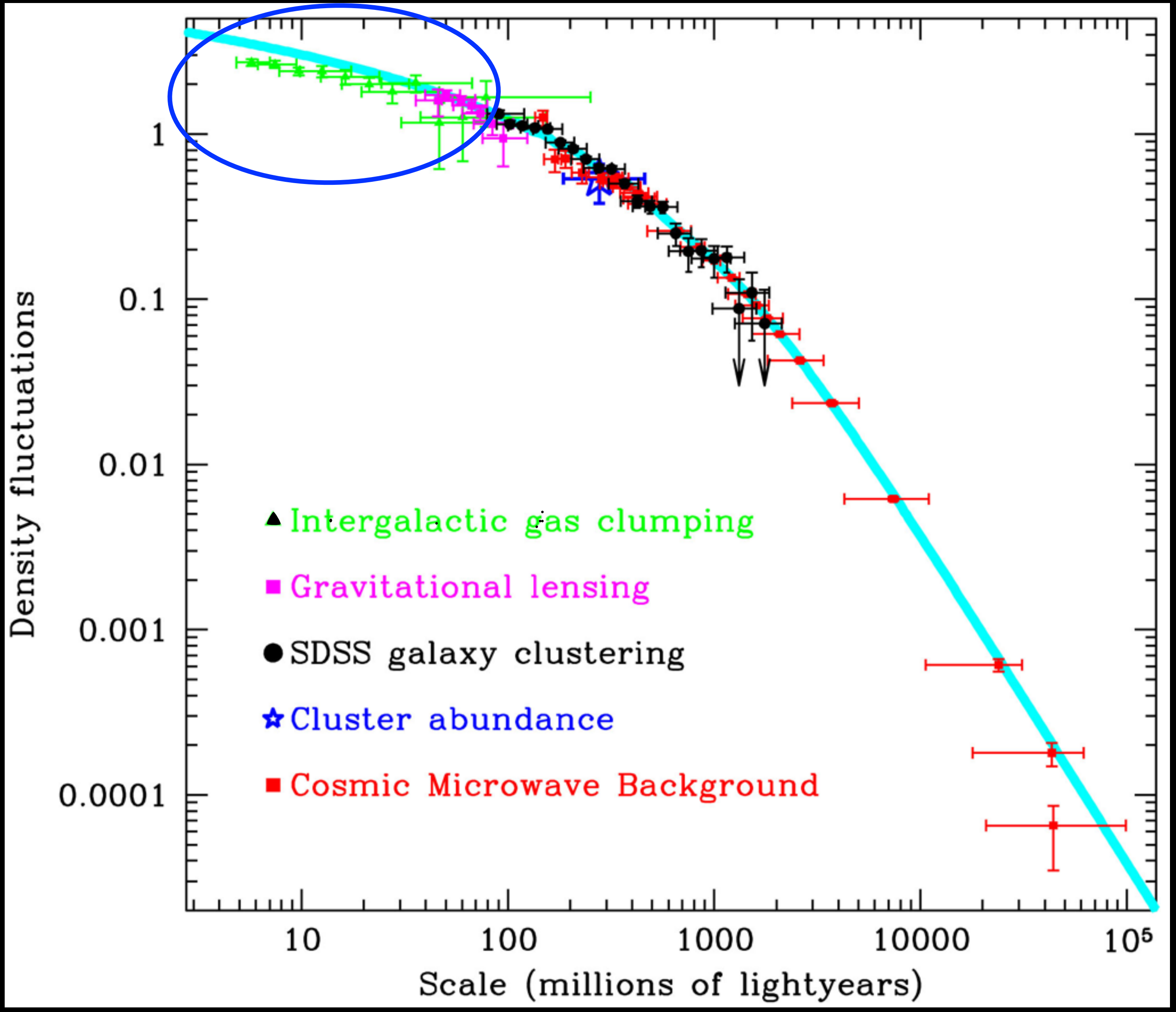

Constraining the WDM candidate mass through the abundance of low-mass galaxies

Structure formation in WDM models suppressed on small mass scales.

Small mass galaxies are the first to form.

The most powerful for probe for these scenarios is the abundance of high-redshift galaxies

Constraining the WDM candidate mass through the abundance of low-mass galaxies

Schultz et al. 2014

Compare predicted abundance of low-mass DM halos at z>6 with observed abundance of faint galaxies in the HUDF

Delicate issue: relate UV luminsity of observed galaxies to the mass of the host DM halo

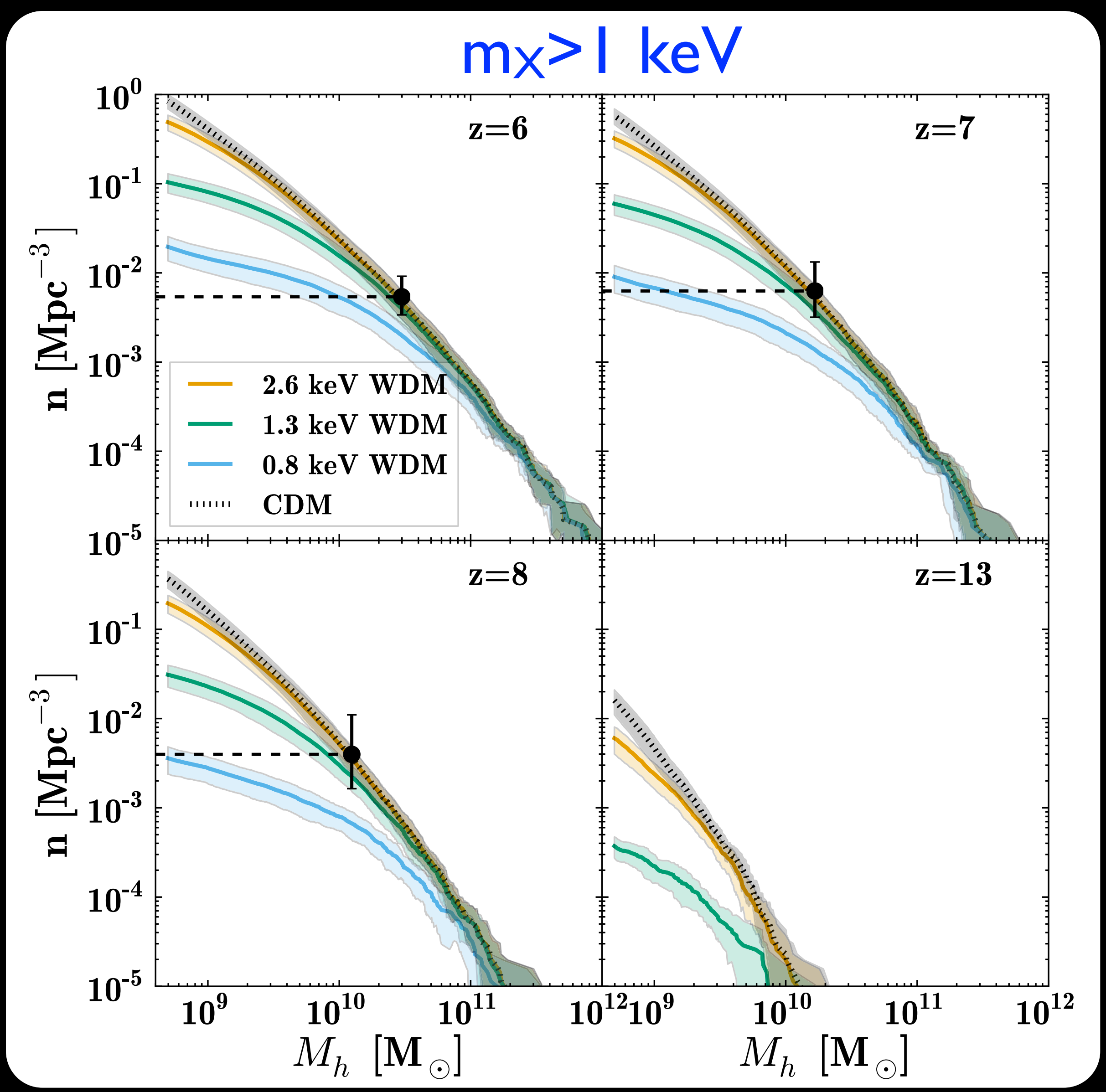

Magnitude limit mag=30

at z=6 this corresponds to M_{UV}=-18

Constraints on m_X from the abundance of low-mass galaxies: getting rid of degeneracy with astrophysics of gas and stars

At masses close to the Half-Mode mass WDM mass functions exhibit a down turn.
Observed galaxy densities larger than the maximum predicted abundance of a given WDM model would rule out the corresponding WDM particle mass independently of L/M relation

m_X>1 keV

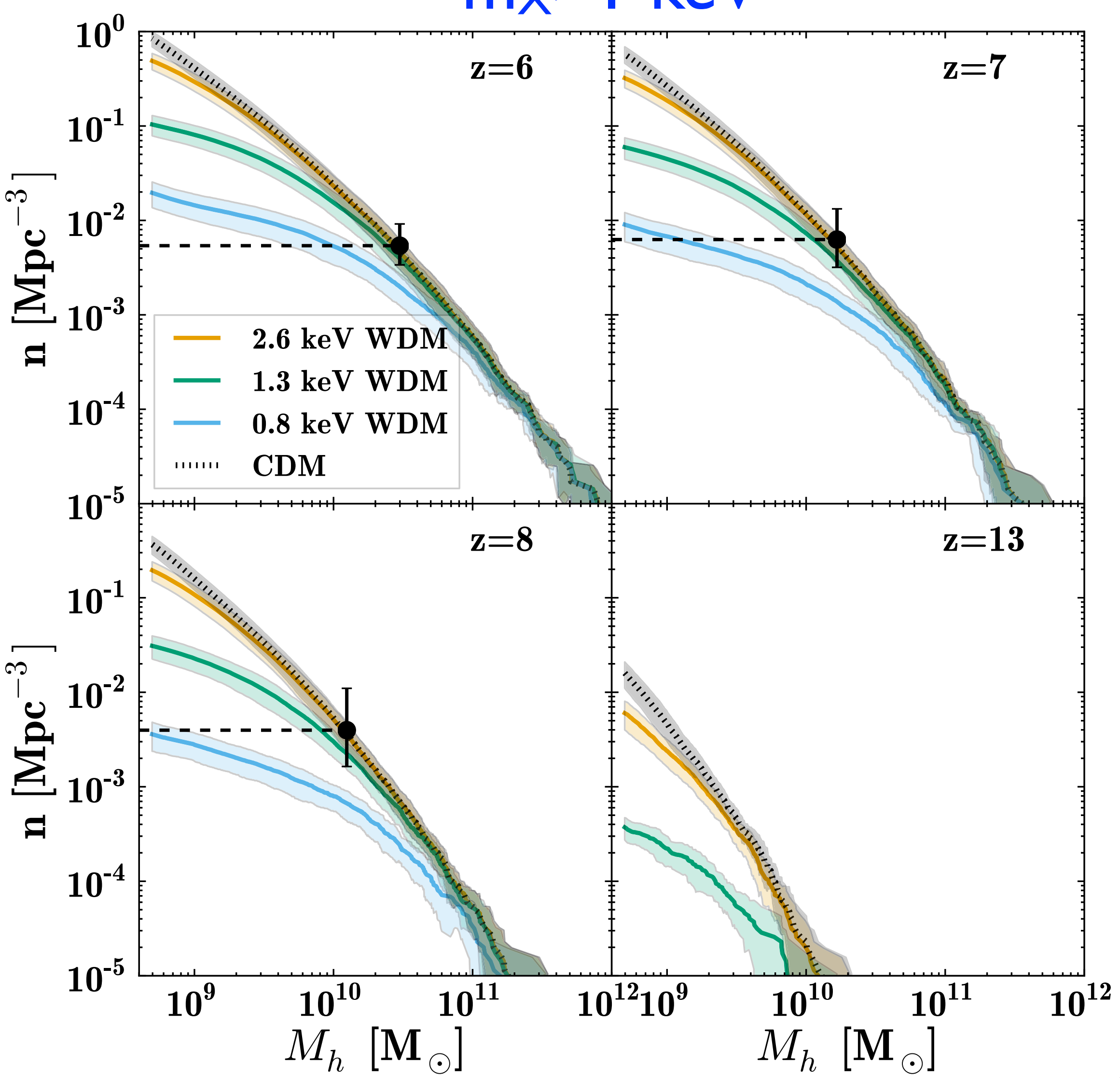

Probing the Half-mode mass of ~ 2 keV WDM models requires reaching $M_{UV} \approx -13$

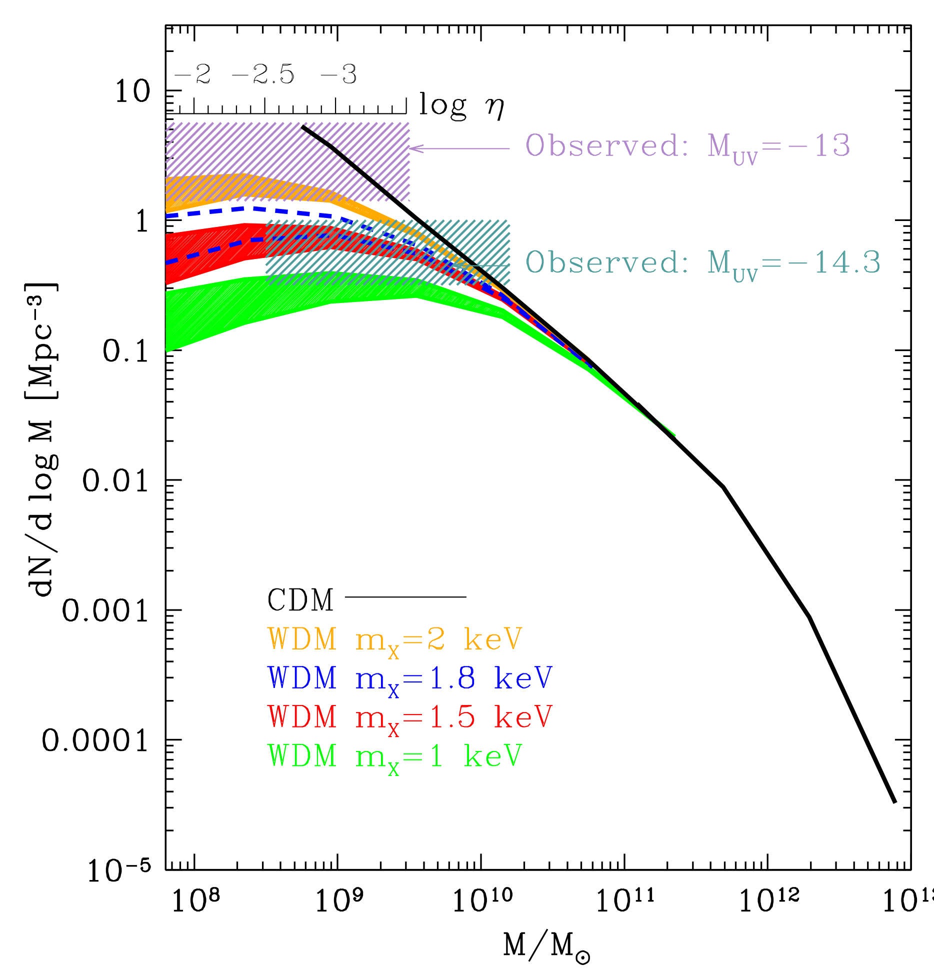

Constraints on m_X from the abundance of low-mass galaxies: getting rid of degeneracy with astrophysics of gas and stars

At masses close to the Half-Mode mass WDM mass functions exhibit a down turn.
Observed galaxy densities larger than the maximum predicted abundance of a given WDM model would rule out the corresponding WDM particle mass <u>independently of L/M relation</u>

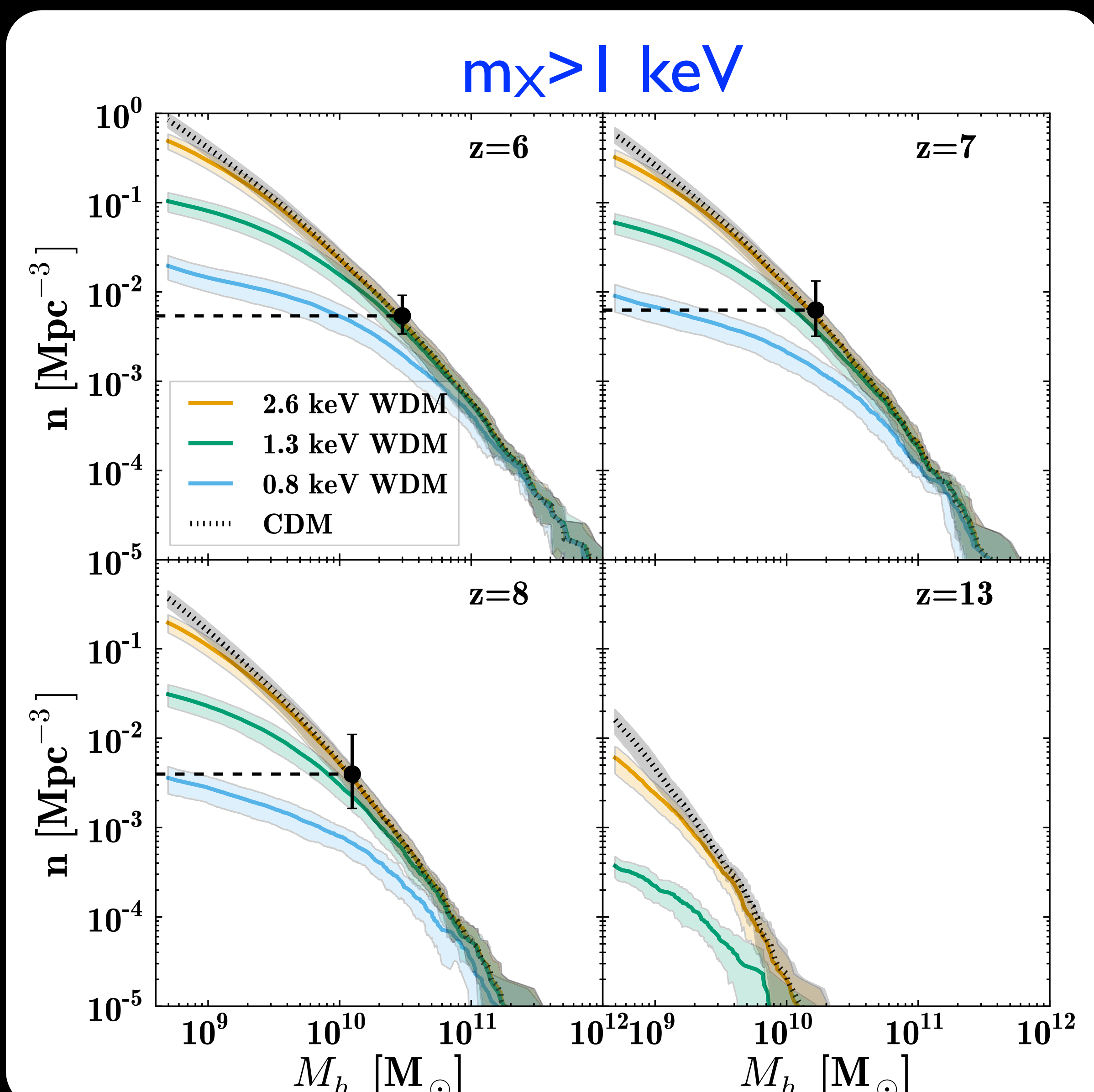

Probing the Half-mode mass of ~ 2 keV WDM models requires reaching $M_{UV} \approx -13$ much, much deeper than present limit of HST

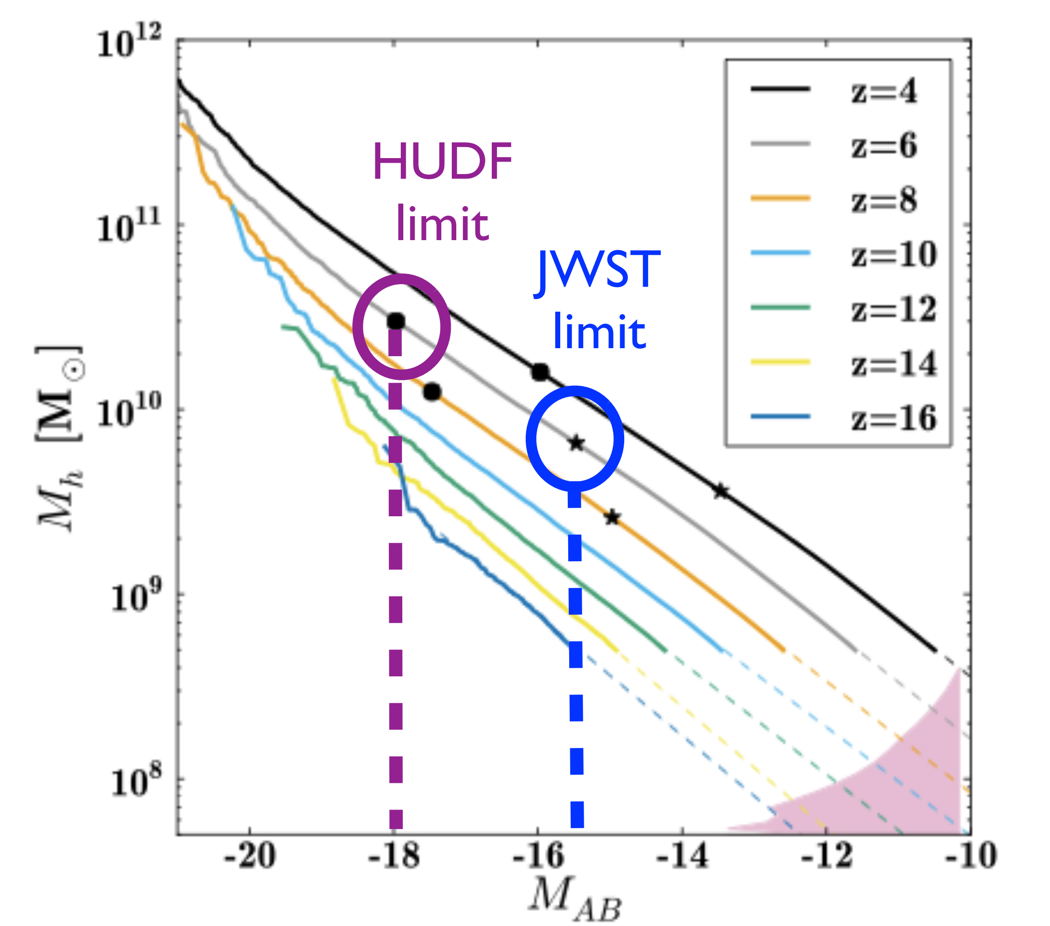

Hubble Frontier Field

The Frontier Fields Goals

Using Director's Discretionary (DD) observing time, HST is undertaking a revolutionary deep field observing program to peer deeper into the Universe than ever before and provide a first glimpse of JWST's universe.

These Frontier Fields will combine the power of HST with the natural gravitational telescopes of high-magnification clusters of galaxies. Using both the Wide Field Camera 3 and Advanced Camera for Surveys in parallel, HST will produce the deepest observations of clusters and their lensed galaxies ever obtained, and the second-deepest observations of blank fields (located near the clusters). These images will reveal distant galaxy populations ~10-100 times fainter than any previously observed, improve our statistical understanding of galaxies during the epoch of reionization, and provide unprecedented measurements of the dark matter within massive clusters.

This program is based upon the 2012 recommendations from the Hubble Deep Fields Initiative Science Working group: SWG Report 2012

Six Frontier Fields

Cluster Name	z	Cluster		Parallel Field	
		RA	Dec	RA	Dec
Year 1:					
Abell 2744	0.308	00:14:21.2	-30:23:50.1	00:13:53.6	-30:22:54.3
MACSJ0416.1-2403	0.396	04:16:08.9	-24:04:28.7	04:16:33.1	-24:06:48.7
Year 2:					
MACSJ0717.5+3745	0.545	07:17:34.0	+37:44:49.0	07:17:17.0	+37:49:47.3
MACSJ1149.5+2223	0.543	11:49:36.3	+22:23:58.1	11:49:40.5	+22:18:02.3
Year 3:					
Abell S1063 (RXCJ2248.7-4431)	0.348	22:48:44.4	-44:31:48.5	22:49:17.7	-44:32:43.8
Abell 370	0.375	02:39:52.9	-01:34:36.5	02:40:13.4	-01:37:32.8

Abell 2744 Cluster

Clusters as lensing telescopes

slide by Jennifer Lotz

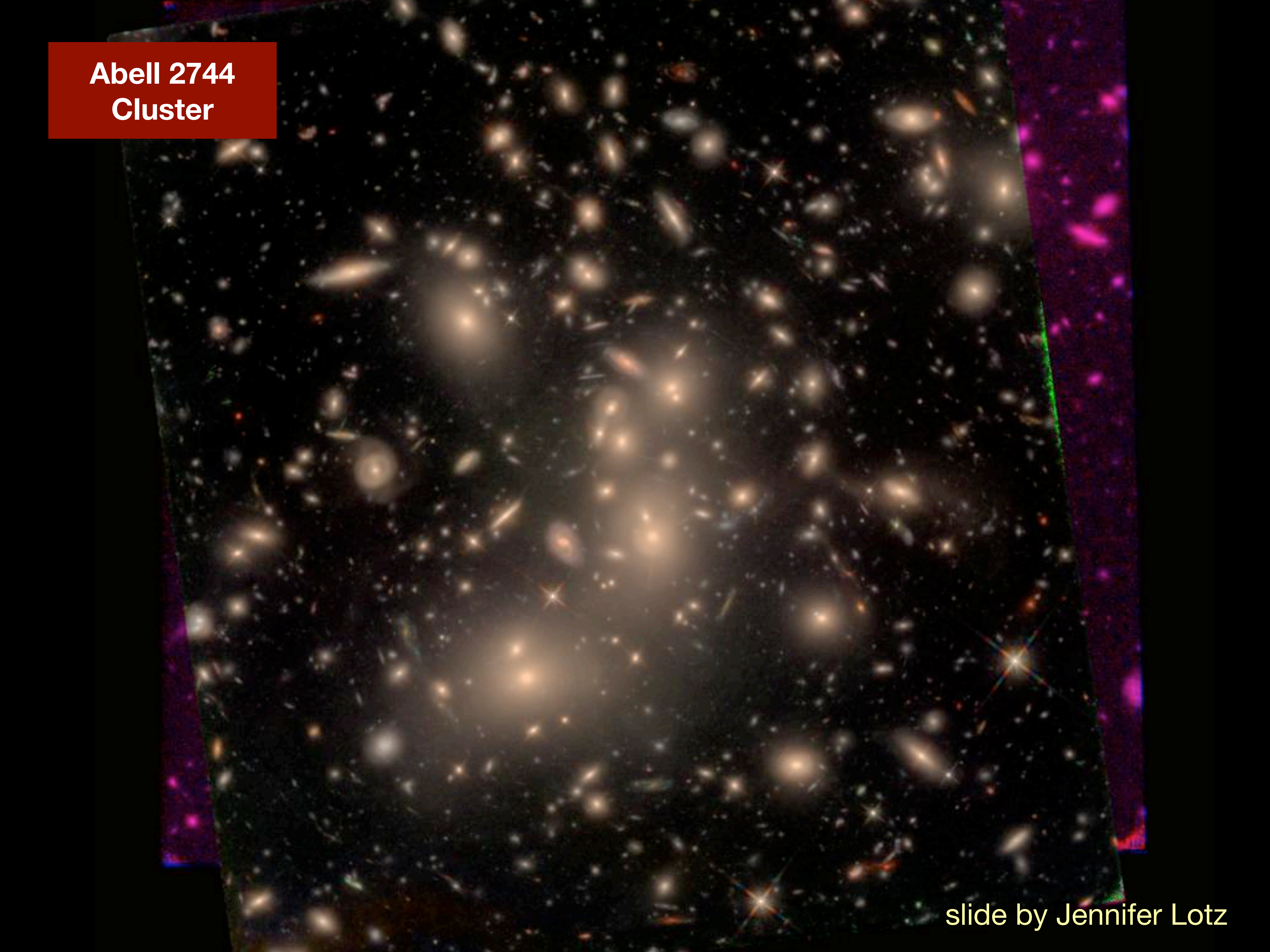

Abell 2744
Cluster
slide by Jennifer Lotz


Abell 2744
Cluster
slide by Jennifer Lotz


Abell 2744
Cluster
a model of the cluster's 'optics' gives us the magnification power
model credit: J. Richard, CATS team
slide by Jennifer Lotz

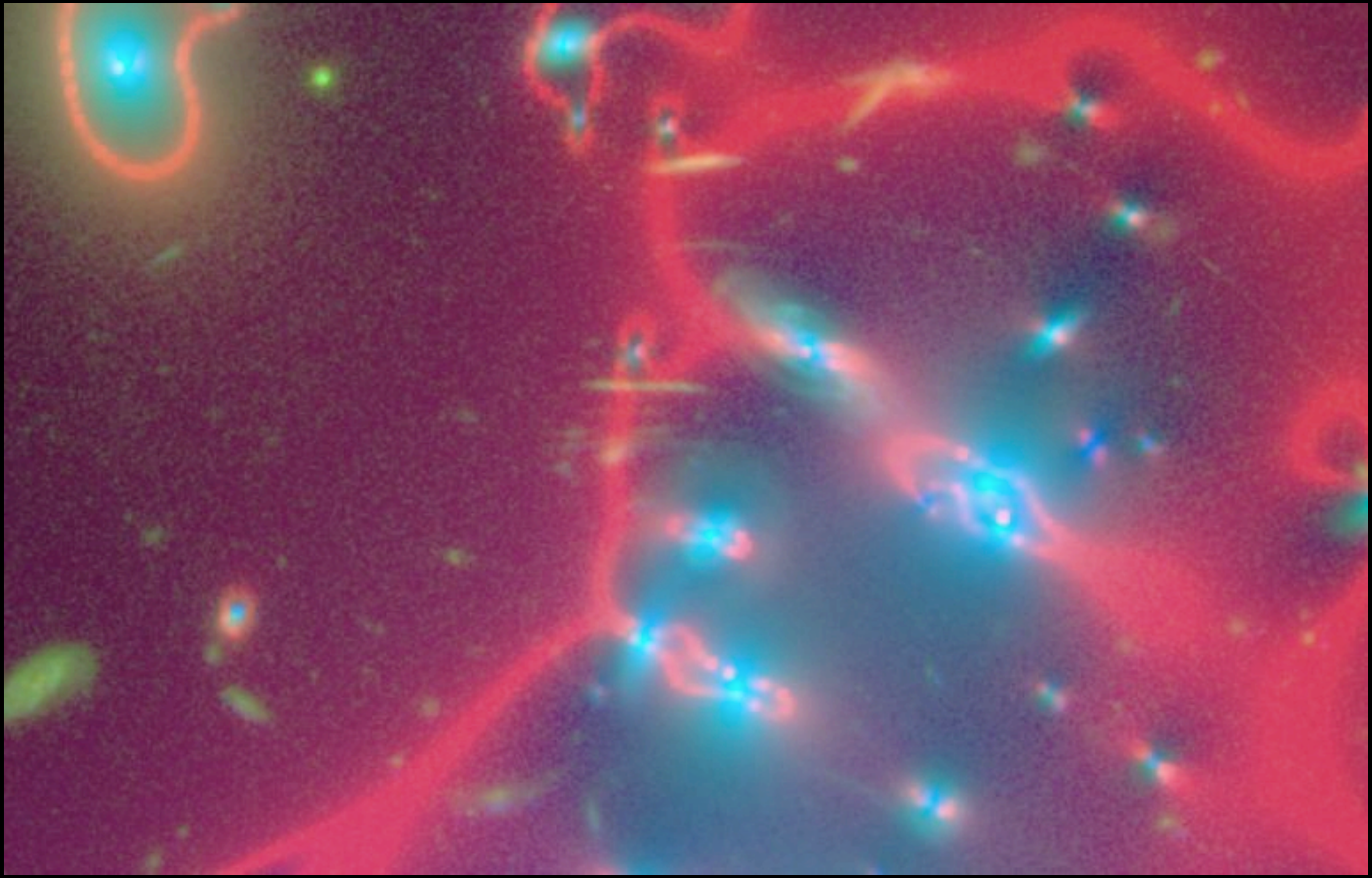

background galaxies are magnified by factors up to ~10-20,
providing the deepest yet view of the universe

slide by Jennifer Lotz

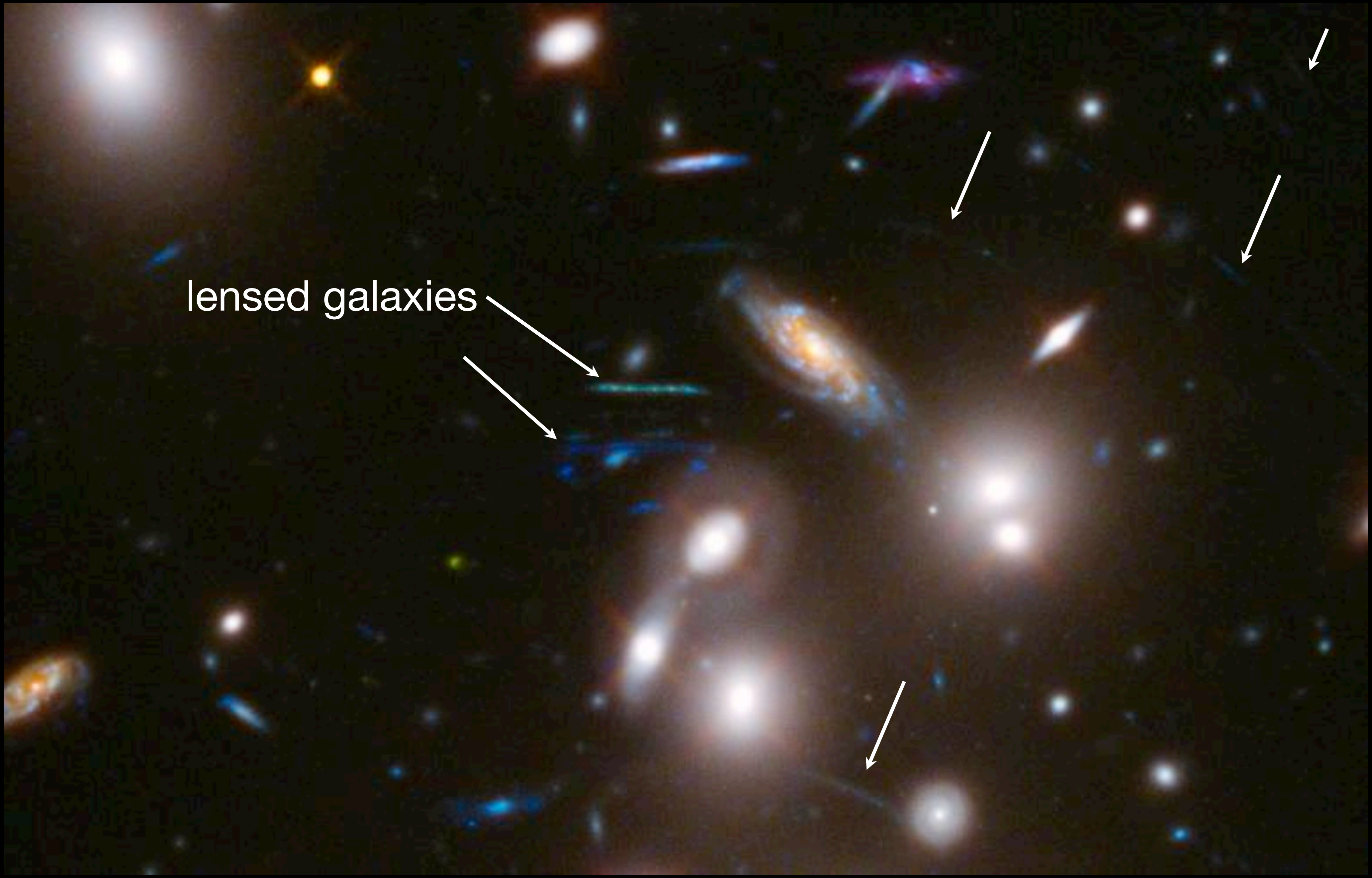

background galaxies are magnified by factors up to ~10-20, providing the deepest yet view of the universe

slide by Jennifer Lotz

Deepest view yet into the distant universe:

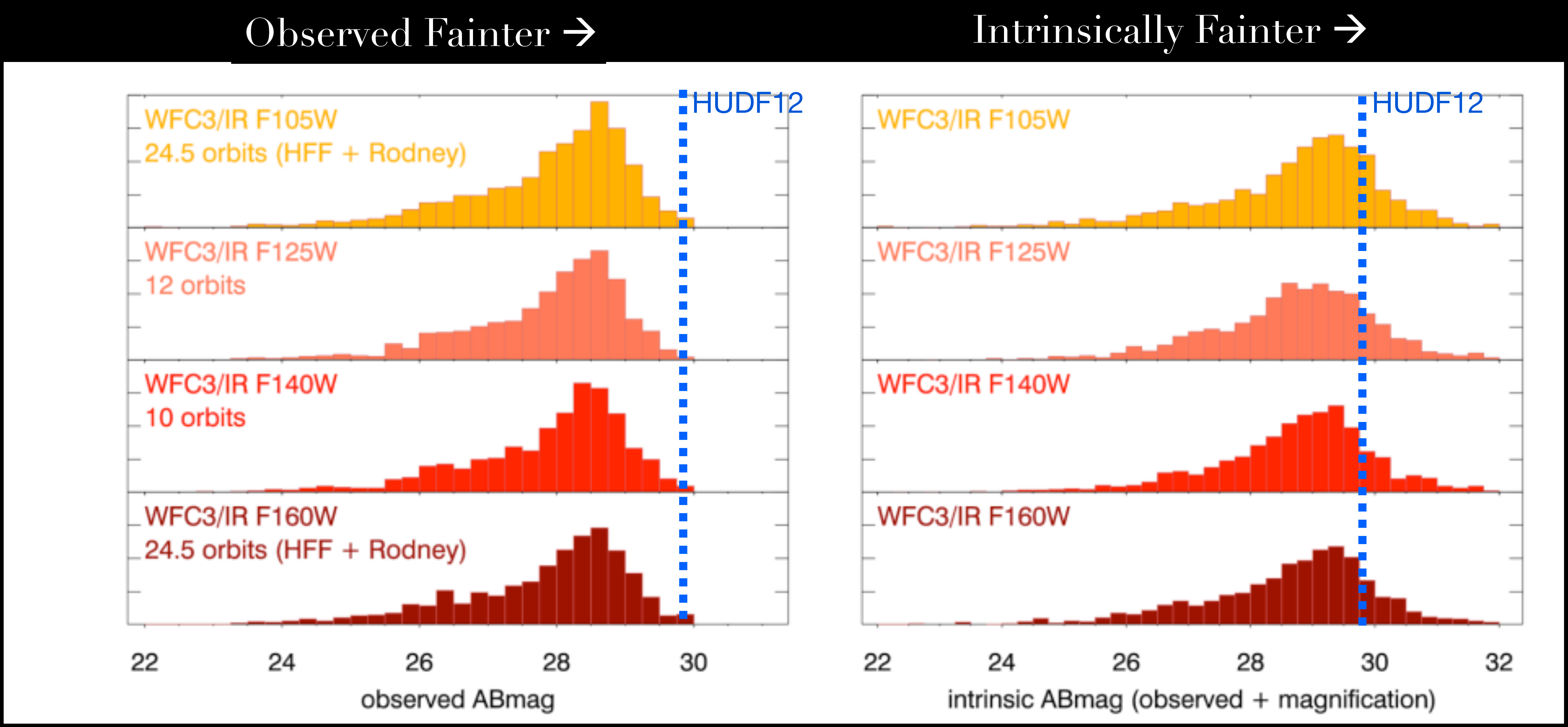

Take observed fluxes x lensing magnifications (average ~1.8x, max ~80x)

⇒ intrinsically faintest Frontier Fields galaxies ~2.5 magnitudes (10x) fainter than Ultra Deep Field (blue dashed line)

slide by Jennifer Lotz

A single cluster lens provided a significant step forward

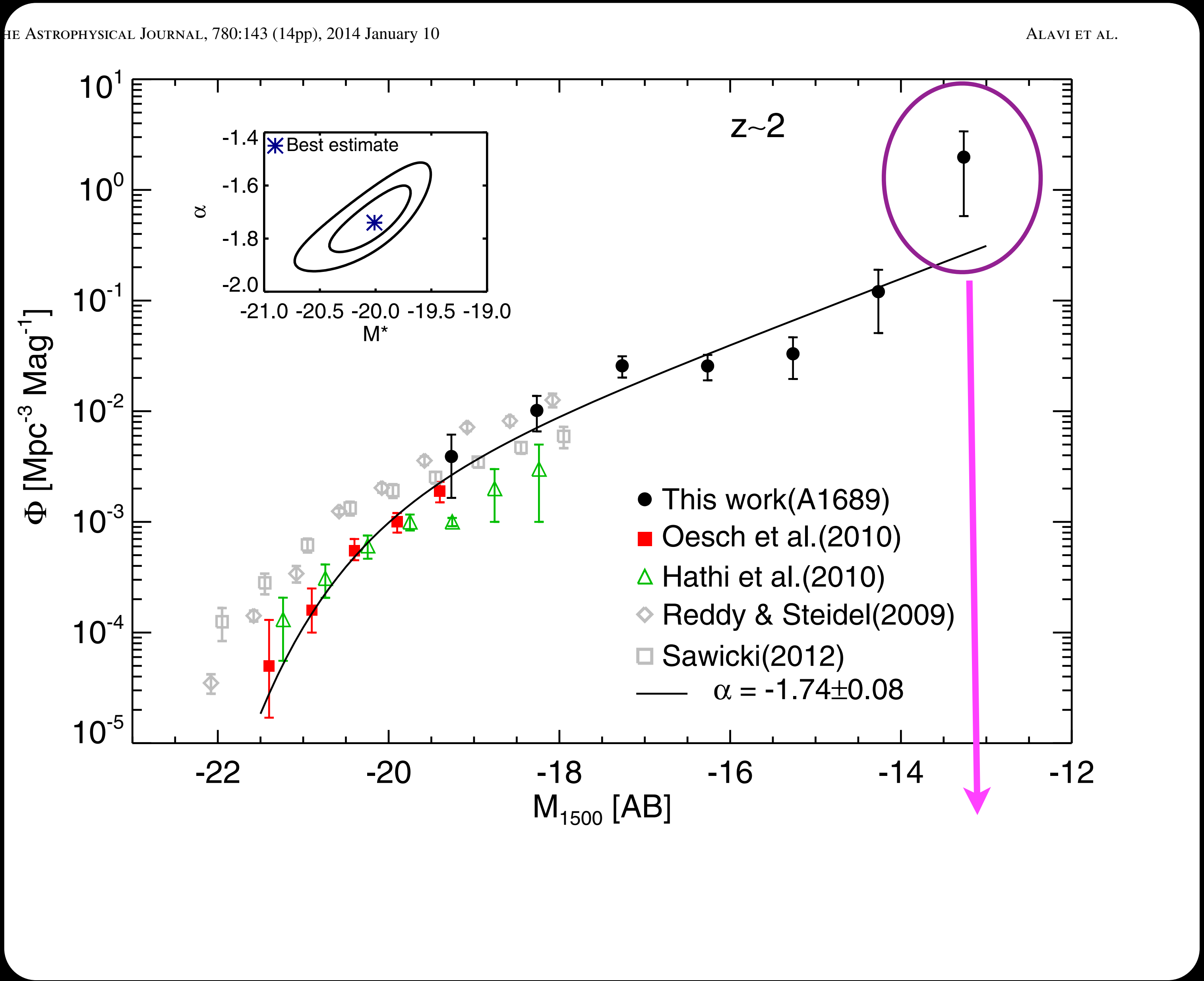

Alavi et al. 2015
Deepest Luminosity Function measured so far at z=2

Magnifications between 30 and 300

Statistics is still poor
4 galaxies in the faintest bins
$-14 \leq M_{UV} \leq -13$

Deep ultraviolet imaging of the lensing cluster A1689 with the WFC3/UVIS camera on *Hubble Space Telescope* in the F275W (30 orbits) and F336W (4 orbits) filters.
Identify z ~ 2 star-forming galaxies via their Lyman break. Because of the unprecedented depth of the images and the large magnification provided by the lensing cluster, we detect galaxies 100× fainter than previous surveys at this redshift.

A single cluster lens provided m_X>1.8 keV (thermal relic mass)

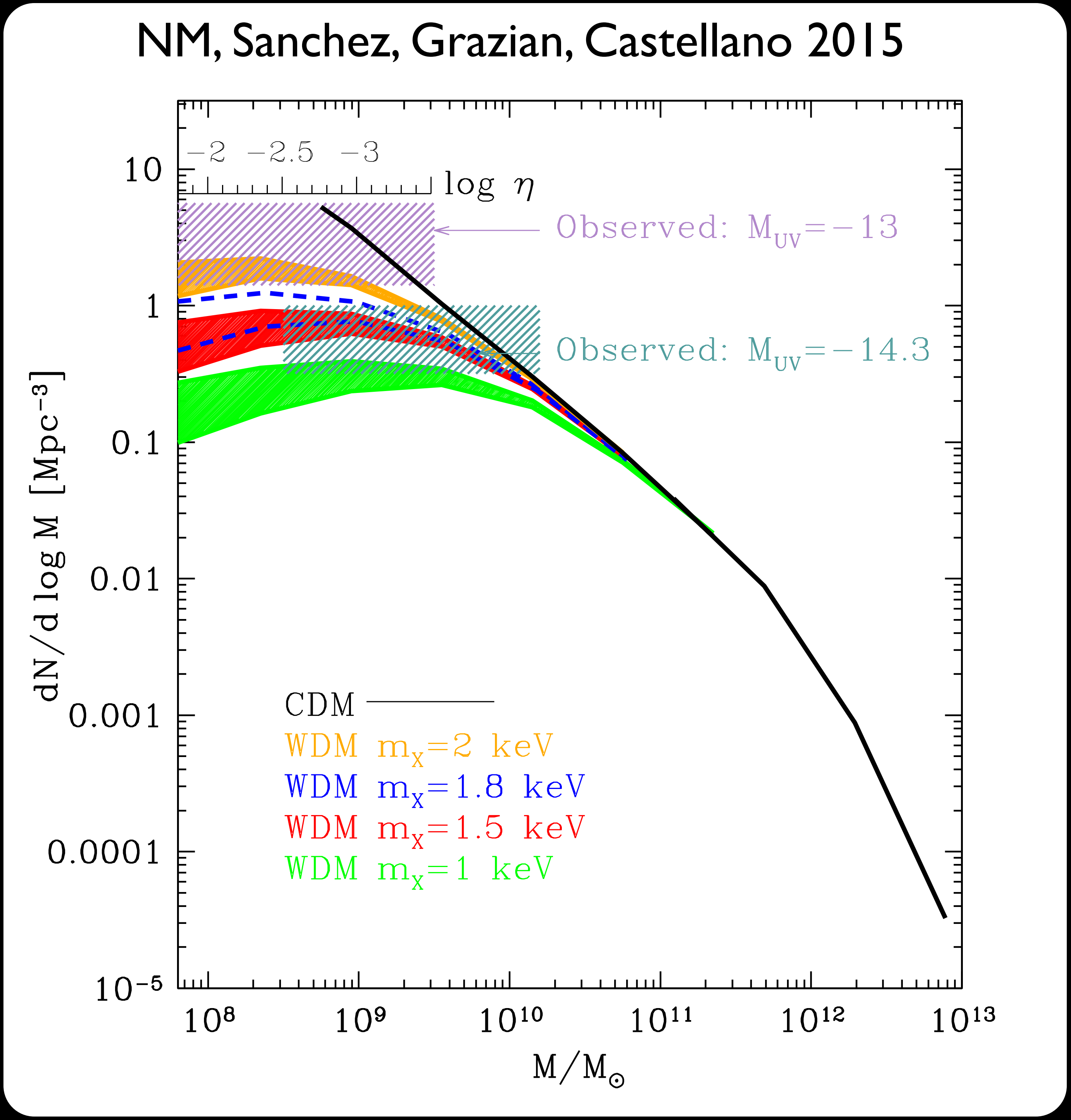

lower m_X do not provide the observed abundance. Note: baryonic processes can make the LF flatter but not steeper !

The result is robust with respect to

The effect of baryonic processes included in η. Observations probe the mass function in the mass range around the half-mode mass where the DM mass functions are characterized by a maximum value.

The modeling of residual DM dispersion velocities. Their would yield a sharper decrease of the mass function at small masses (see, e.g., Benson et al. 2013), thus yielding tighter constraints.

The kind of DM clumps hosting the UV emitting galaxies. In fact, the upper boundaries of the solid filled regions correspond to predictions including also proto-halos.

The possible effects of UV background and reionization. Such effects would further suppress the abundance of galaxies in low-mass halos (Sawala et al. 2015).

Recently Livermore, Finkelstein, Lotz 2016 obtained LFs of z=6 galaxies down to M_{UV}=-12.5

Based on 2 HFF lensing clusters Abell 2744 and MACS 0416

164 galaxies at z>6

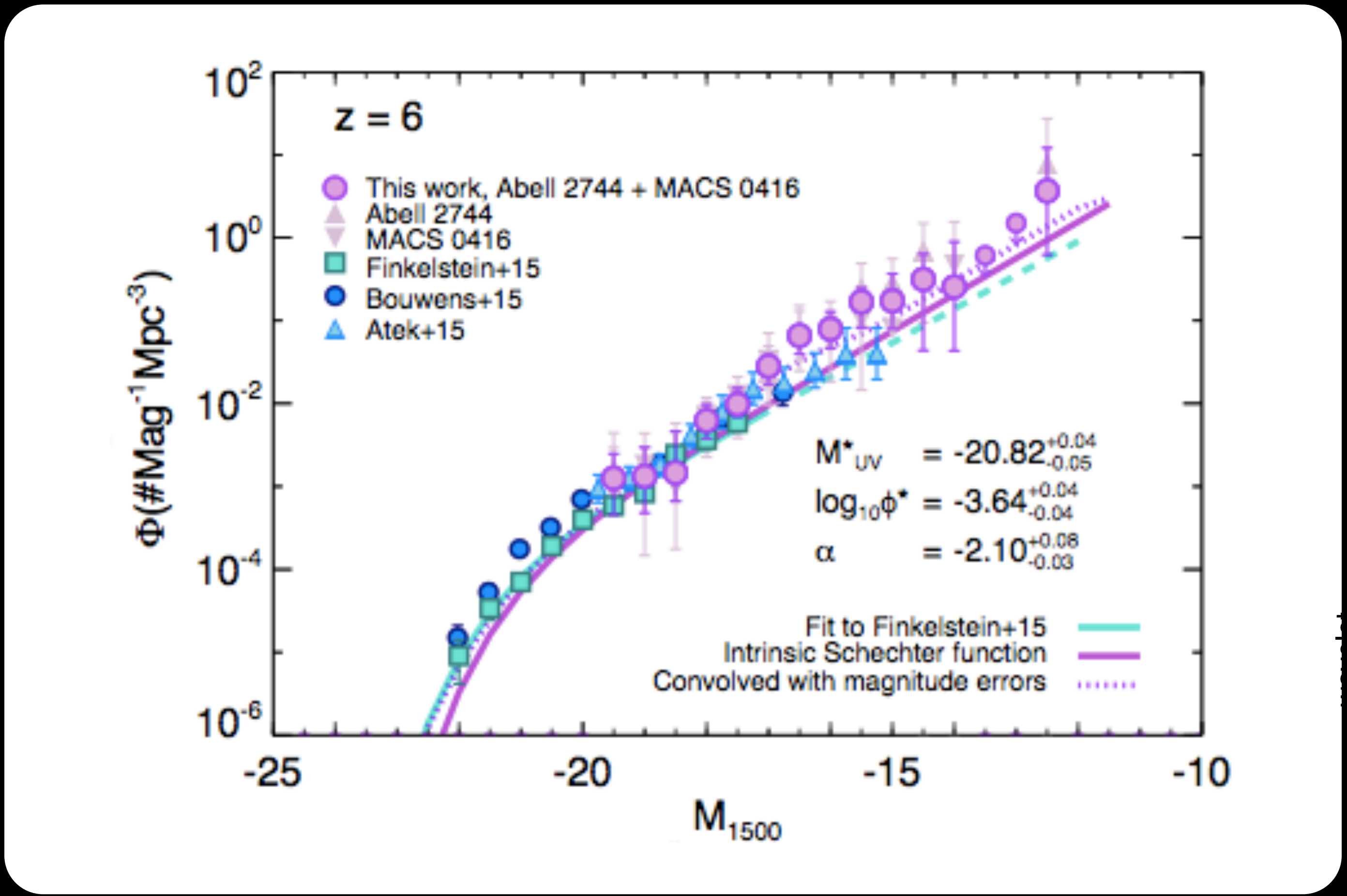

Lensing magnifications >50X

Magnifications have been derived by adopting the full range of possible lens models produced for the HFF by seven independent groups who used different assumptions and methodologies.

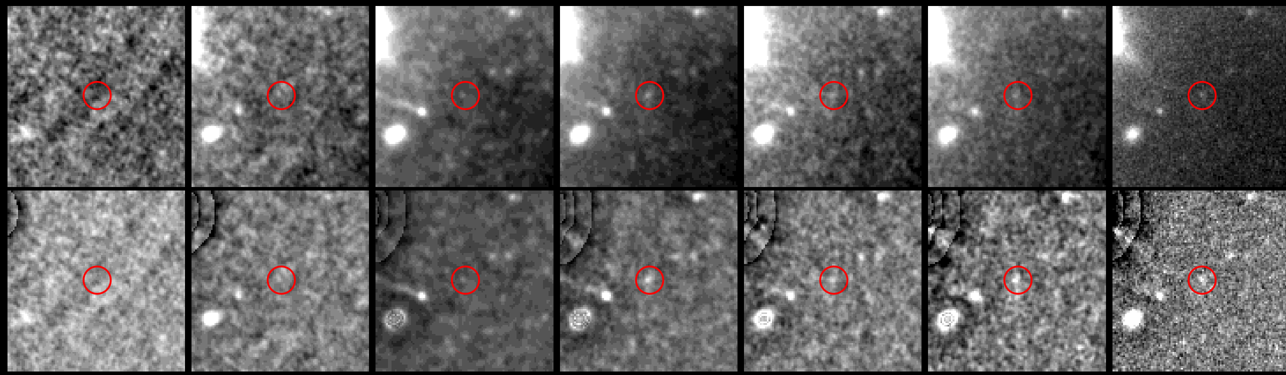

Postage stamp image of a2744 z6 3341, from the z ~ 6 sample detected in the Abell 2744 cluster field. The circle shows a 0.4" aperture. This galaxy is magnified by a factor ~ 20×, giving it an intrinsic UV magnitude of MUV = −14.54, but was not detected in previous studies due to the bright foreground object close to the line of sight (top row). It is easily detected in the wavelet-subtracted images (lower row

Such measurements have been shown to provide important constraints on the contribution to reionization, and on the star formation and feedback processes of primeval galaxies.

Recently Livermore, Finkelstein, Lotz 2016 obtained LFs of z=6 galaxies down to M_{UV}=-12.5

When compared with maximum number density of DM halos in WDM models

we find a limit m_X>3 keV (1σ), m_X>2,4 keV (2σ)

The tighter limits on mX derived so far independently of astrophysical processes

NM NM, Grazian, Castellano, Sanchez 2016

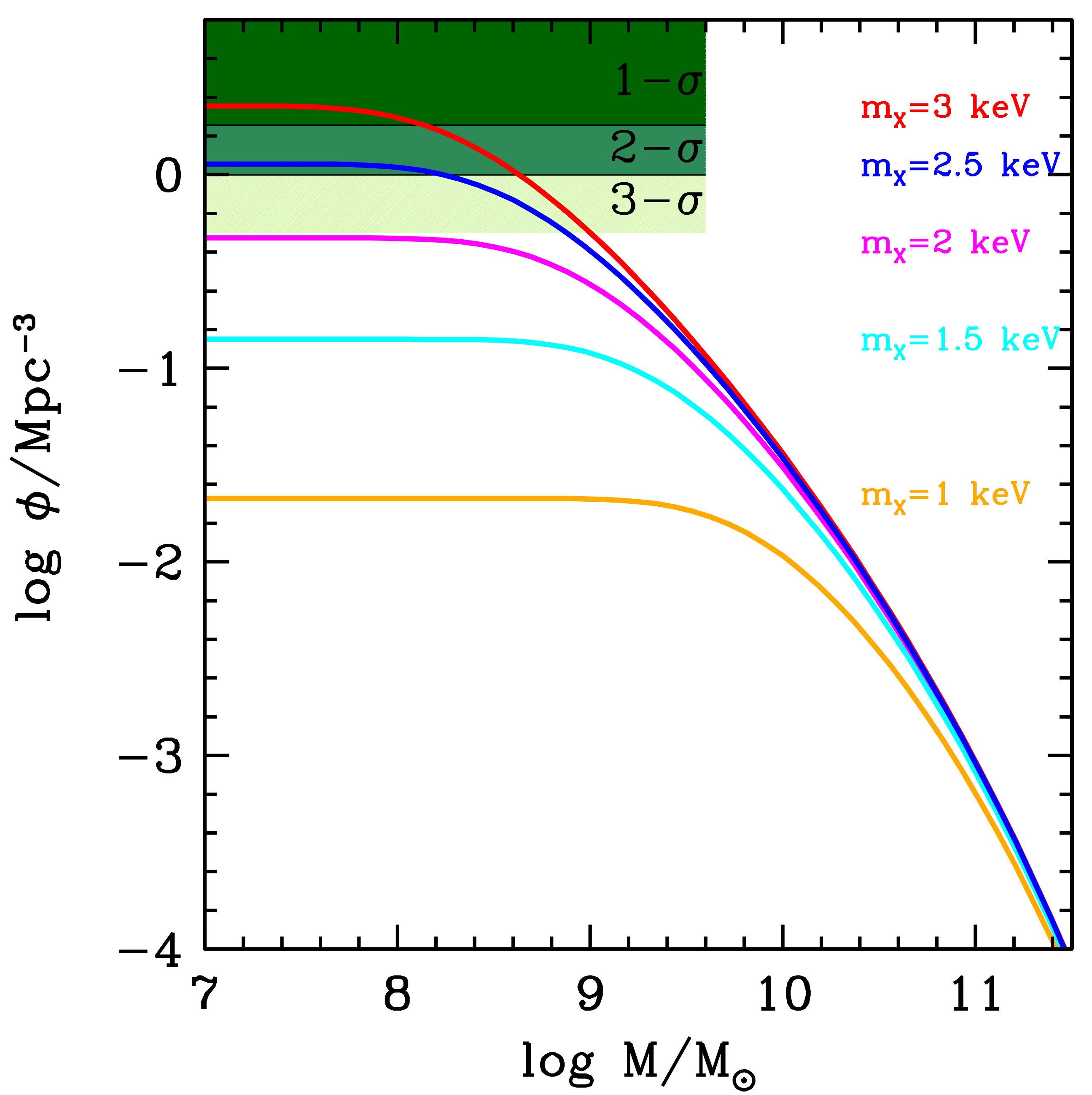

No matter what are the gas and star formation processes involved in galaxy formation visible galaxies cannot outnumber their host DM haloes

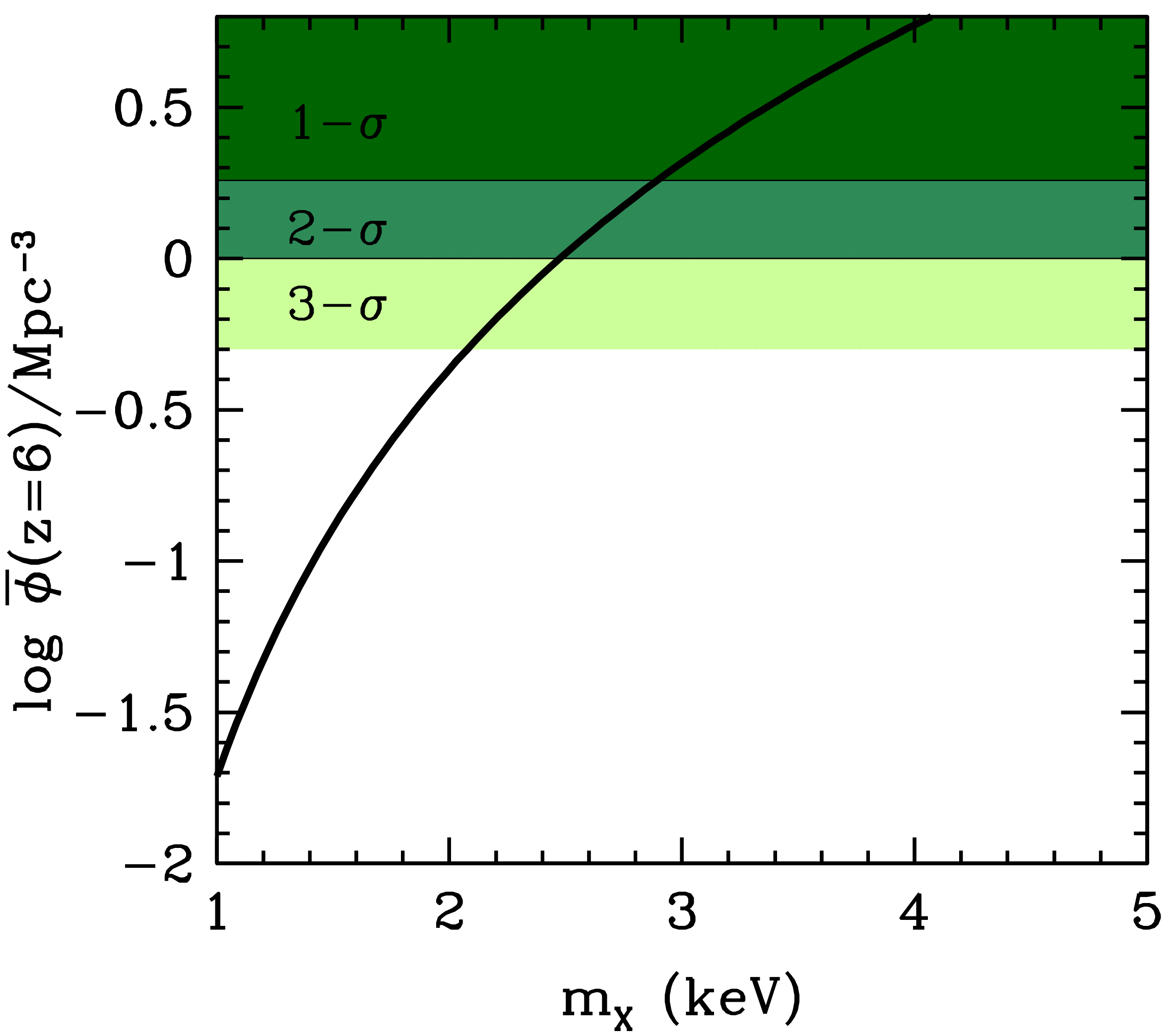

Comparison with previous limits based on galaxy abundances

NM+2016b

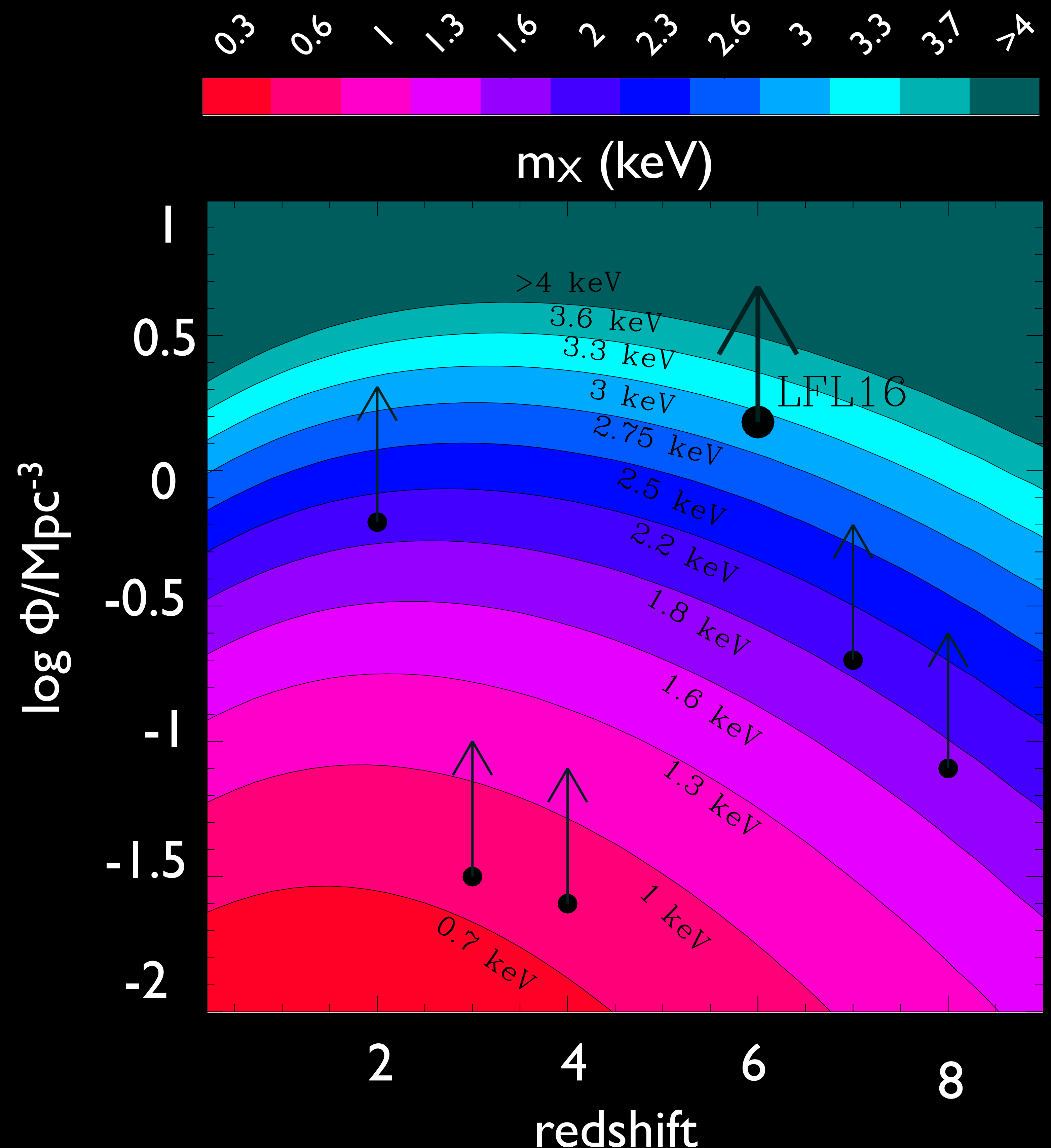

Data from

Alavi et al. 2015 z=2

Parsa et al. 2015 z=3-4

Livermore et al. 2016 z>6

The ultra-deep LF at z=6 constitute an extremely powerful probe
Ex. sterile neutrinos from scalar decay (Merle 2016)

courtesy A. Merle

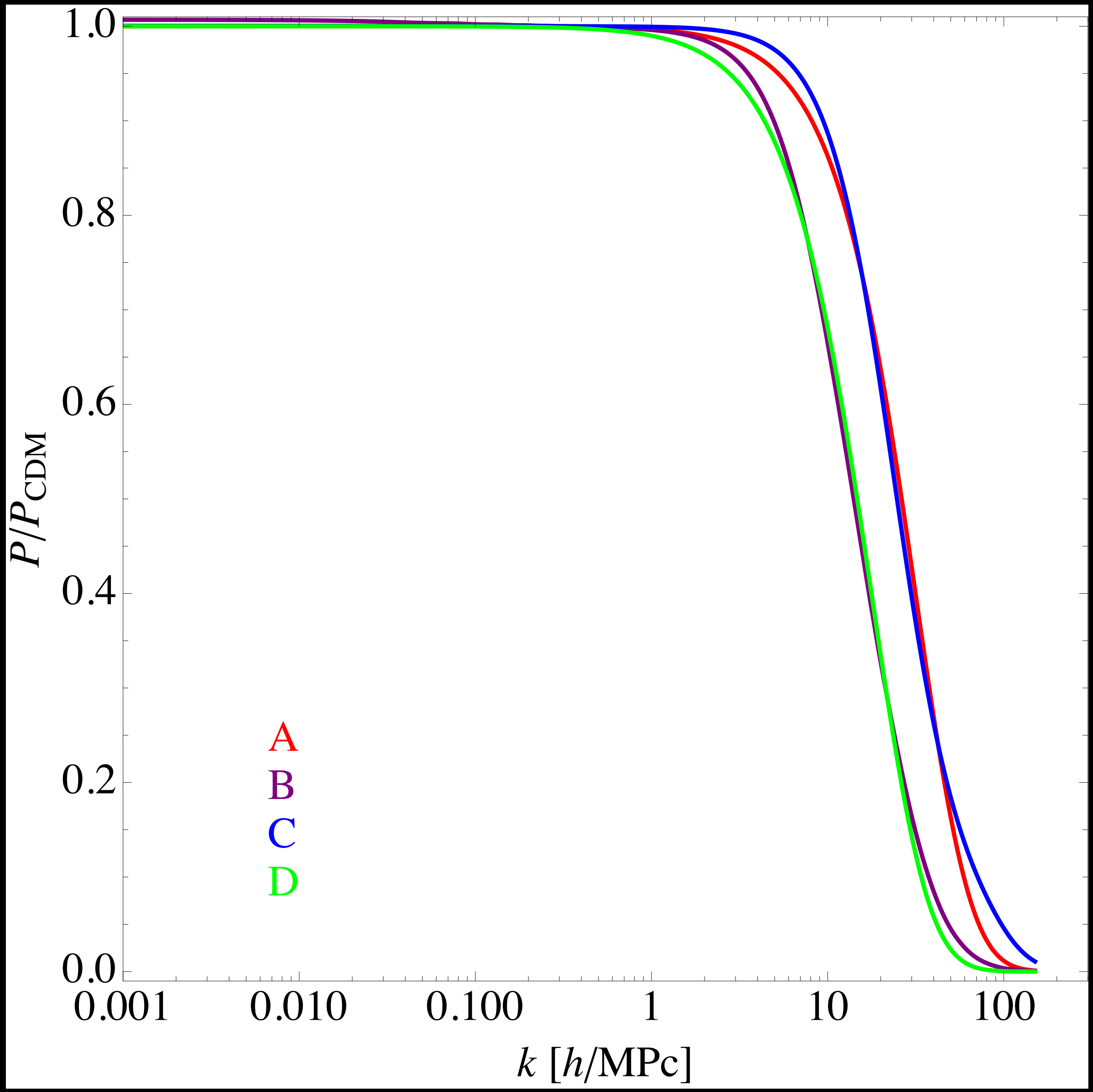

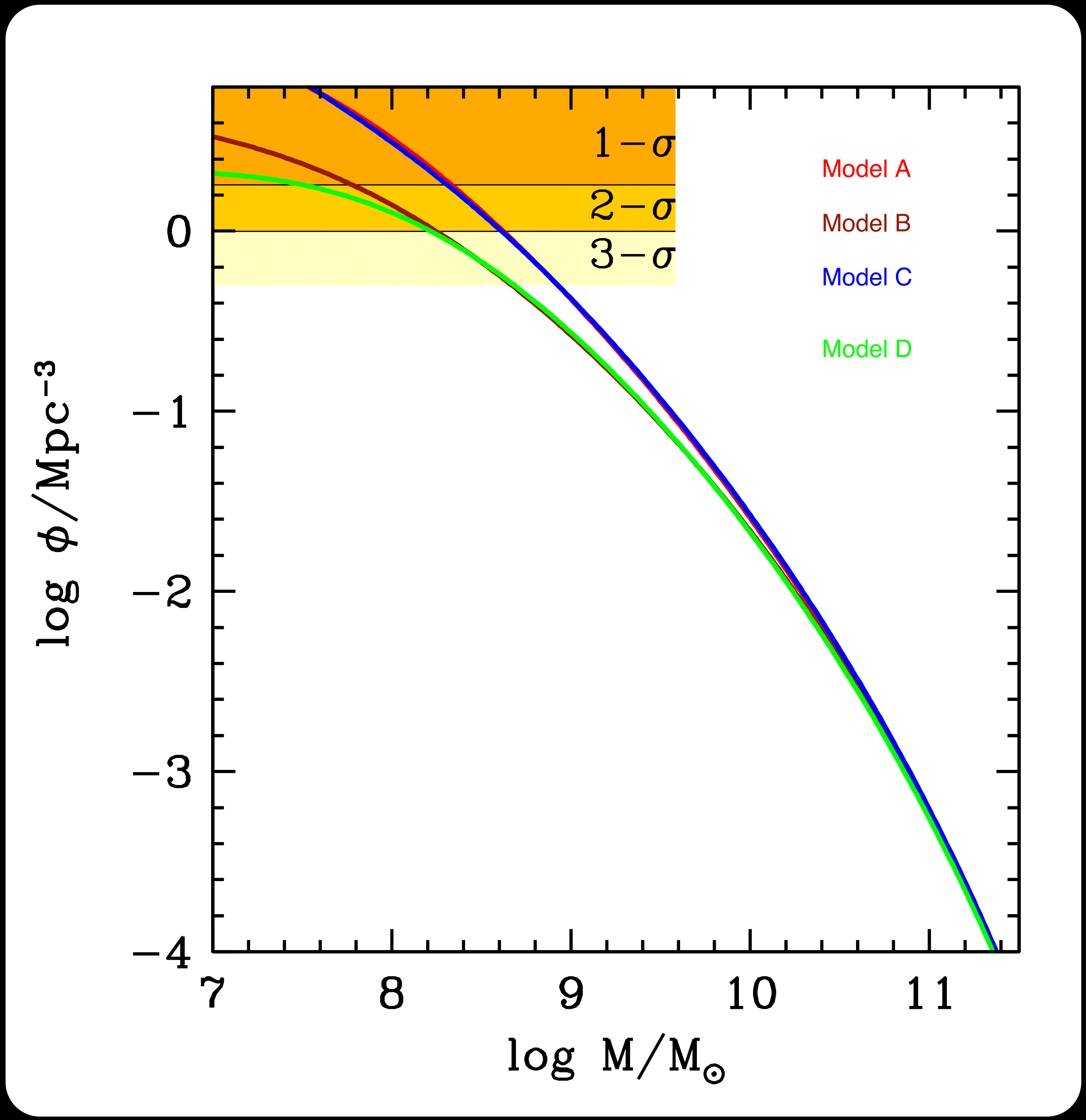

Wave DM (ultra-light axion like DM $m_X \sim 10^{-22}$ ev) is ruled out

Matching the dwarf profiles requires $m_{22}<1.2$, but abundances rule out $m_{22}<5$

Schive et al. 2016

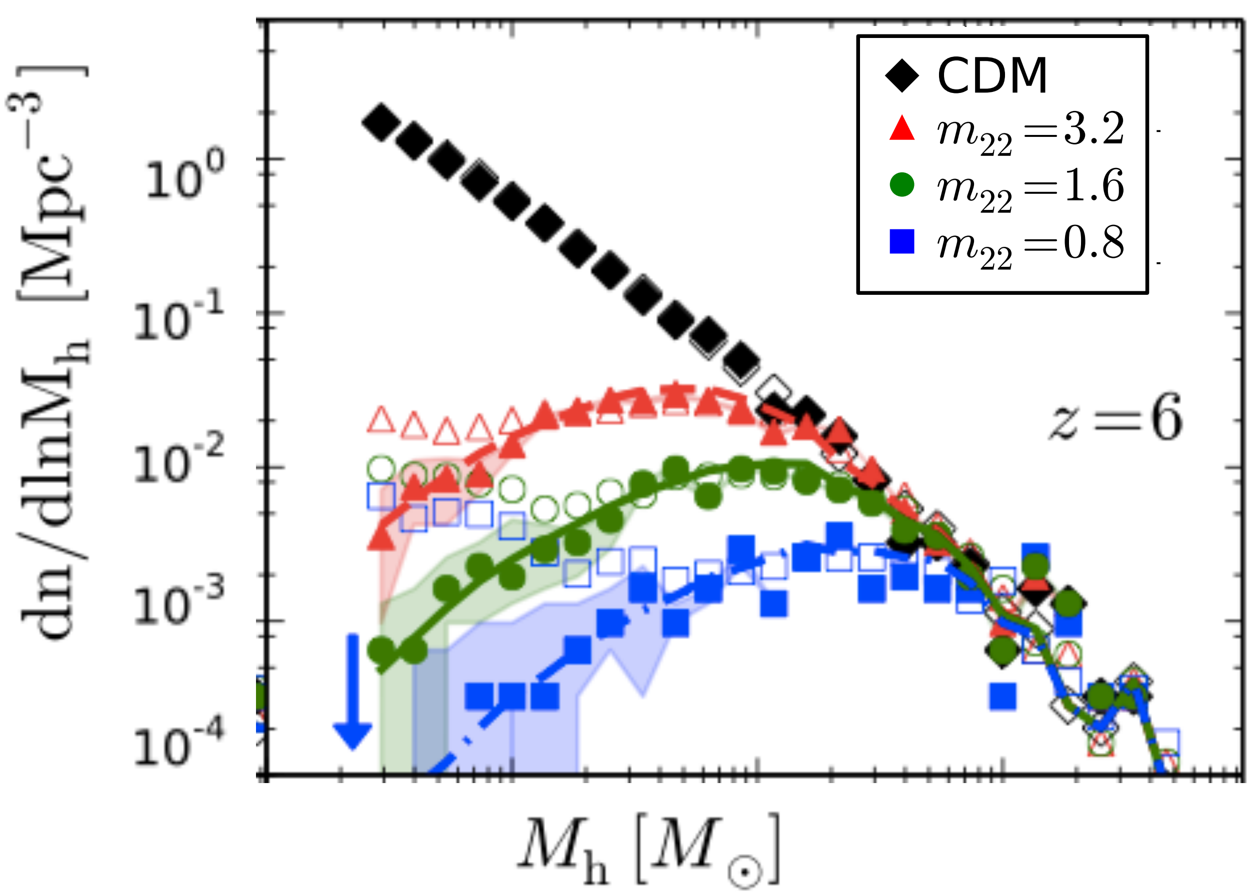

NM NM, Grazian, Castellano, Sanchez 2016

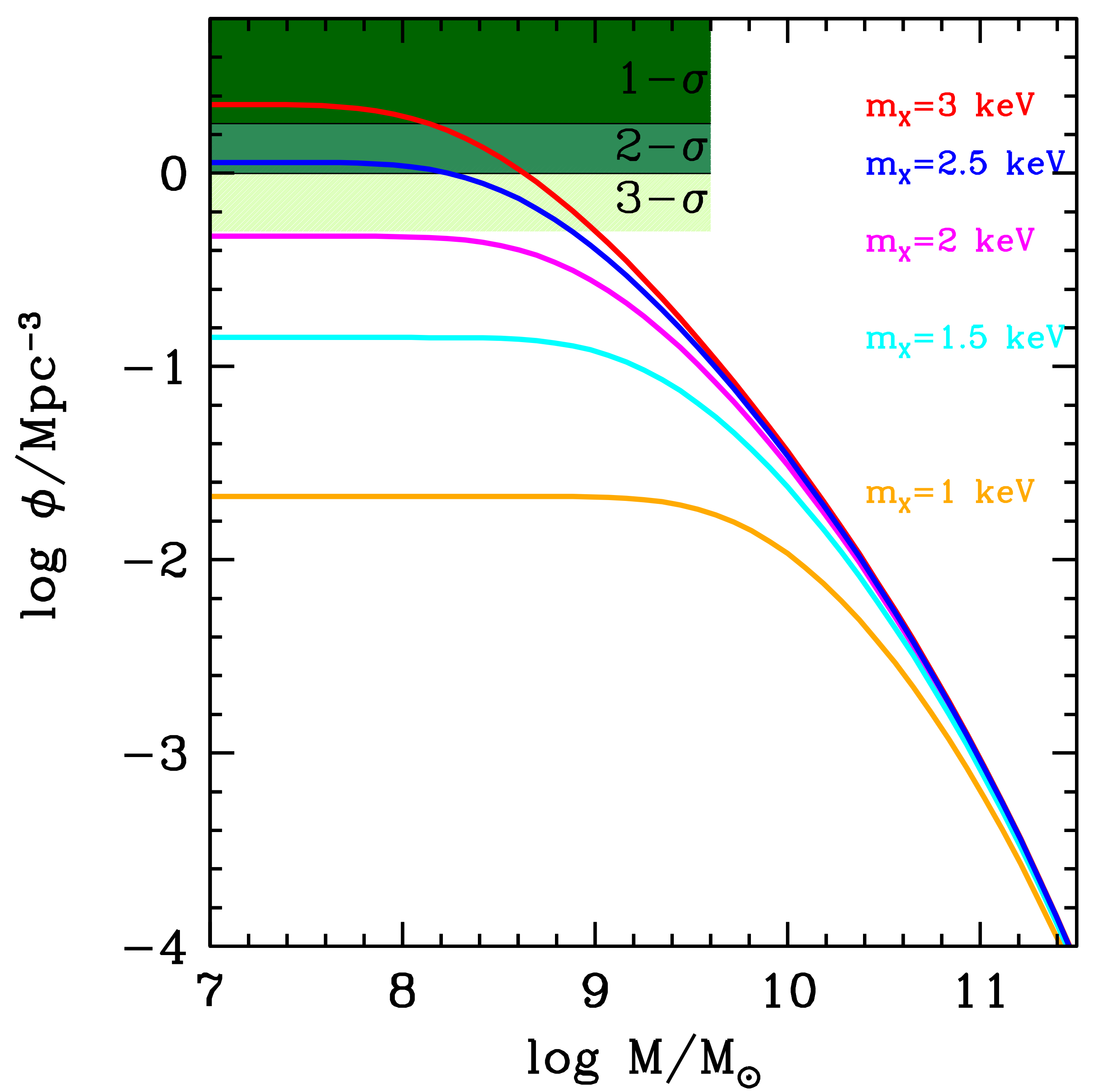

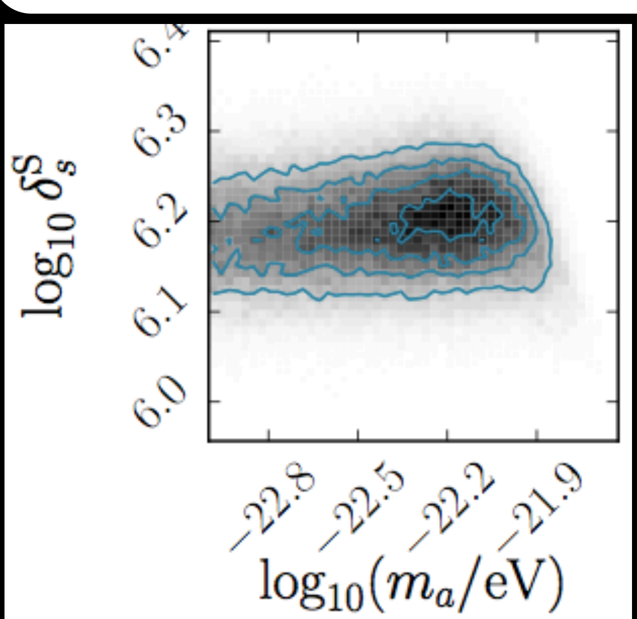

Marsch et al. 2015

Conclusions

Unsolved issues exist in current CDM galaxy formation model at small mass scales $M \lesssim 10^9 M_\odot$

WDM models with spectra corresponding to thermal relic mass $m_X \sim$ keV constitute viable solutions provided $m_X < 4$ keV (models with larger m_X are undistinguishable from CDM as far as galaxy formation is concerned)

The tremendous improvement in the observations of faint galaxies at high redshift through WFC3+lensing (HFF) allows to measure the abundance of z=6 galaxies down to M_{UV}=-12.5. This allows to set strong limits on m_X.
$m_X > 2.4$ keV at 2-σ level
independent on the modeling of astrophysical processes involving of gas and star formation
This corresponds to $m_{sterile} > 7$ keV for neutrinos produced via the Dodelson-Widrow mechanism

IF sterile neutrinos are the origin of the 3.5 keV line observed in spectra of X-ray clusters (i.e., $m_{sterile}$=7 keV) the above limit on m_X rules out the Dodelson-Widrow model for the production of sterile neutrino from oscillations with